4

N00014-90-J1913

Progress Report

STUDY OF BRIGHTNESS AND CURRENT LIMITATIONS IN INTENSE CHARGED PARTICLE BEAMS

For the period

July 1, 1992 - June 30, 1993

Submitted to

Office of Naval Research

Submitted by

Laboratory for Plasma Research
University of Maryland, College Park

Principal Investigators

M. Reiser and S. Guharay

UNIVERSITY OF MARYLAND

LABORATORY FOR PLASMA RESEARCH
COLLEGE PARK, MARYLAND
20742-3511

DISCLAIMER NOTICE

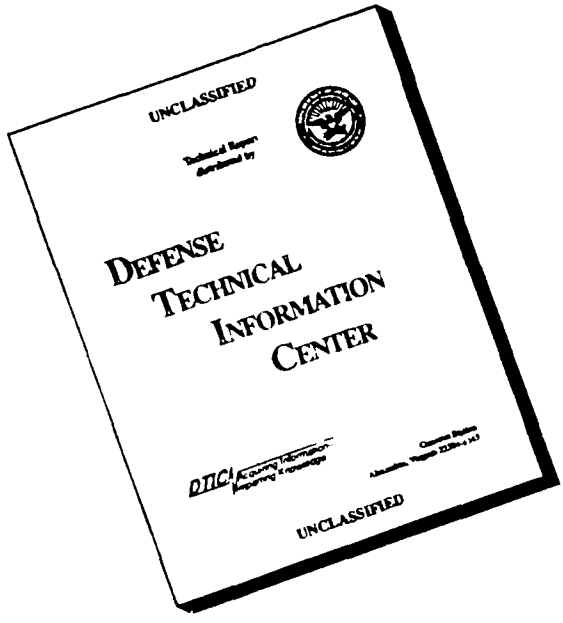

THIS DOCUMENT IS BEST QUALITY AVAILABLE. THE COPY FURNISHED TO DTIC CONTAINED A SIGNIFICANT NUMBER OF PAGES WHICH DO NOT REPRODUCE LEGIBLY.

STUDY OF BRIGHTNESS AND CURRENT LIMITATIONS IN INTENSE CHARGED PARTICLE BEAMS

M. Reiser and S. Guharay
University of Maryland, College Park, MD 20742 (301) 405-4960

INDIVIDUAL RESEARCH ABSTRACT

Over the past several years of ONR support for our research program we have mainly studied the various schemes for intense, high-brightness H^- beam transport and focusing in the context of its application in space defense. Detailed theoretical studies revealed that the conventional gas focusing system is not suitable as a low-energy beam transport (LEBT) system and also that there are too many unknown parameters to model accurately the behavior of partially charge-neutralized particle beams. We concluded that the electrostatic quadrupole lens system will be a good choice. We have developed a large number of simulation codes and also accessed into the existing codes in the accelerator community (e.g., PARMILA, SNOW-2D, PARMTEQ, etc.) to strengthen our analysis.

During the 1992-93 contract period we focused our attention to the experimental activities on H^- beam characterization and on the installation of a LEBT system for beam transport experiments. We have simultaneously improved our code by incorporating many practical features that we encountered during the analysis of experimental data.

We have studied H^- beams from two types of ion sources: a volume ionization type and a magnetron type source. One of the major problems in this work is to transform a highly diverging beam from the source into a highly converging one so that the output beam from the LEBT can be matched into the acceptance ellipse of an RFQ. Furthermore, the emittance budget is quite restricted. After a detailed beam dynamics studies, we have been finally successful to design an optimized LEBT system that can deliver a matched beam to the RFQ; this is the first time that such good beam matching has been simulated in the context of the particular experiment.

We have set up an experimental facility in-house to perform various tests of the LEBT system. We have made several important modifications of our ESQ LEBT system which was

developed last year. The electrical layout of the lens assembly has been changed and this required to modify the vacuum vessel. The system is expected to have a long-term reliability in terms of voltage holding. The ESQ LEBT is supported in the vacuum vessel using a vacuum manipulator developed in-house. This allows to align the system in-situ. Various tests of the ESQ LEBT are being conducted.

We have received a magnetron ion source from the Superconducting Super Collider Laboratory (SSCL). This allows us to set up an in-house test stand facility for H^- beams.

In theoretical work supported by this contract, Christopher Allen, a graduate research assistant working towards his Ph.D. has developed a new moment-method Laplace solver for low-energy beam transport codes. This technique is expected to increase both speed and accuracy of electrostatic field calculations.

St-A per telecon, Mr. Shlesinger, ONR/Code 1112A1. Arl., VA 22217

JK 8/23/93

STUDY OF BRIGHTNESS AND CURRENT LIMITATIONS IN INTENSE CHARGED PARTICLE BEAMS

M. Reiser and S. Guharay, University of Maryland

RESEARCH OBJECTIVES:

Intense, high-brightness neutral beams have a strong potential to strengthen the space defense program. In recent years a strong emphasis has been laid on pushing the state-of-the-art of negative ion beams, especially the H^- beams. This has occurred due to several special features of the negative ions, e.g., non-Liouvillean stacking to generate intense beams, efficient charge-exchange process to generate high-energy neutral beams, and furthermore, future application of H^- beams in ion-beam microlithography. Such a demand from multiple disciplines has set a strong challenge to the community involved in research on ion sources and ion-beam dynamics, and a rapid progress of the field is visible. Our research program on nigh-brightness H^- beams involves both experimental and theoretical work on the generation and transport of the beams; the major emphasis here is on the study of the beam emittance.

After a detailed investigation of the various methods of transporting a high-brightness H^- beam we have determined that an electrostatic quadrupole lens system is a good choice. We have set up a strong infrastructure on simulation of beam dynamics. This work is being continuously examined in the light of experimental results. Consequently, many practical features are included in our simulation codes and the simulation predictions are expected to be very reliable. Experiments with an ESQ LEBT system, which was developed in-house, are in progress. We have also initiated an experimental program to set up a test stand facility at Maryland.

STUDY OF BRIGHTNESS AND CURRENT LIMITATIONS IN INTENSE CHARGED PARTICLE BEAMS

M. Reiser and S. Guharay, University of Maryland

STATUS OF RESEARCH IN PROGRESS

Our research during the current contract period has been mainly motivated towards the experimental work on transport of high-brightness H^- beams and focusing. The experimental studies are being carried out at the test stand facility of the Superconducting Super Collider Laboratory (SSCL) using ion beams from a volume ionization source; a new in-house program is also established with some support for equipment from SSCL to set up a test stand using a magnetron-type ion source. As the characteristic parameters of H^- beams from these two different ion sources are quite different, these studies allow us to address a number of key physics issues on beam dynamics as well as to evaluate some practical problems in terms of long-term stable operation, ease of handling, etc. This work is described below.

High-Brightness H^- Beam Transport and Focusing

As was mentioned earlier in our previous reports to ONR, the study of high-brightness H^- beams is motivated towards the development of an efficient low-energy beam transport channel. After a detailed investigation of the characteristics of various types of transport systems, we decided to focus our attention on an electrostatic system, mainly the electrostatic quadrupole configuration, in the context of transporting short-pulse beams which are particularly relevant to our beam transport experiments with volume and magnetron sources (typically, pulse length $\ll$ beam neutralization time). Our approach is to initially develop a good understanding of the beam dynamics through simulation studies, and to build up a close link between experimental results and simulation predictions. This procedure helps to continuously improve upon any weak points of the simulation schemes, and it, therefore, enhances the confidence level of the simulation predictions.

The goal of this work is to deliver a matched beam to the RFQ in the linac section without any significant emittance dilution. In the case of the SSC RFQ the matching condition is given by the acceptance ellipse parameters: $\alpha = 1.26$, $\beta = 1.86$ cm/rad, $\pi\tilde{\epsilon}_n = 0.2\pi$ mm-mrad. This demands a strong convergence of the beam from the LEBT section. We find that a short einzel lens module between the ESQ LEBT and the RFQ will allow us to handle the emittance budget efficiently, especially when a large drift space ($\sim$ few cm) exists to accommodate the mechanical structures as the front wall of the RFQ; however, this space should be kept to a minimum to deliver a good beam to the RFQ. It is estimated using the SNOW-2D code that the einzel lens geometry, shown schematically in Fig. 1a, can satisfy the nominal matching condition at a distance of about 3.0 cm from the front end of the RFQ wall without any noticeable emittance growth (Fig. 1b); the third electrode at ground potential simulates the front wall of the RFQ here. This result corresponds to the following beam parameters at the input of the einzel lens: beam current = 30 mA, $\tilde{\epsilon}_n = 0.23\pi$ mm-mrad, $X \sim 7$ mm and $X' \lesssim -50$ mrad. Our ESQ LEBT is chosen to deliver an output beam so that it can satisfy the aforementioned requirements for matching with the einzel lens.

A. H^- beams from a volume source

The emittance measurements of a 30 mA, 35 kV H^- beam from the SSCL volume source are shown as contour plots in Fig.2. These data are taken at a distance of about 10 cm from the extraction electrode (aperture radius = 4 mm). The beam parameters at this location are: beam size = 2.38 cm, full divergence $\Delta\theta = 260$ mrad, $\pi\tilde{\epsilon}_n = 0.1537\pi$ mm-mrad. The drift space of 10 cm long is due to the insertion of an electron suppression system which separates out the electron component (initial electron-to-ion current ratio is about 40.) from the extracted current. Such a long drift space causes a significant blow-up of the H^- beam envelope. It is currently planned to replace the electron suppression system by a shorter one of about 5 cm long.

In order to estimate the beam parameters at the extraction electrode the aforementioned beam data at $z = 10$ cm are given as input to the envelope simulation code which solves the K-V equations. This code, developed here, has a number of important features that allow to include several practical considerations, e.g., the space-charge effects due to the accum-

accumulation of extraneous charge elements (electrons and positive ions) in the neighborhood of the extraction region, plausible profiles of the extraneous charge elements, etc. Figure 3(a) shows the assumed space-charge correction factor, f, due to the electrons. Note that f is negative here, and the beam perveance is to be multiplied by a factor of $(1-f)$ to include the effect of the electrons in the space-charge force term in K-V equations. The estimated beam envelope upstream towards the extraction electrode (here, at $z = 0$) is shown in Fig. 3(b). This suggests that the beam forms a waist close to the extraction electrode and it fills up almost the full aperture.

Using the above information of the beam parameters at the extraction electrode, the characteristics of the ESQ LEBT system and the behavior of the beam through the LEBT are determined. Figure 4 shows the envelope of the H^- beam through the ESQ LEBT. It may be noted that the aperture of the ESQ lenses are about a factor of two larger than what we mentioned in our last year's report; this change has been necessary to accommodate the large beam at the end of the 5 cm-long electron suppressor in this experiment. The distribution of the beam particles through the ESQ LEBT is estimated using the modified PARMILA code. Figure 5 shows the particle distribution in phase space. The output beam parameters are: $X = 7.2$ mm, $Y = 7.3$ mm, $X' = -51$ mrad, $Y' = -51$ mrad, $\tilde{\epsilon}_{nf}/\tilde{\epsilon}_{ni} \sim 1.5$. The emittance growth is mainly due to chromatic aberrations. Note that the output beam parameters match closely to the desired characteristics of the input beam for the einzel lens.

Details of this work are given in reference 4. Note that the reference numbers referred to in this section correspond to the numbers in the list of presentations, publications and invited talks (p. 23) of this report.

B. H^- beams from a magnetron source

The emittance measurement of the H^- beam from the SSCL magnetron source is shown in Fig. 6. These data were taken at 11.75 cm downstream from the extraction slit of the source; the beam size is about 3.5 cm, full beam divergence is about 300 mrad, and $\pi\tilde{\epsilon}_n = 0.12\pi$ mm-mrad. In the case of a magnetron source the ratio of e/H^- in the extracted current is about 1-2; hence the space-charge effect of the electrons may not be important. Following the method as described in the previous case, the beam parameters at the extractor is estimated

using the aforementioned emittance data, and it is found that $X \sim 1.1$ mm and $X' \sim 70$ mrad.

The beam envelope through the ESQ LEBT is shown in Fig. 7. It is noted from the particle simulation results that the emittance growth for the full beam current is quite large here – a factor of about 3. Scraping off about 15% of the beam particles the emittance growth drops to a factor of 1.5; Fig.8 shows the phase-space distribution of the particles. The beam parameters are: $X = 4.7$ mm, $Y = 4.4$ mm, $X' = -49$ mrad, $Y' = -48$ mrad. These results also match reasonably well with the requirements of the einzel lens input as discussed earlier.

Details of this work are given in reference 1.

C. ESQ LEBT system and tests

It is planned to initially use a prototype ESQ LEBT system which has already been developed in-house at Maryland. The compatibility of the LEBT system with the SSC volume source environment has been checked. Figure 9 shows an initial experimental set-up of the LEBT on the SSCL test stand. Figure 10 shows the test facility at Maryland to perform voltage hold-off tests. The experiment is now in progress.

D. Magnetron ion source facility at the University of Maryland

We have received a magnetron ion source with numerous supporting electronics from SSCL. Figure 11 shows a few major components of the experimental facility. In order to bring the test stand to operation and run the ion source meaningfully, it will be necessary to develop the computer control system, and also some diagnostic equipment, e.g., Faraday cup, toroids, emittance scanner, etc., should be procured.

E. Theoretical studies

1. Laplace/Poisson Solver

An efficient Laplace/Poisson Solver has been developed. It is fully 3D and capable of running practical problems on an IBM PC. The technique relies on a combination of the method of moments and fast iterative techniques for solving linear systems. Specifically, we

proceed by reformulating Laplace's equation into an integral equation over the boundary surface, reducing the dimensionality of the original system. The new problem is approximated by the method of moments to yield the matrix-vector equation $A_x = y$. We then use conjugate gradient algorithms to solve this equation; this is an iterative method which seems to provide fastest convergence.

The above technique has been implemented on an i486 PC operating at 33 MHz and running Windows 3.1 operating system. A 3D potential problem is the modeling of an electrostatic quadrupole lens. Figure 12 shows the computer model of an ESQ lens. It is formed from 4 cigar-shaped electrodes, the beam would enter from the left. Each electrode is 59 mm long and has a radius of 12 mm. The aperture of the entire lens is 10.5 mm. Two grounding shunts are located at $z = \pm$ 31 mm (they are not shown in Figure 12 to avoid clutter) which provide isolation from adjacent lenses.

The single particle focusing effect (the kappa function $\kappa(z)$) from such lenses can be determined from the on axis derivatives dE_x/dx and dE_y/dy. Figure 13 shows the computed data for the y-plane for the case in which the x-plane electrodes are driven to 1 V and the y-plane electrodes are held at -1 V. The grounding shunts at either end of the lens cause the rapid decay in dE_y/dy.

We can use the Poisson extension to simulate a uniform charge density ellipsoid in a conducting cylinder. This situation is useful in modeling cold bunched beams propagating through a beam pipe. There exists an analytic solution for the potential of such an ellipsoid in free space. Thus, it is only necessary to model the pipe (surface charge) numerically. The above simulations can be used to determine the so called "g-factor" for bunched beams in cylindrical pipes.

Details of this work are given in reference 3.

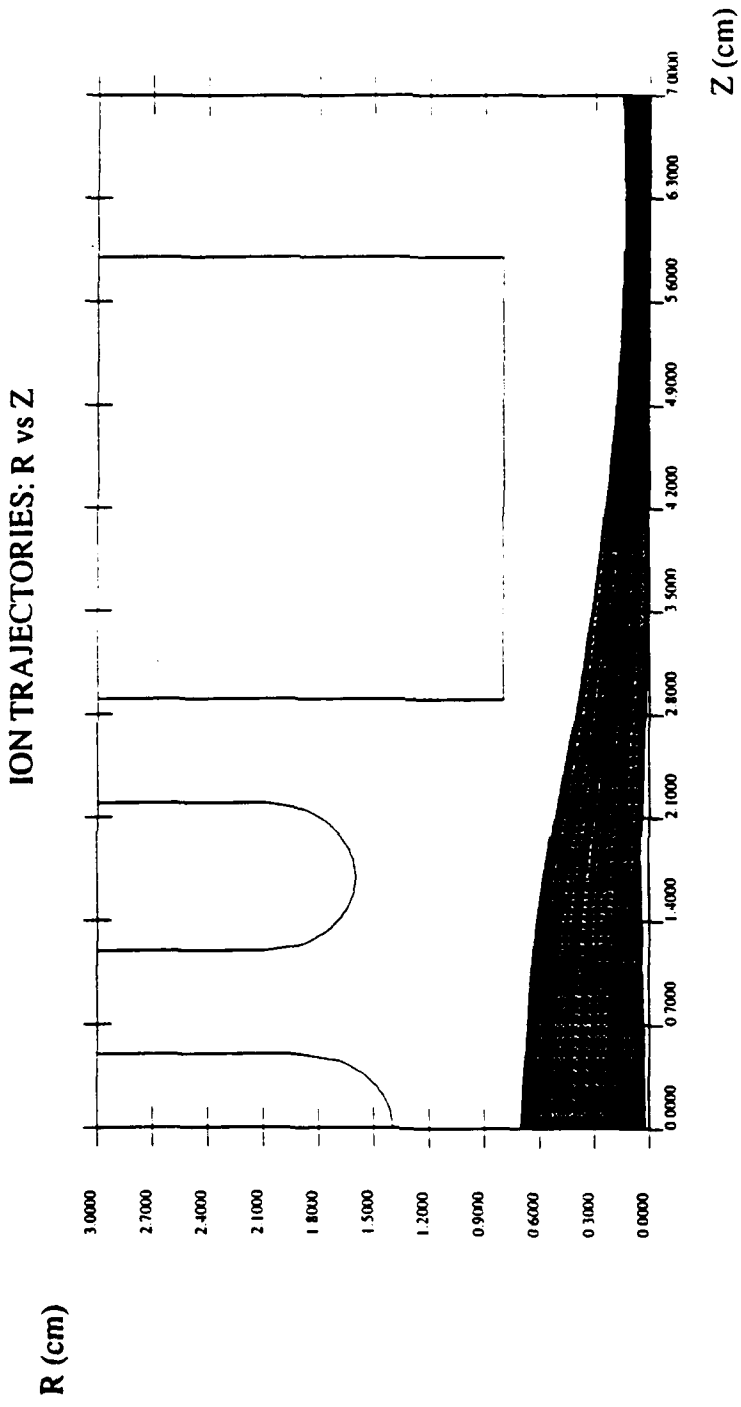

Figure 1(a). Trajectory of the beam particles through the single-stage einzel lens between the ESQ LEBT and the RFQ;

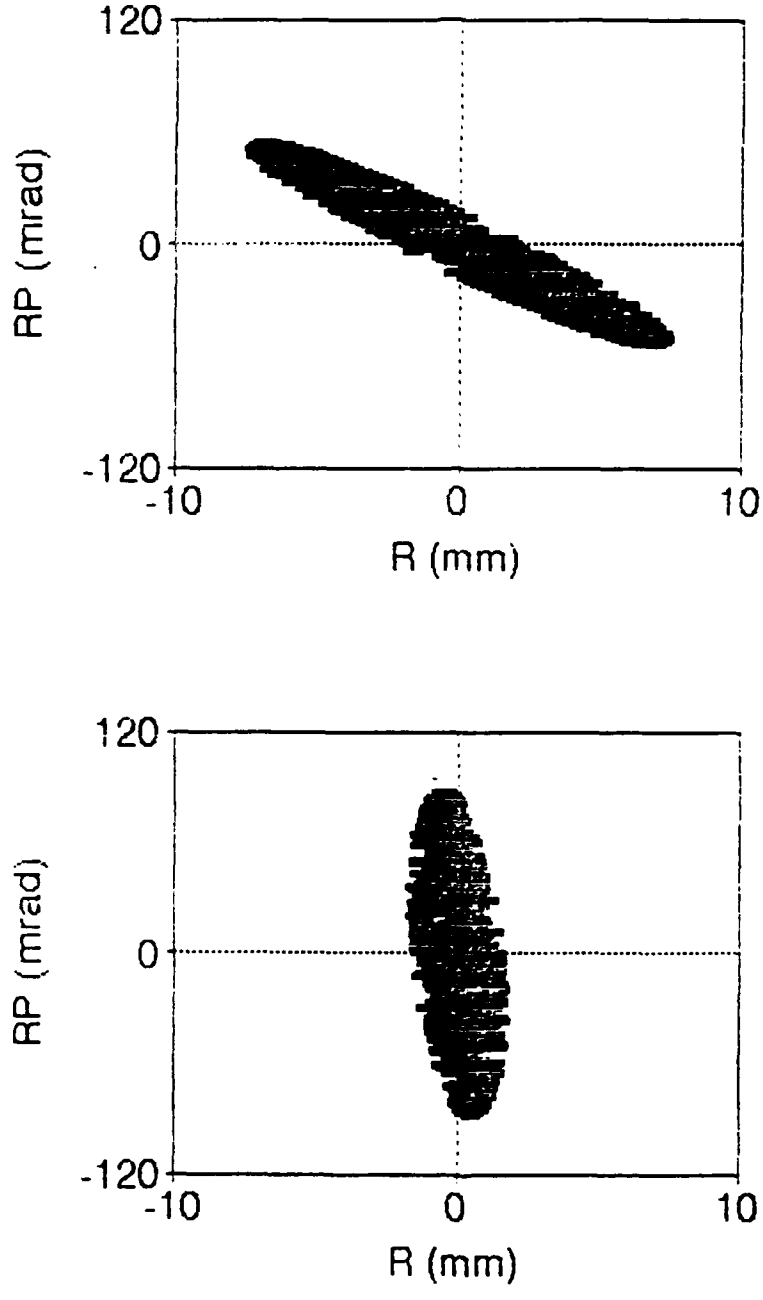

Figure 1(b). SNOW-2D results of the particle distribution: input beam (top), output beam (bottom).

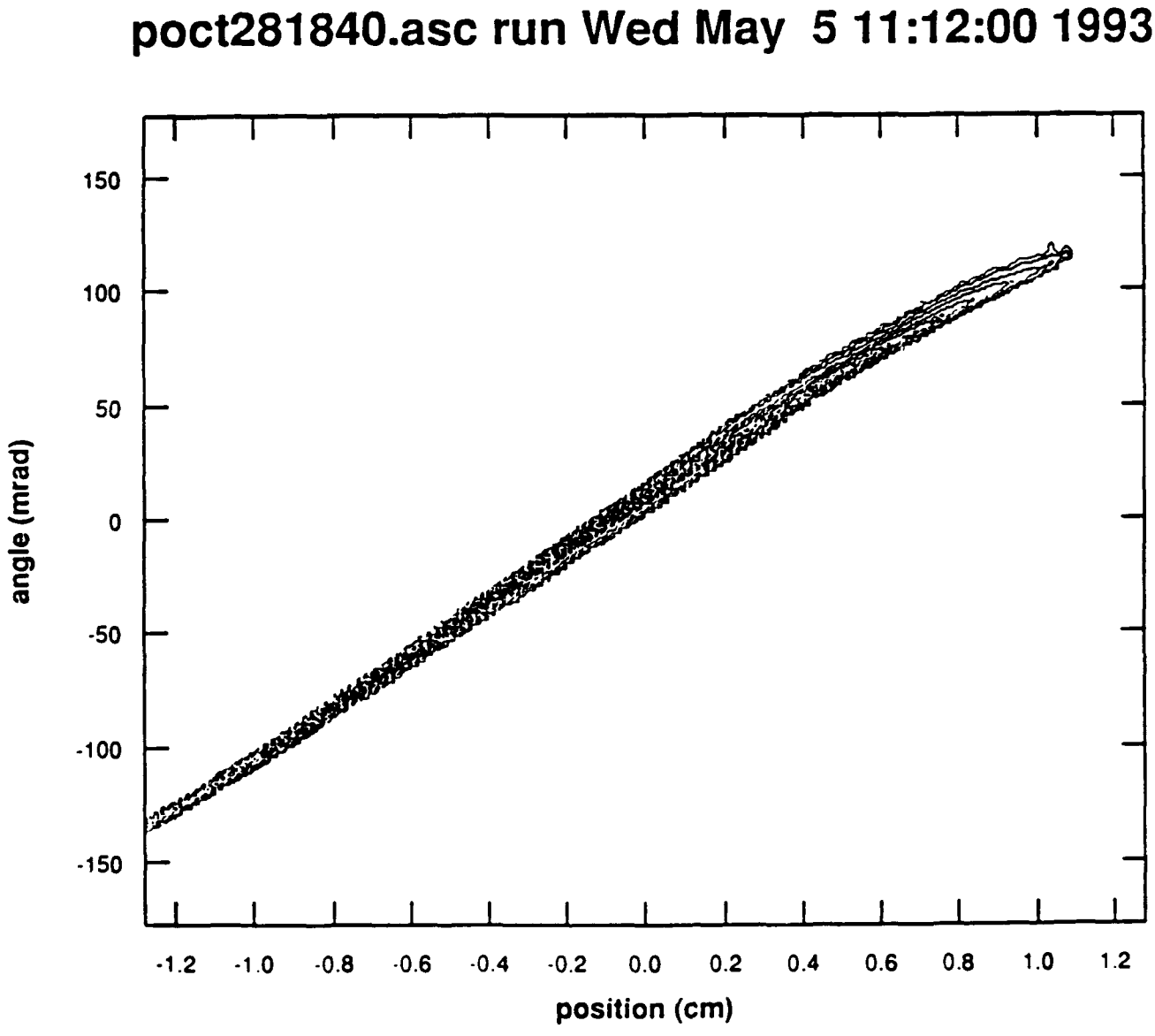

Figure 2. Contour plots of the beam from the SSC volume source at a distance of 10 cm downstream from the extractor.

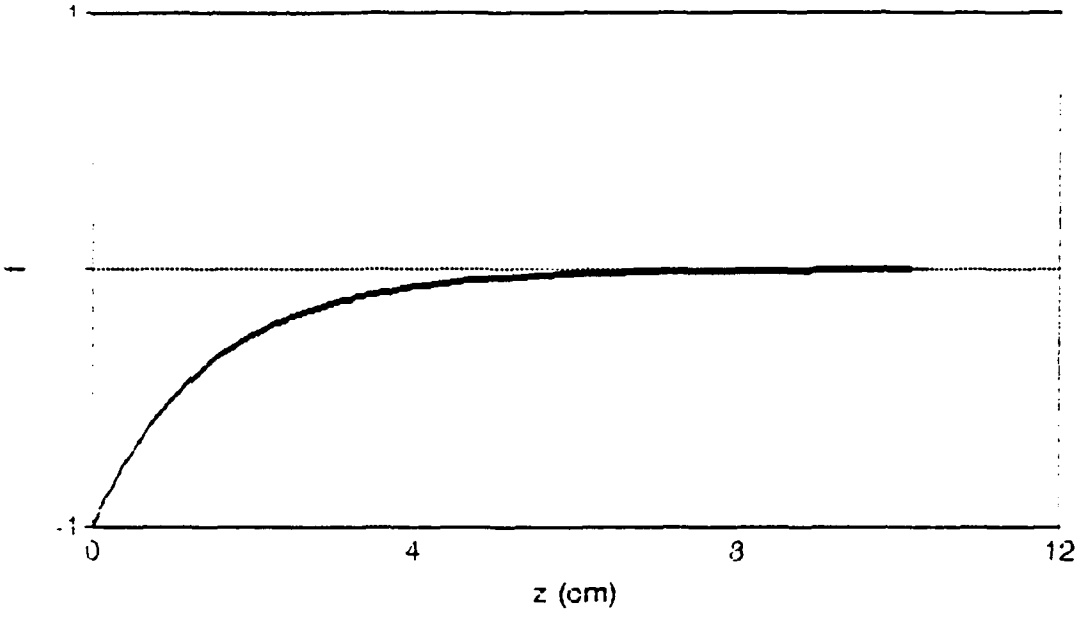

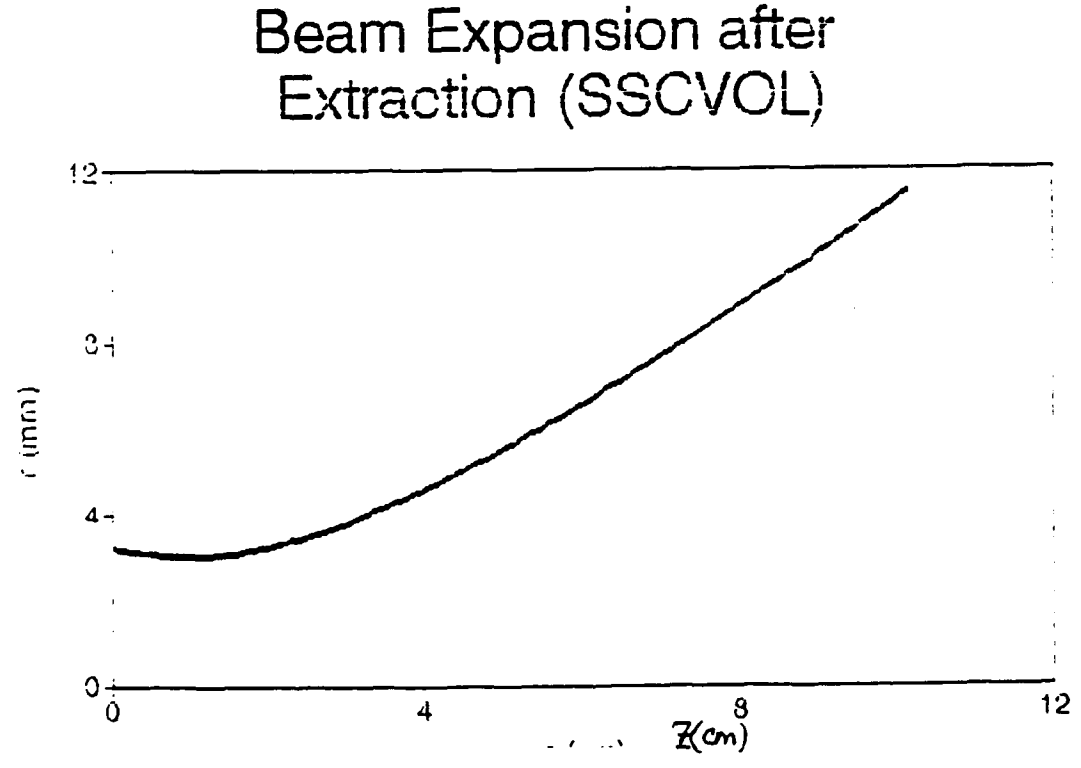

Figure 3. Estimation of beam characteristics at the extractor.

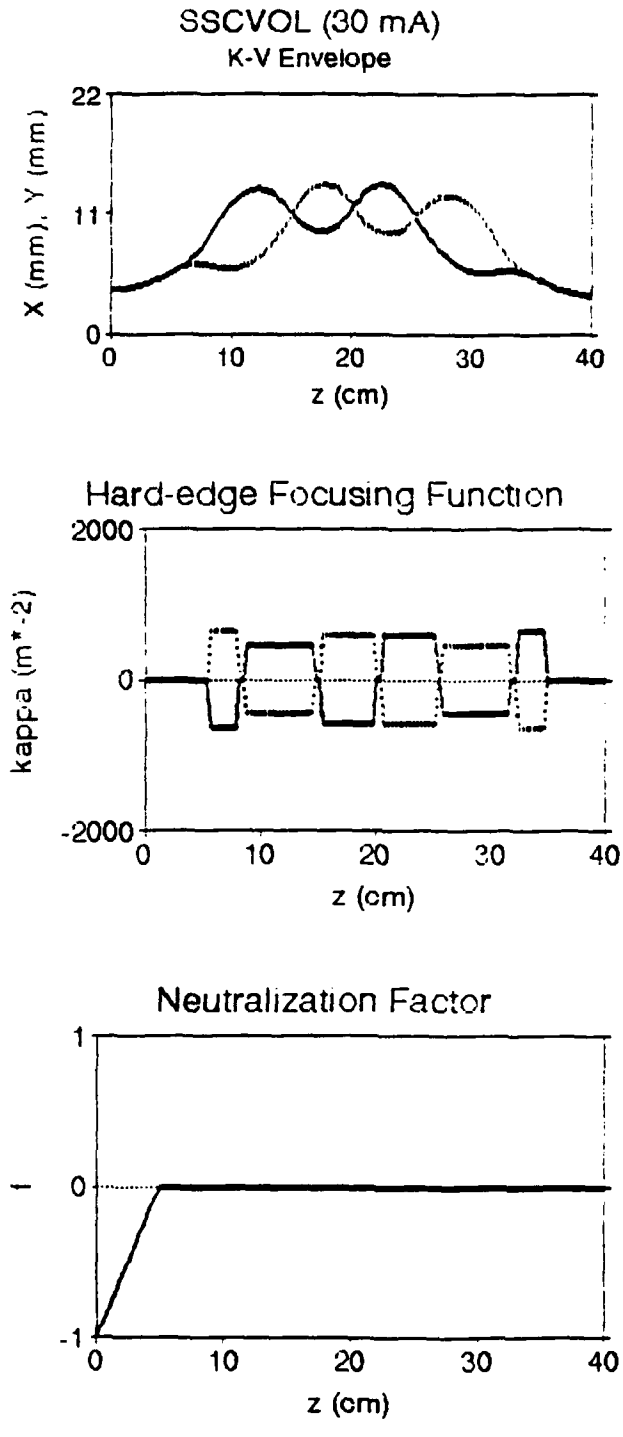

Figure 4. K-V envelope solution for an H^- beam from the volume source.

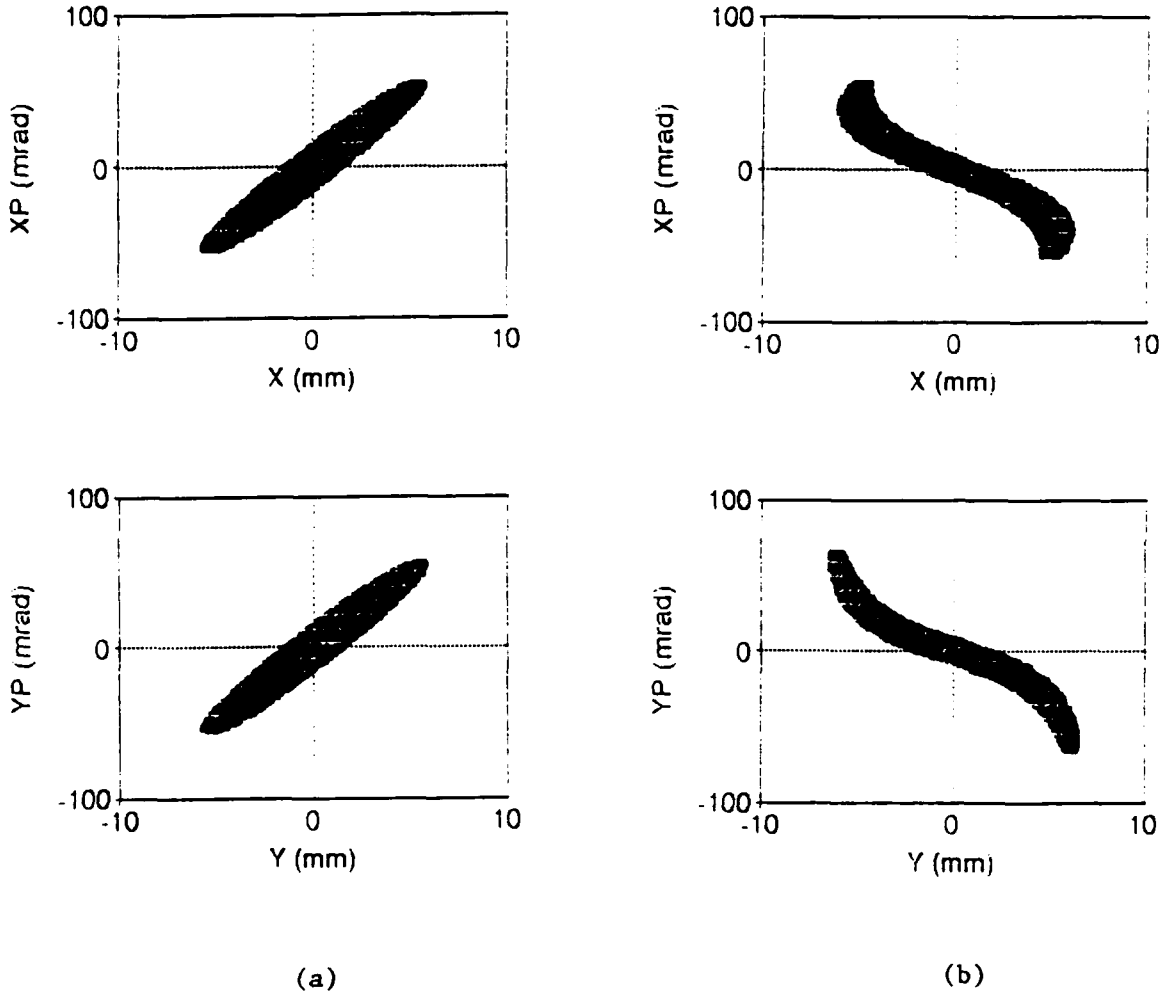

Figure 5. (a) Particle distribution at the input of the ESQ LEBT; (b) particle distribution at the output of the ESQ LEBT.

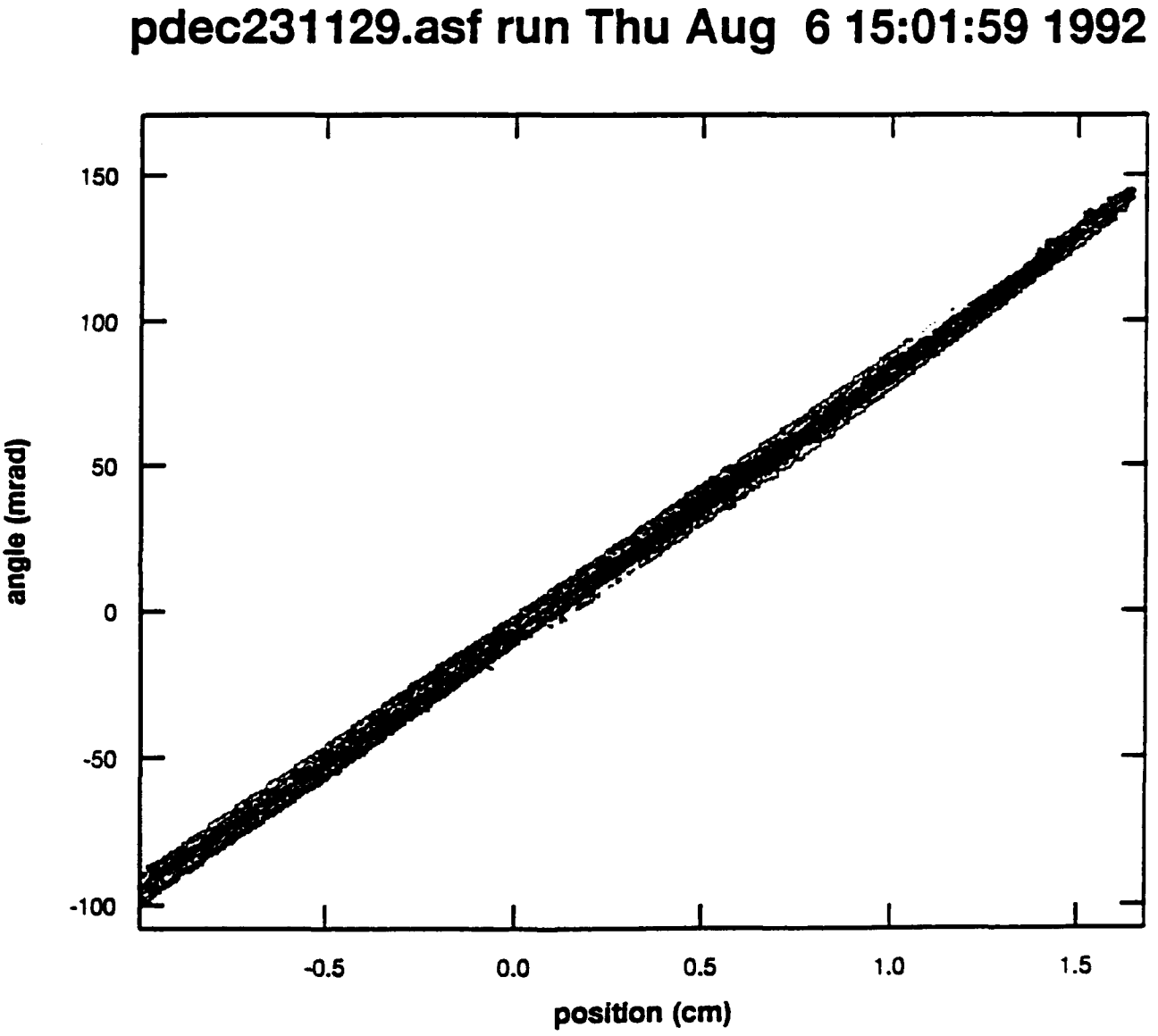

Figure 6. Contour plots of the beam from the SSC magnetron source.

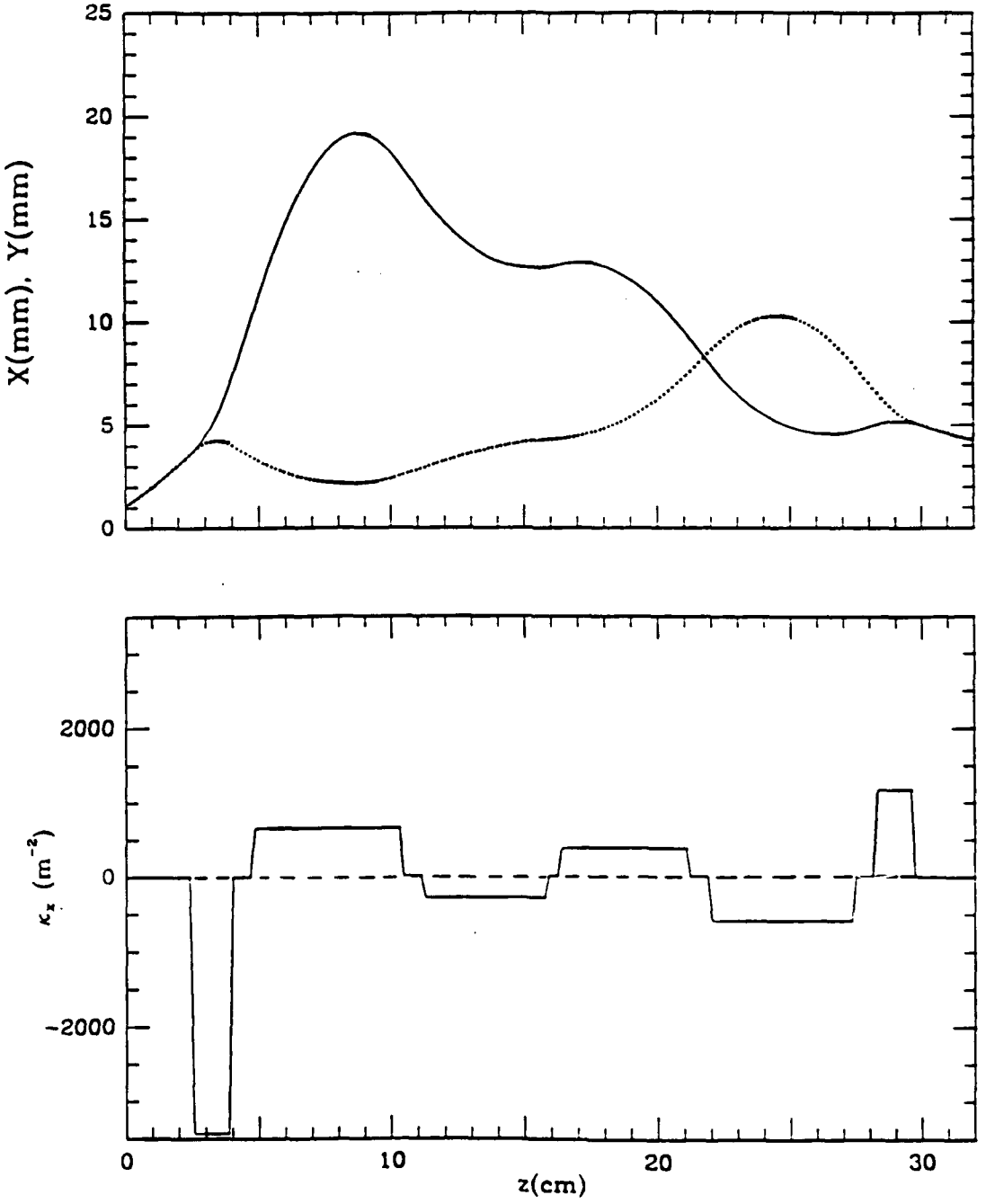

Figure 7. K-V envelope solution for an H^- beam from the magnetron source.

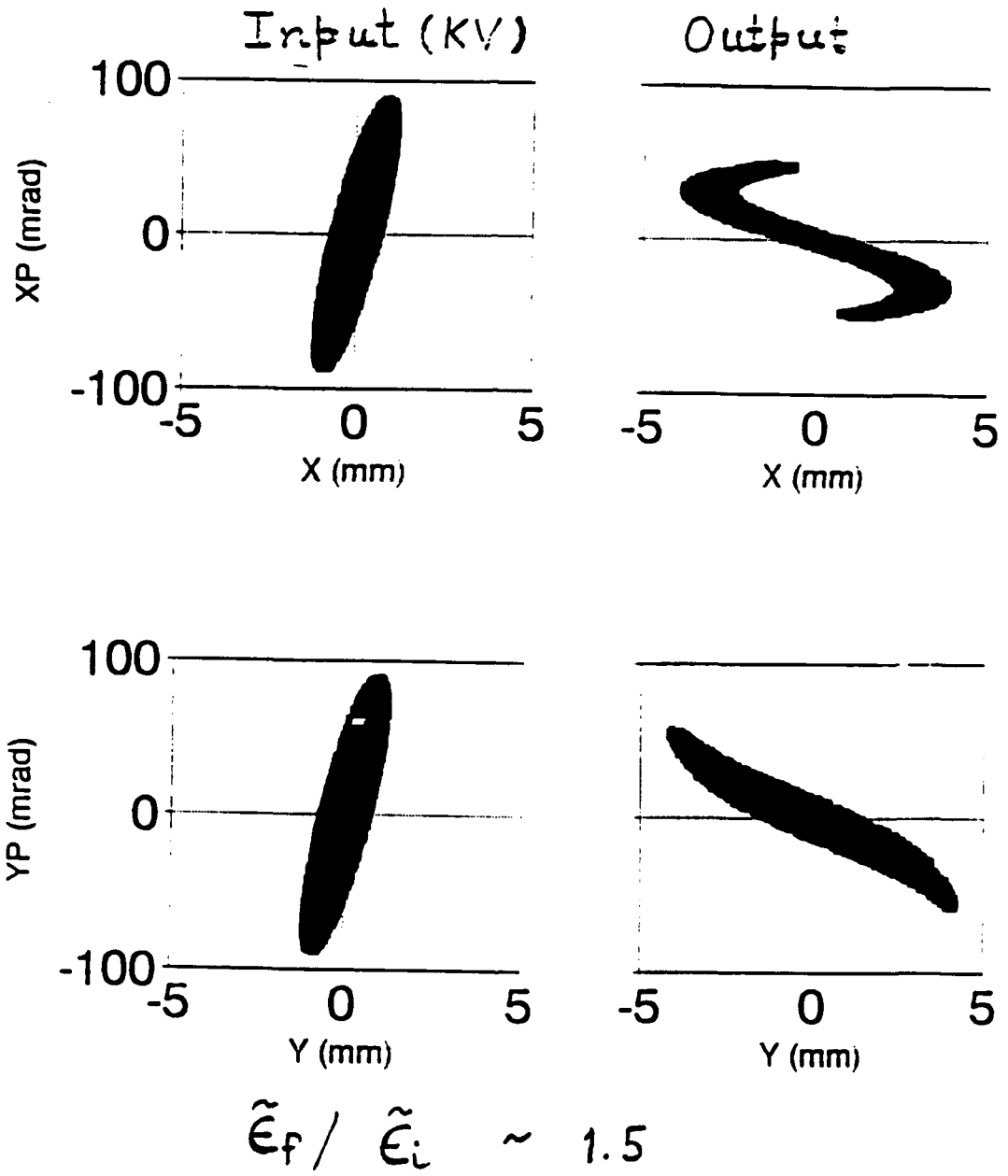

Figure 8. Particle distribution from modified PARMILA.

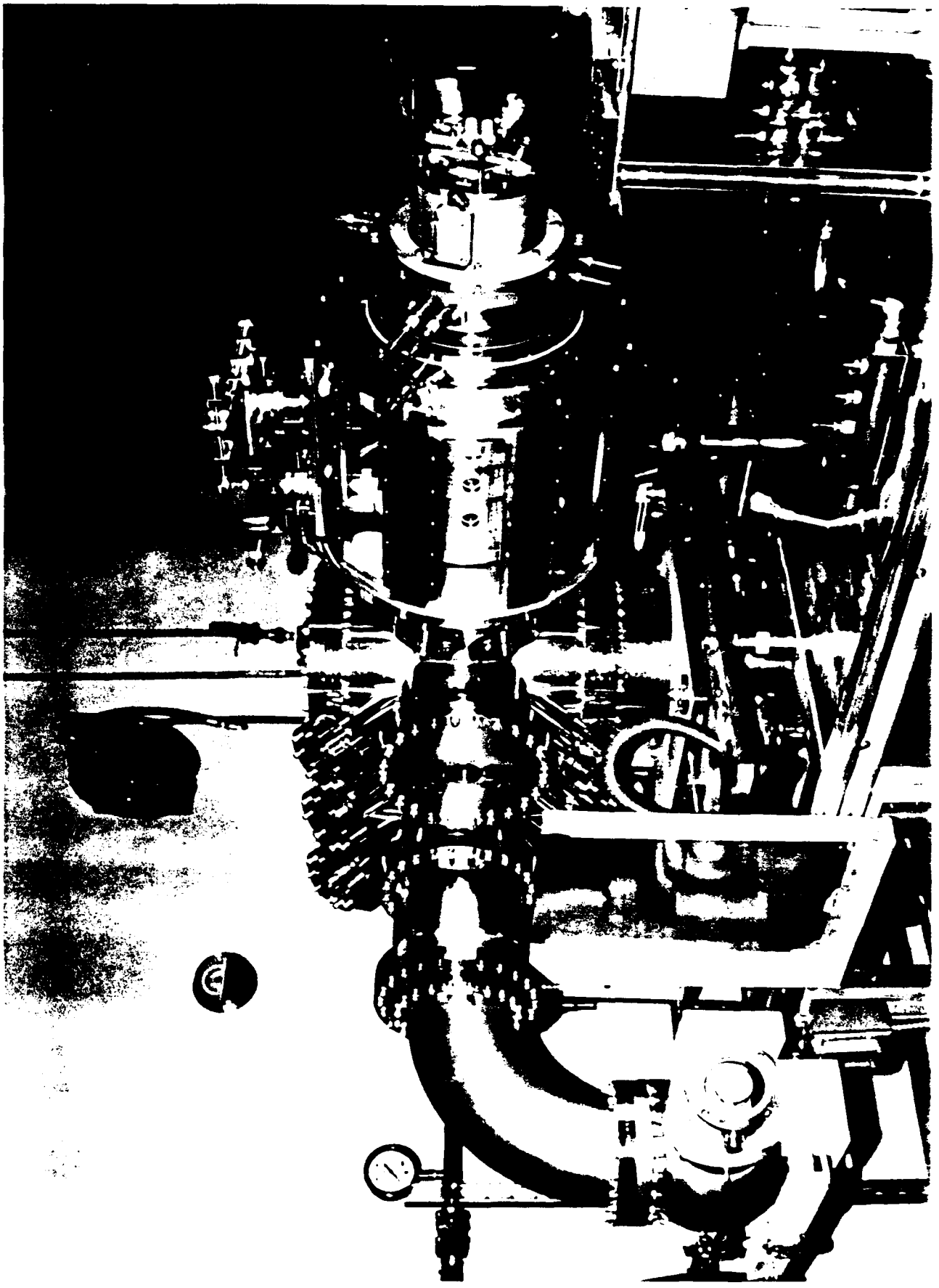

Figure 9. Initial Experimental set-up of the Maryland FSO LEBT system on the SSCL test stand.

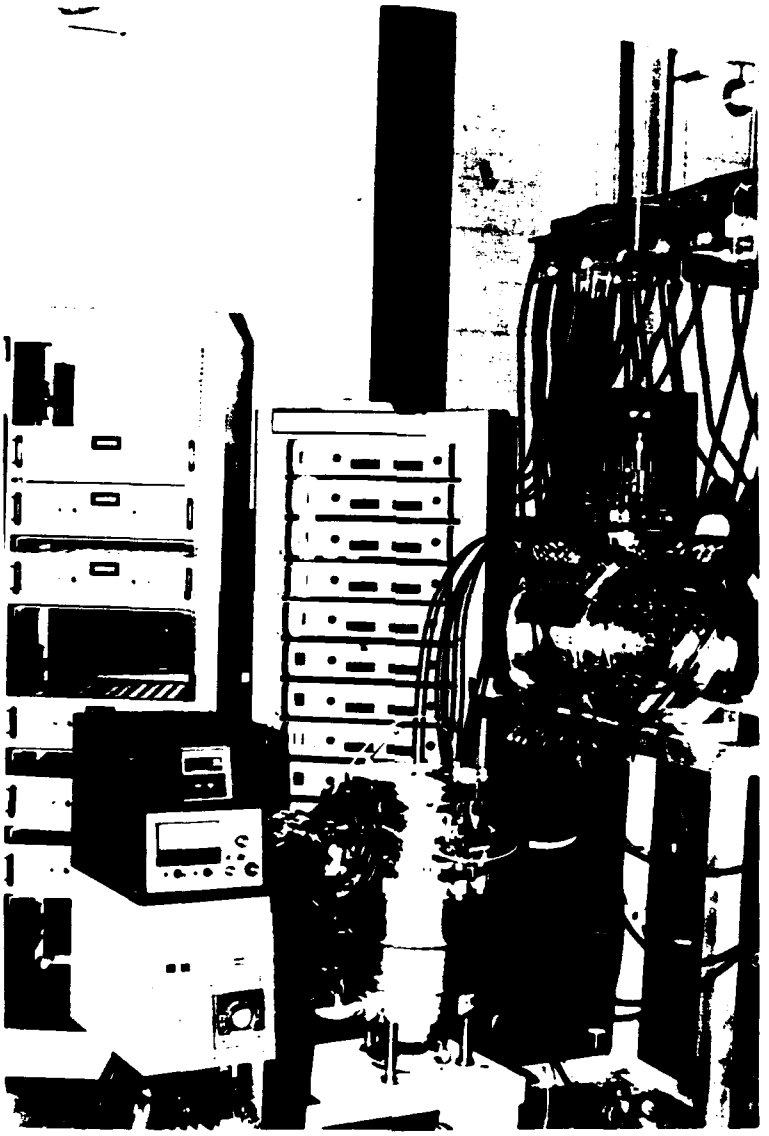

Figure 10. LEBT test facility at Maryland

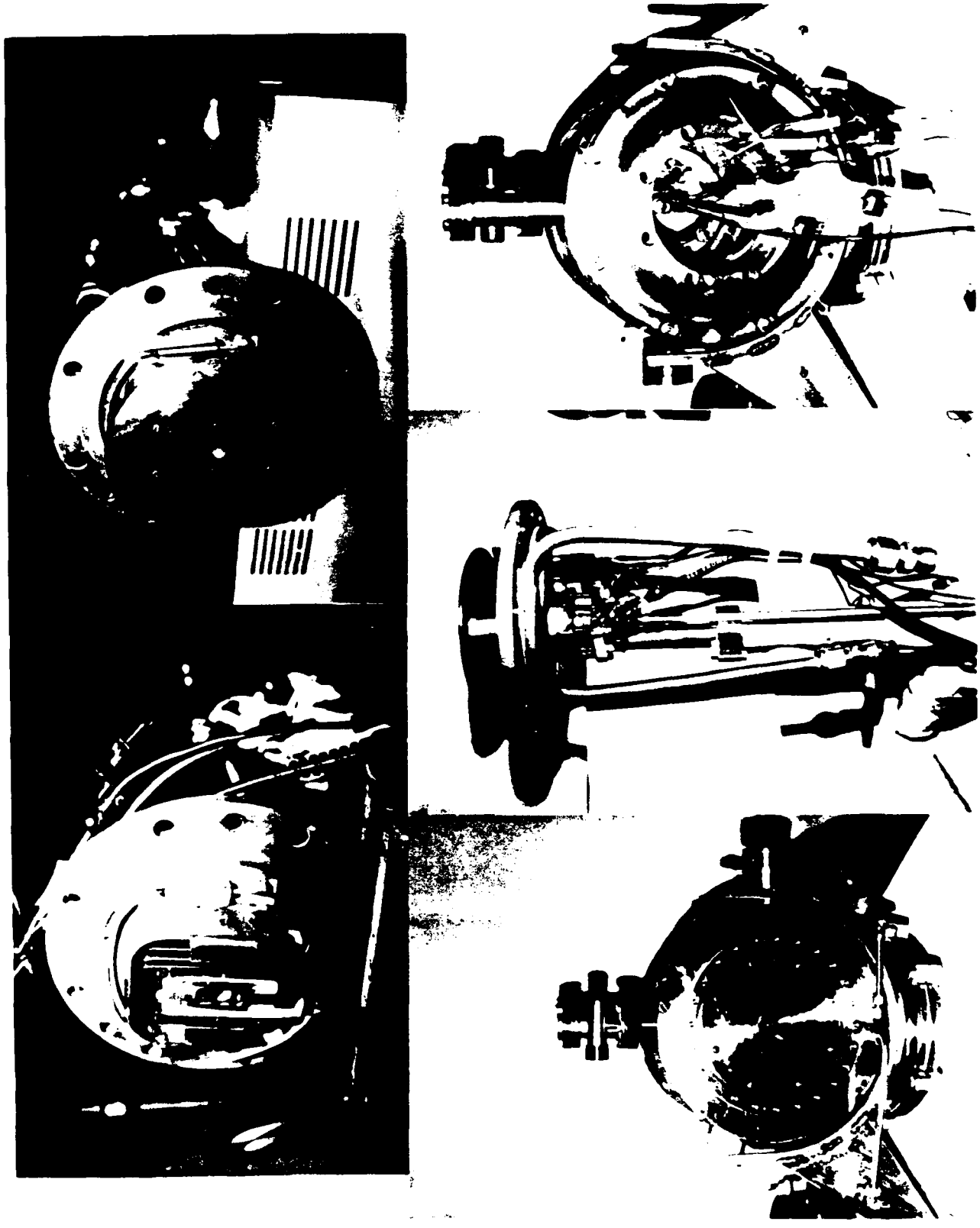

Figure 11. Magnetron source components of the test facility at Maryland.

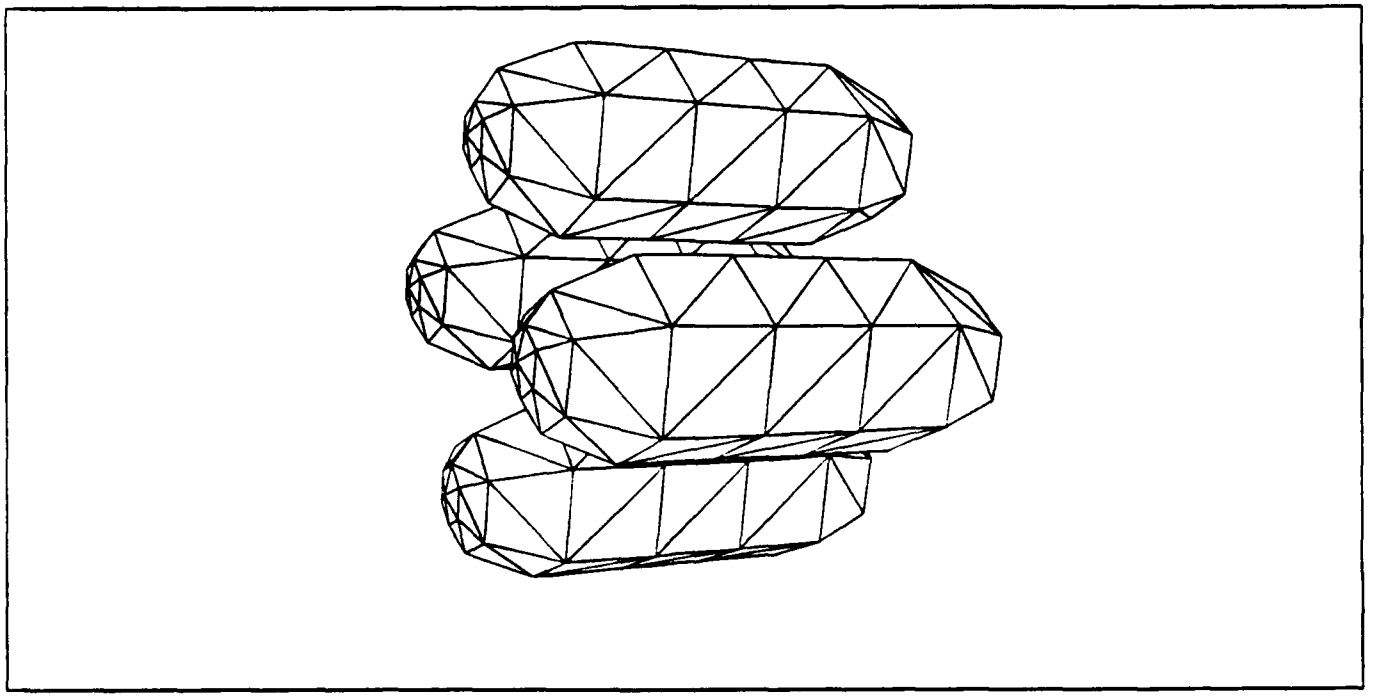

Figure 12: Triangulated ESQ Lens

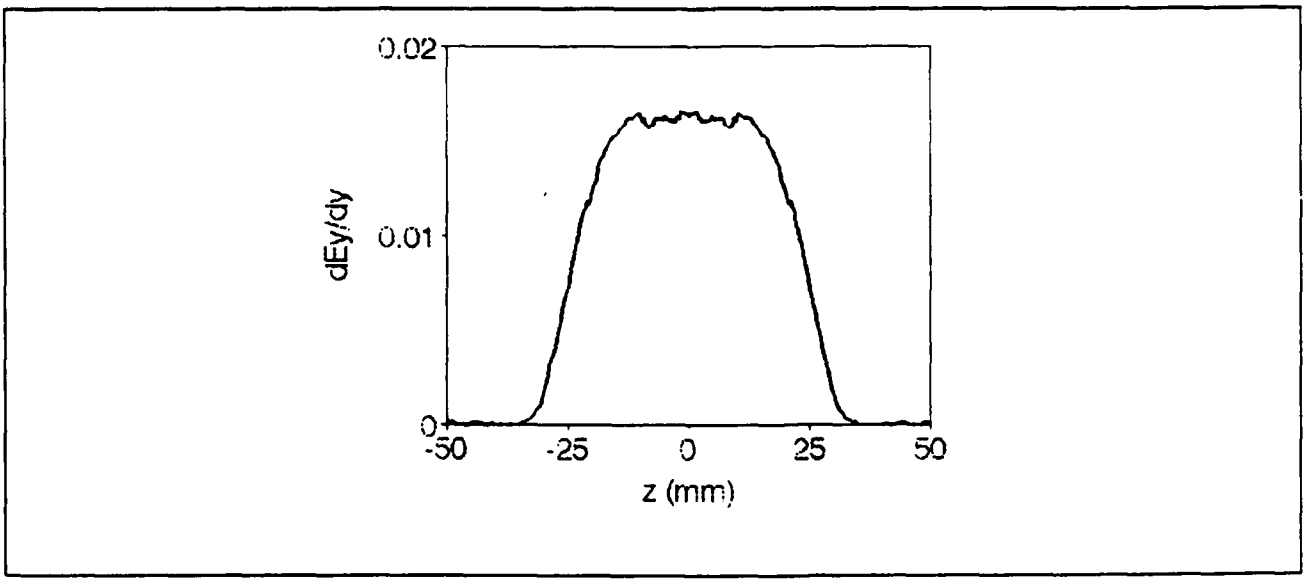

Figure 13: ESQ Lens Focusing Function

STUDY OF BRIGHTNESS AND CURRENT LIMITATIONS IN INTENSE CHARGED PARTICLE BEAMS

M. Reiser and S. Guharay, University of Maryland

PRESENTATIONS, PUBLICATIONS, AND INVITED TALKS

1. S.K. Guharay, C.K. Allen, M. Reiser, K. Saadatmand, and C.R. Chang, "Study of emittance growth and its control for a low-energy H^- beam transport system," AIP Conference Proceedings on Production and Neutralization of Negative Ions and Beams (to be published).

2. S.K. Guharay, C.K. Allen, and M. Reiser, "ESQ focusing for an intense, high-brightness H^- beam: Emittance growth and its remedy," Proceedings of the 9th International Conference on High Power Particle Beams (to be published).

3. C.K. Allen, S.K. Guharay, and M. Reiser, "Solution of LAPLACE's equation by the method of moments with application to charged particle transfers," AIP Conference Proceedings on the Computational Accelerator Physics (to be published).

4. S.K. Guharay, C.K. Allen, M. Reiser, K. Saadatmand, and C.R. Chang, "An ESQ lens system for low energy beam transport experiments on the SSC test stand," Proceedings of the 1993 Particle Accelerator Conference, May 17-20, 1993, Washington, DC (to be published).

5. S.K. Guharay, C.K. Allen, M. Reiser, K. Saadatmand, and C.R. Chang, "A compact ESQ system for transport and focusing of H^- beam from ion source to RFQ," 1992 LINAC Conference Proceedings, vol. 1, p. 338.

6. S.K. Guharay, C.K. Allen, and M. Reiser, "Study of beam dynamics and desing of a low energy beam transport for intense, high-brightness H^- beams," submitted to Nuclear Instruments and Methods in Physics Research.

7. C.K. Allen, S.K. Guharay, and M. Reiser, "A moment method Laplace solver for low energy beam transport codes," Proceedings of Particle Accelerator Conference, Washington, DC (1993) (to appear).

8. S.K. Guharay, C.K. Allen, M. Reiser, "A compact, precision electrostatic quadrupole lens system for high-brightness ion beam transport and focusing," SPIE Conf. on Charged Particle Optics, San Diego, CA, July 15, 1993.

Paper published in AIP Conference Proceedings 287

STUDY OF EMITTANCE GROWTH AND ITS CONTROL FOR A LOW ENERGY H^- BEAM TRANSPORT SYSTEM*

S. K. Guharay, C. K. Allen, M. Reiser
University of Maryland, College Park, MD. 20742
K. Saadatmand, C. R. Chang
Superconducting Super Collider Laboratory, Dallas, Texas 75237

ABSTRACT

A compact 6-lens electrostatic quadrupole lens system in conjunction with a short, single einzel lens section has been developed with the aim of transporting a 30 mA, 35 kV H^- beam (normalized beam brightness of about 10^{11} A/(m-rad)^2) over a length of about 30 cm and focusing it into an RFQ. The effect of a neutral background gas on the measurements of the beam from the ion source is studied in order to evaluate reliably the input beam parameters for the lens design. The beam dynamics calculations have been made using simulation codes for typical H^- beam parameters from two different ion sources: a magnetron type and a volume source type. The simulation results show a relatively modest emittance growth, that is within about 50-60% even in the case of an input beam with very small beam radius (1.1 mm) and very large divergence (72 mrad).

INTRODUCTION

Over the past few years our research has been primarily focused on simulation studies of charged-particle beam dynamics with the aim of developing an efficient low-energy beam transport (LEBT) system for intense, high-brightness H^- beams. While dealing with the problem of design and development of an LEBT, we encountered several problems of practical interest. One of the puzzling issues is related to the assumption of input beam parameters. Often, the beam parameters are measured at a certain distance, typically ~10 cm, downstream from the extraction aperture of the . source. This leads to some uncertainty in predicting beam parameters at the extraction point as this information is required to define the input beam parameters in designing a LEBT. Second, the beam parameters at the extraction aperture depend very much on the mechanism of ion source operation and the extraction optics. It is thus of practical interest to adapt an LEBT scheme which may function reasonably well for a certain range of the input beam parameters. Such a system is less susceptible to failure in the event the source parameters drift to a certain extent; this situation is encountered quite commonly in experiments with ion sources. Third, in the injectors of high-energy accelerators a good buffer space, ~20 - 30 cm, between the ion source and the first stage of acceleration, commonly an RFQ (radio-frequency quadrupole), is desired

*Supported by ONR/SDIO and DoE

as it offers some practical advantages in terms of clean operation of the RFQ and flexibility in achieving satisfactory transformation of beam parameters.

The present article addresses the aforementioned problems when widely different beam parameters are used as input conditions. Special considerations are given to meet the matching condition dictated by the acceptance ellipse parameters of the RFQ in the Superconducting Super Collider (SSC).[1]

INPUT BEAM PARAMETERS AND THE ROLE OF NEUTRALIZING BACKGROUND

Beam characterization experiments were done on the SSC test stand with H^- beams from both magnetron and volume ion sources. In this article, we will mainly deal with the magnetron beam parameters; some analysis is done using typical beam parameters of the Brookhaven National Laboratory (BNL) volume source. Sadaatmand et al. reported some recent results on the characteristics of H^- beams from the SSCL volume source[2]; we plan to use these results in the future to study beam dynamics in the context of our LEBT system.

Figure 1 shows the phase-space distribution of the beam particles, when the emittance scanner slit was located at 11.75 cm downstream from the extraction slit of the source. Using the best fit to the data by an ellipse, the Twiss parameters were determined. The values of the beam size in the two orthogonal directions (X and Y) and the respective slopes (X' and Y') were obtained as: X = 14.5 mm, X' = 132.2 mrad; Y = 18.9 mm, Y' = 175.4 mrad. In order to estimate the beam parameters at the extraction slit, a linear beam optics code is used. This code takes the above values of the beam parameters at z = 11.75 cm as input, and it integrates the Kapchinskij-Vladimirskij (K-V) envelope equations backwards towards the extraction aperture. The background gas may have an important role in this analysis, particularly in relation to the evaluation of the space-charge neutralization factor f_N which enters in the calculation of the space-charge force. Various spatial profiles of f_N have been considered: the results are rather insensitive to the variation of f_N . We have shown two cases in Fig. 2: (a) $f_N = 0$, and (b) $f_N = 1.0$ at the extraction aperture and it falls off exponentially afterwards. From this analysis we predict a beam radius of 1.1 mm and slope of 72 mrad at the extraction slit.

In order to further understand the role of a neutralizing background on measurements of the spatial evolution of beam parameters, we studied three cases of practical relevance: (a) a 30 mA, 35 kV beam with a beam radius of 1.1 mm and beam divergence of 72 mrad, representing a magnetron source as described above, (b) a 30 mA, 35 kV beam with a beam radius of 5.6 mm and near-parallel extraction, representing a BNL volume source,[3] and (c) for higher current - 120 mA, 30 kV beam with a beam radius of 2 mm and near-parallel extraction. The effective emittance values in the three cases are almost similar, the range being $5.0 - 6.6 \times 10^{-5}$ m-rad. Figure 3 shows the spatial evolution of the beam envelopes when several different values of the space-charge neutralization factor (f_N = 0,

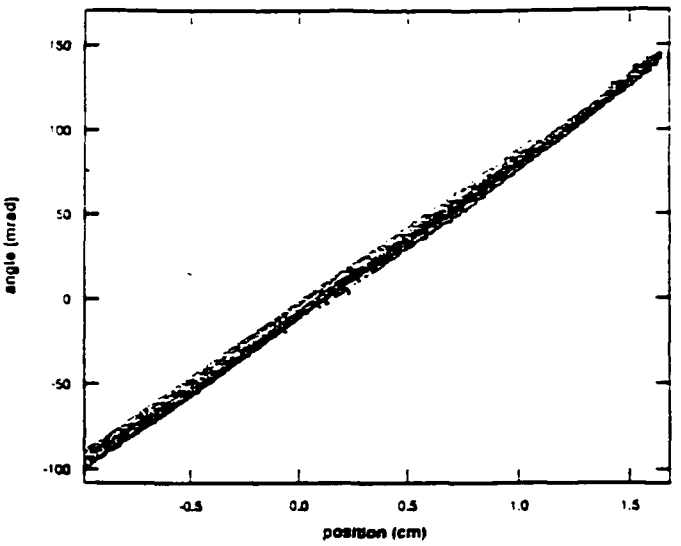

Figure 1: Phase-space distribution of H^- beam from the SSCL magnetron source. The measurements were made at 11.75 cm downstream from the extraction aperture.

0.5, 1.0, and 1.04) were assumed. As a typical example, f_N is taken constant, C, up to $z = 10$ cm, and then it linearly drops to zero at $z = 15$ cm. The results suggest that the space-charge neutralization factor significantly changes the beam envelope for the cases (b) and (c), and that the effect is not as strong in the case (a). Comparing the various terms in the K-V envelope equations, we note that the ratio of the space charge force to the emittance force, Ka^2/ϵ^2, is initially (at $z = 0$) much larger than 1 in the cases (b) and (c); while this ratio is close to 1 in the case (a). ($K = 2I_b/I_0\beta^3\gamma^3$ is the generalized beam perveance, I_b is the beam current, I_0 is the characteristic current (3.1×10^7 A for H^- beam), $\beta = v/c$, $\gamma = (1 - \beta^2)^{-1/2}$, a is the initial beam radius, and ϵ is the effective beam emittance.) In the cases where the space-charge force is the most dominant factor, it may be postulated that the aforementioned method to estimate initial beam parameters may introduce some ambiguity, unless a good understanding of the gas dynamics is achieved and is incorporated properly in the analysis.

SIMULATION OF BEAM DYNAMICS THROUGH A LEBT SYSTEM

(a) H^- Beam from the SSC Magnetron Source

A proto-type ESQ LEBT system has been developed in-house at Maryland, and the system has been described in detail elsewhere.[4] Figure 4 shows the geometry of the LEBT system. In a previous article,[5] we reported that the aperture of the lenses in the proto-type ESQ LEBT system needs to be increased by a factor of two to accommodate the large excursion of the SSC magnetron H^- beam. Further details of the beam dynamics are presented here, where the ESQ lens

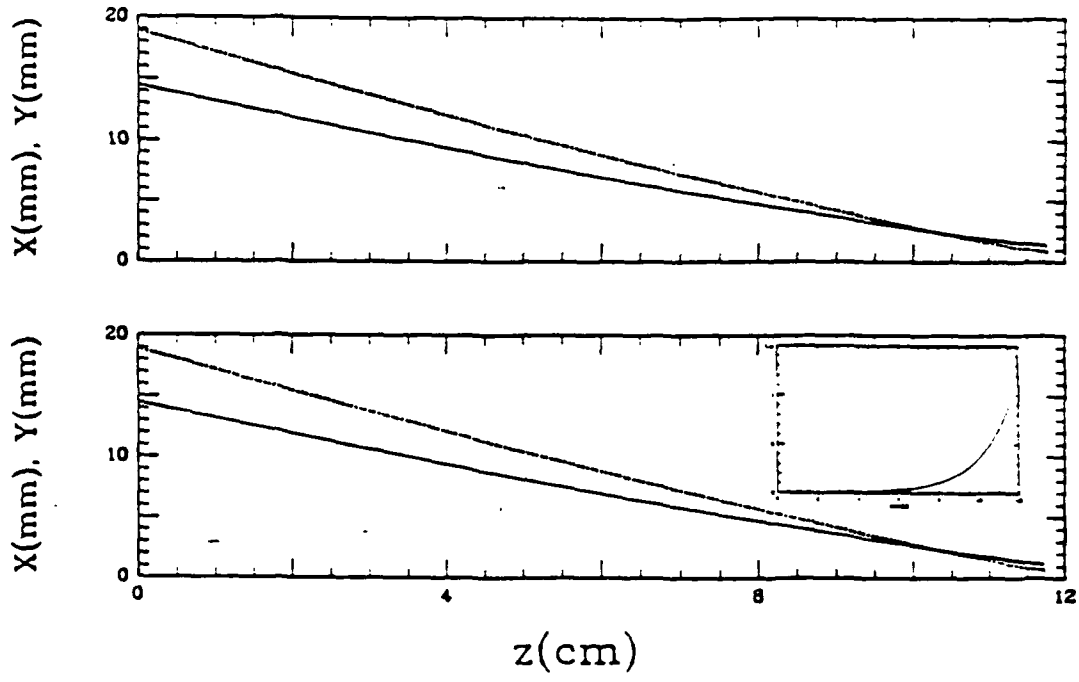

Figure 2: K-V envelope solution for H^- beam propagating over the drift space between the extraction aperture of the magnetron source and the slit of the emittance diagnostic. Here $z = 0$ is considered as the location of the slit of the emittance diagnostic; the beam envelope is calculated backward toward the extraction slit which is here at $z = 11.75$ cm. Space-charge neutralization factor, f_N, is taken as: (a) zero (upper figure), and (b) exponentially falling with the peak value as 1.0 at $z = 11.75$ cm (lower figure). The inset in the lower figure shows the spatial profile of f_N.

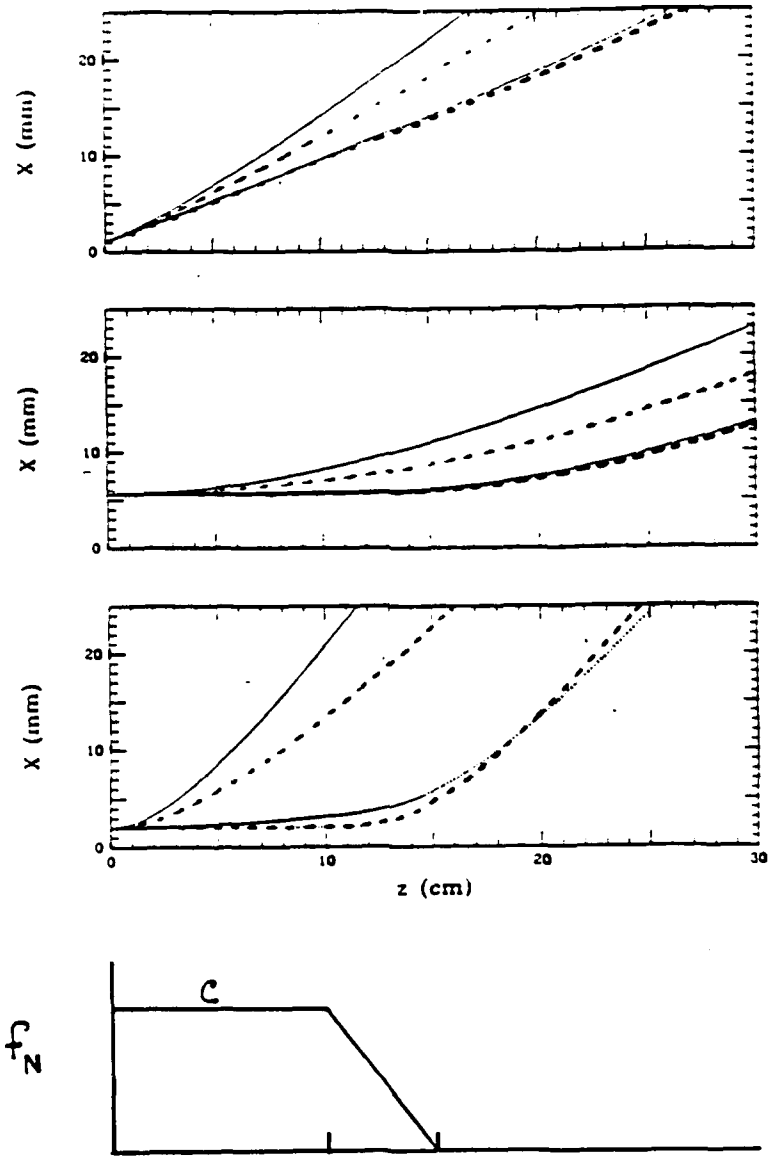

Figure 3: Spatial evolution of the beam envelope for three different cases: (a) beam current I = 30 mA, beam voltage V = 35 kV, initial beam radius a = 1.1 mm, initial beam divergence $r'|_{r=a}$ = 72 mrad; (b) I_b and V_b are same as in (a), a = 5.6 mm, $r'|_{r=a}$ = 0; (c) I_b = 120 mA, V_b = 30 kV, a = 2.0 mm, $r'|_{r=a}$ = 0. The bottom figure shows the nature of the assumed space-charge neutralization factor f_N. The four different curves in each figure correspond to different values of the constant C. Going from the leftmost side of each figure, solid line: C = 0, next dashed line: C = 0.5, dotted line: C = 1.0, next dashed line: C = 1.04.

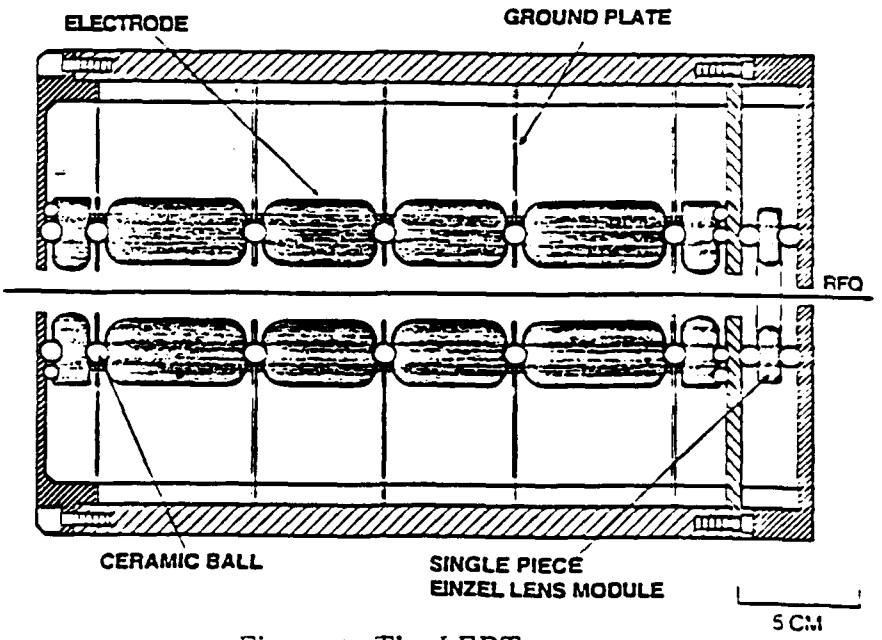

Figure 4: The LEBT system.

parameters, especially the voltages, are further optimized and also the design of the end section of the LEBT consisting of a short einzel lens is further developed.

Figure 5 shows the most optimized envelope solution that we have obtained until now after a number of iterations of our numerical scheme.[6] The maximum beam excursion in one plane (about 17 mm) is found significantly larger than in the other orthogonal plane (about 10 mm). Initially we obtained an envelope solution with symmetric beam excursions in both X and Y-planes; however, the emittance growth was higher in this situation. This is an artifact of nonlinear beam dynamics. As a rule of thumb, nonlinear effects, which contribute to the distortion of the beam optics and thus enhance the beam emittance, are not important if the beam does not occupy more than about 75% of the quadrupole aperture. Hence it is clear from Fig. 5 that the emittance growth should primarily occur in the X-plane. The phase-space distribution of the particles, obtained from the modified PARMILA code (a $2\frac{1}{2}$-D code) is shown in Fig. 6; the results conform to the physical picture revealed in Fig. 5. Here a beam current of about 25 mA is transported. The remaining part of the 30 mA input beam current contributes enormously (more than 300%) to the emittance growth. This group of particles, which behaves like a "halo" and occupies a large phase-space boundary, is eliminated by a beam scraper. The emittance growth for about 25 mA of beam current is estimated to be about 50% assuming a K-V type distribution of the input beam (Fig. 6); the estimated emittance growth is about 60% for a Gaussian input beam as shown in Fig. 7.

From the modified PARMILA results shown in Fig. 6 it is estimated that the output beam parameters at 6 mm downstream from the last lens of the ESQ LEBT

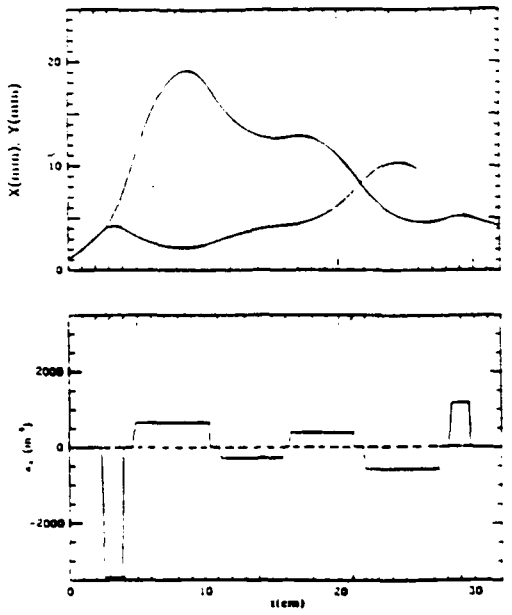

Figure 5: Envelope solution for the ESQ LEBT section using SSCL magnetron beam parameters. A hard-edge type external focusing function $\kappa(z)$, as shown in the bottom figure, is assumed.

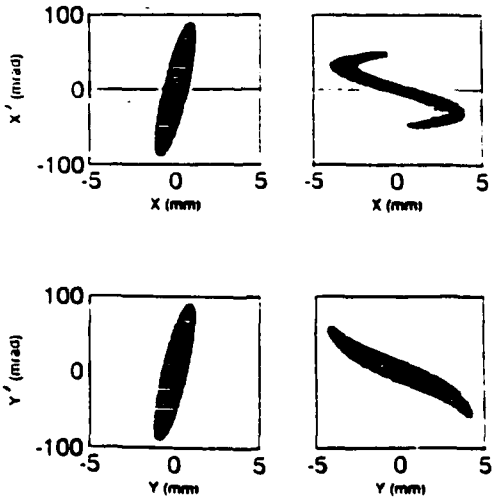

Figure 6: Modified PARMILA results on phase-space distribution of particles through the ESQ LEBT section (magnetron beam case). Left-side figure: input beam distribution (K-V type); right-side figure: output beam.

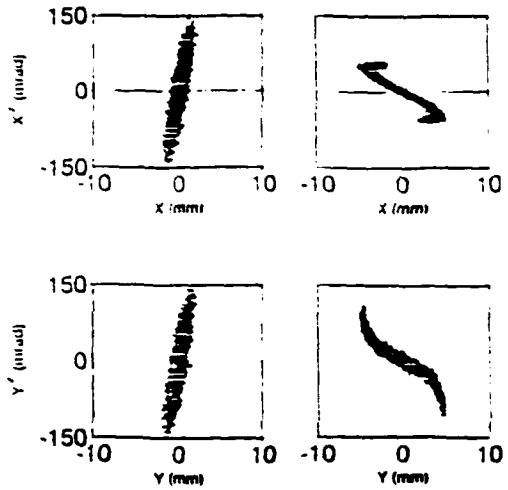

Figure 7: Modified PARMILA results for the same case as in Fig. 6 using a Gaussian input beam distribution.

are: $X = 4.68$ mm, $Y = 4.38$ mm, $X' = -49$ mrad, and $Y' = -48$ mrad. This beam is given as input to a short, single einzel lens section cascaded to the ESQ LEBT. The einzel lens is composed of three electrodes as shown in Fig. 8 (top figure) – the first and the third electrodes are at ground potential, and the center electrode is at a high negative potential close to the beam voltage. In our experimental configuration, the two grounded electrodes of the einzel lens are made as common elements, respectively, with the last shunt plate of the ESQ LEBT and the front wall of the RFQ. The output from the einzel lens is determined using the SNOW-2D code. The output beam distribution in Fig. 8 shows the results at a downstream location of 1.0 cm from the front of the RFQ's ground wall: an effective ellipse representing the output beam in Fig. 6 is given as input here. The beam parameters at this location match well with the acceptance ellipse of the RFQ. However, if the input vane of the RFQ is located further away, the lens parameters need to be adjusted. It may be noted that the einzel lens section does not introduce any emittance growth. Hence the overall emittance growth in the entire LEBT channel is about 50%.

(b) H^- Beam from a Volume Source

The beam parameters of BNL volume source[3] are used in this case. The prototype ESQ LEBT system developed at Maryland is well suited to transport such beams. Figure 9 shows the K-V envelope solution; we have aimed here to obtain a beam convergence of about -20 mrad at the output as the final focusing will be done by an einzel lens.

The phase-space distribution of particles in the input and output beams for the ESQ LEBT section is shown in Fig. 10. The output beam is almost free from

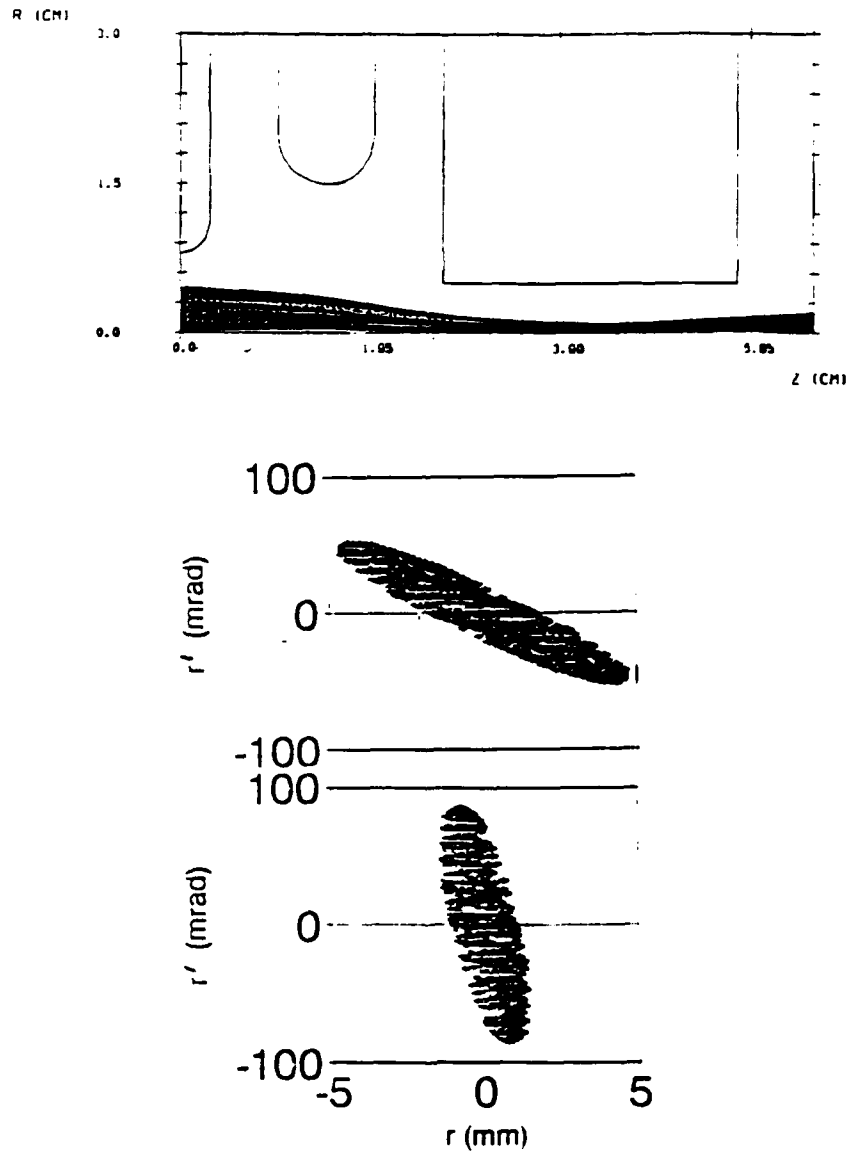

Figure 8: SNOW-2D results for the einzel lens section using the output beam from the ESQ LEBT (magnetron case). Top figure: beam envelope through the lens. Middle figure: phase-space plot of the input beam. Bottom figure: phase-space plot of the output beam.

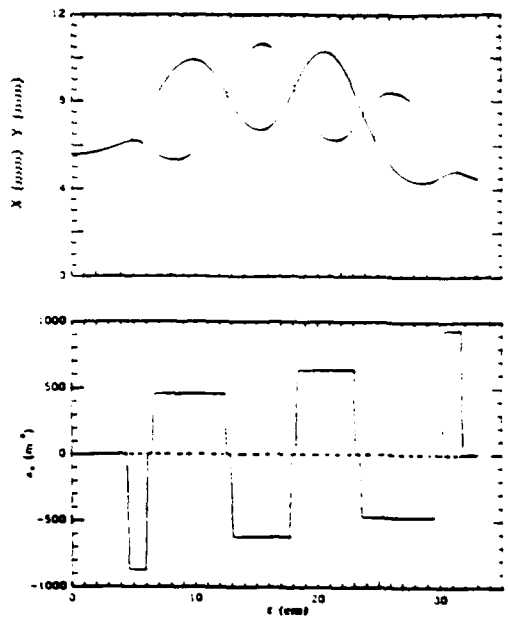

Figure 9: Envelope solution for the ESQ LEBT section using volume source parameters.

distortions, and the emittance growth is insignificant. The SNOW-2D code results showing the behavior of the beam particles as they move from the end of the ESQ LEBT section and are being focused by the einzel lens, are shown in Fig. 11. The output beam distribution is taken here at a distance of 1.0 cm downstream from the front end of the third electrode (at ground potential) in the einzel lens; the third electrode should be considered as the front wall of the RFQ in reality. The emittance growth in the entire LEBT channel is very small, <15%, here.

CONCLUSIONS

One of the major points in this article is the simulation analysis to estimate beam parameters at the extraction aperture from the measured data at a certain distance away, typically about 10 cm downstream. It is noted that an uncertainty in the analysis generally occurs due to the lack of precise knowledge about the neutralizing gas background. The importance of this issue depends significantly on the initial conditions of the beam, primarily the ratio of Ka^2/ϵ^2. For $Ka^2/\epsilon^2 \sim 1$ close to the extraction aperture, as in the case of the SSC magnetron beam, the spatial evolution of the beam envelope over a distance of about 10 cm is quite insensitive to the variation of the space-charge neutralization factor, f_N. The beam envelope is found to be significantly affected by the variation of f_N for $Ka^2/\epsilon^2 \gg 1$; examples are given for a 30 mA volume source beam and a situation with large beam current (120 mA).

The beam dynamics through a LEBT system, comprising of 6-ESQ lenses and one einzel lens, have been studied in detail using simulation codes. The

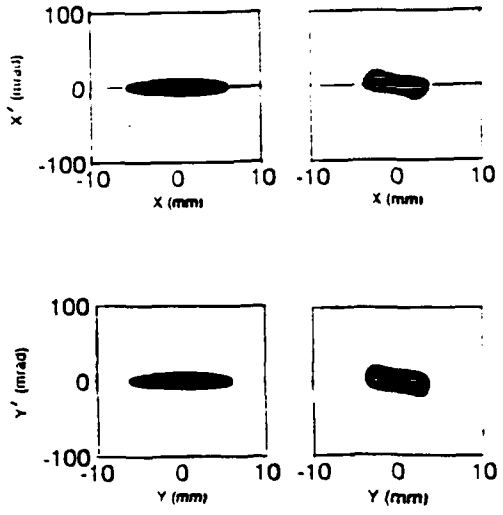

Figure 10: Modified PARMILA results on phase-space distribution of particles through the ESQ LEBT section (volume source case). Left-side figure: input beam distribution (K-V type); right-side figure: output beam.

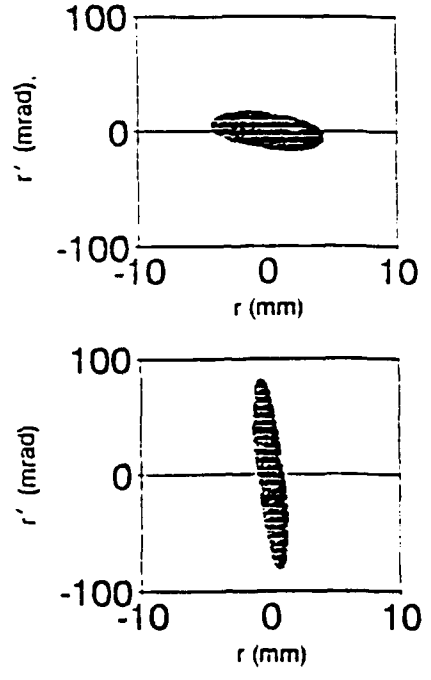

Figure 11: SNOW-2D results for the einzel lens section using the output beam from the ESQ LEBT (volume source case). Top figure: phase-space plot of the input beam. Bottom figure: phase-space plot of the output beam.

analyses have been done using two widely different input beam parameters, and the LEBT systems have been designed accordingly. The present LEBT system is very compact, and it has a good tunability to control the emittance growth. In the case of a 30 mA, 35 kV SSC magnetron beam when the input beam radius is taken as 1.1 mm and the beam divergence is 72 mrad, the beam into the RFQ has an emittance growth of about 50 to 60%. Here a scraper in the ESQ LEBT system is used to deliver 25 mA of output beam current, which appears to be the nominal SSC injector beam current. This part of the beam conforms to a good core geometry, and hence it suffers less due to aberrations. While dealing with a larger beam (5.6 mm in radius and near-parallel extraction) corresponding to the BNL volume source case, the LEBT system is shown to behave very nicely, and the full beam (30 mA) can be matched into the RFQ with practically no emittance growth.

The present LEBT system has several strong features. The transport section of about 30 cm length creates a good buffer space between the ion source and the RFQ. It thus insures a clean operation of the RFQ. Several tuning knobs allow us to handle some variation of the input beam characteristics and maintain an acceptable level of emittance growth. Anderson et al.[7] reported intriguing experimental results with similar LEBT systems based on a combination of ESQ lenses and one einzel lens (referred as a ring lens in their paper); near-parallel input beams with brightness about an order of magnitude lower than in the presently investigated cases were considered there.

A comment is made in the context of the present experimental effort. The current LEBT system will satisfy the RFQ's matching condition approximately 1 cm downstream from the RFQ aperture. With intense, high-brightness beams the problem of matching will be formidable if the drift space between the end of the LEBT and the RFQ entrance is too large; the emittance growth may need to be sacrificed enormously.

REFERENCES

1. T. S. Bhatia, J. H. Billen, A. Cucchetti, F. W. Guy, G. Neuschaefer, L. M. Young, "Beam Dynamics Design of an RFQ for the SSC Laboratory", Proc. IEEE Particle Accelerator Conf., San Francisco, CA, May 6-9, 1991, p.1884.

2. K. Saadatmand, J. E. Hebert, N. C. Okay, "RF Volume H^- Ion Source for the Superconducting Super Collider", these proceedings.

3. J. G. Alessi, Private communication.

4. S. K. Guharay, C. K. Allen, M. Reiser, V. Yun, "Low Energy H^- Beam Transport Using an Electrostatic Quadrupole Focusing System", Proc. Particle Accelerator Conf., San Francisco, CA, May 6-9, 1991, p. 1961.

5. S. K. Guharay, C. K. Allen, M. Reiser, K. Saadatmand, C. R. Chang, "A Compact ESQ System for Transport and Focusing of H^- Beam from Ion Source to RFQ" Proc. Linear Accelerator Conf., Ottawa, Canada, August 24 - 28, 1992, p. 338.

6. S. K. Guharay, C. K. Allen, M. Reiser, P. G. O'Shea, "Experimental Study of a High-Brightness H^- Beam and Its Transport Through an ESQ Focusing System", Intense Microwave and Particle Beams III, SPIE vol. 1629, 421 (1992); S. K. Guharay, C. K. Allen, M. Reiser, "Electrostatic Focusing and RFQ Matching System for a Low Energy H Beam", Intense Microwave and Particle Beams II, SPIE vol. 1407, 610 (1991).

7. O. A. Anderson, L. Soroka, J. W. Kwan, R. P. Wells, "Application of Electrostatic LEBT to High Energy Accelerators" Proc. 2nd European Particle Accelerator Conf., Nice, June 12-16, 1990.

ESQ FOCUSING FOR AN INTENSE, HIGH-BRIGHTNESS H⁻ BEAM: EMITTANCE GROWTH AND ITS REMEDY

S. K. Guharay, C. K. Allen, M. Reiser
University of Maryland, College Park, MD 20742 U.S.A.

Abstract

A simple, novel electrostatic quadrupole (ESQ) lens system has been developed to transport and focus an intense, high-brightness (normalized beam brightness ~ 10^{11} A/m^2 rad^2) H⁻ beam. The physics of emittance growth in the ESQ transport system is studied in detail by computer simulation of beam dynamics, when the influence of various factors, e.g., input beam parameters, aberrations, misalignments, etc. has been examined. Possible methods to control the emittance growth have been suggested.

I. Introduction

Although there has been a significant progress in the physics and technology of high-energy accelerators, many new areas of research are still emerging primarily due to a variety of needs of the new accelerators and its applications, e.g., exploration of fundamental particles, space defense by antiballistic neutral particle beams, radio-active waste transmutation, etc. It is recognized that a very good quality beam, defined by its emittance, is required in a high-energy accelerator. This is particularly true in the case of new accelerators, e.g., the Superconducting Super Collider,[1] where the emittance budget through the accelerator chain is very tight due to the stringent requirement for high luminosity (10^{33}cm^{-2}s^{-1}) of the colliding beams. In this pursuit this group at the University of Maryland has been engaged over the last several years in the development of an efficient low-energy beam transport (LEBT) section. This unit lies between an ion source and the first stage of acceleration of the beam (e.g., a radio-frequency quadrupole (RFQ) accelerator) and plays an important role in accelerator research.

The LEBT acts as a phase transformer of the beam from the ion source so that a normally diverging beam from an ion source can be focused with a high convergence angle (~ −100 mrad) into an RFQ. Also, the LEBT creates a buffer space between the ion source and the RFQ; this reduces the possibility of any contamination of the RFQ due to cesium or gas load from the ion source. In spite of an exhaustive body of literature in this field, the state-of-art is not satisfactory. So far the major experimental efforts on LEBT systems in accelerators have been made with solenoidal lenses[2] or magnetic quadrupoles[3] supplemented by gas focusing. The design of such systems has been mainly empirical and control parameters are not known apriori with sufficient accuracy. Significant emittance growth of the beam is noted in this scheme. Other schemes deal with electrostatic lenses (einzel lens,[4] electrostatic quadrupole lens,[5,6] helical electrostatic quadrupole lens[7]) or radio-frequency quadrupole lens.[8] Although such alternate schemes have been tested in some experiments, no experimental effort has been made so far in regard to transporting and focusing intense, high-brightness H⁻ beams (typically, beam current of 30 mA, beam voltage of 35 kV, normalized brightness ~ 10^{11} A/m^{2}rad^2). It is important to focus our attention to such beams as they are relevant to the potential applications of modern accelerators.

The present article delineates the problem of H⁻ beam transport and its matching to an RFQ using a novel 6-lens electrostatic quadrupole (ESQ) system as an LEBT. The main emphasis here is to understand the physics of emittance growth in an ESQ transport system and the possible ways to mitigate the problem. In the past the ESQ LEBT system was used very successfully to transport H⁻ beams;[6] however, the beam perveance was much lower there. Here we consider a highly space-charge dominated, high-brightness beam (beam perveance K = 0.003 and normalized brightness

$\sim 10^{11}$ A/m^{2}rad^2). It is quite a challenging task to transport such beams over a certain distance and focus it into an RFQ without any significant emittance dilution. The design is based on detailed computer simulation of beam dynamics through the transport section. The computer predictions regarding performance of the LEBT system are analyzed in the context of beam parameters of two particular types of H^- ion sources – Penning-Dudnikov source as used in the BEAR experiment,[3] and a volume ionization source of Brookhaven National Laboratory.[9] These two types of sources are particularly suitable to obtain high-brightness H^- beams.[10] In our previous articles, H^- beams from a Penning-Dudnikov source were mainly considered. Here, the emphasis is on the transport of H^- beams from a volume source. We have also addressed the issue of sensitivity of the beam parameters due to misalignments. Finally, the problem of matching the H^- beam to an RFQ is discussed.

II. Beam Dynamics through the ESQ LEBT

The design procedure as reported earlier [11] involves a sequence of computer code analysis: (i) A linear beam optics code integrates the K-V envelope equations and generates the basic geometrical parameters of the lens system. (ii) A 3-D LAPLACE solver calculates the equipotentials and evaluates the fringe-field matrices as suggested by Matsuda and Wollnik.[12] (iii) A modified PARMILA code[13] uses input from the above two steps and evaluates the beam parameters (beam size, emittance growth, etc.). This scheme led us to choose a combination of six ESQ lens system to transport H^- beams over a distance of 30 cm and to provide a moderate convergence ($\sim$ -30 mrad) at the end. The technical details of the LEBT system and some results on the computer code predictions of beam characteristics have been given earlier.[11] The essential points to note from our previous articles are:

1. A unique feature in the design of the ESQ LEBT system is that the entire system is self-aligned mechanically. This demands high precision in the fabrication of the components and their assembly. On the other hand, it eliminates the usually tedious alignment job in the experiment.

2. The performance of the ESQ LEBT has been examined using beam parameters of a Penning-Dudnikov source. Some assumptions of the input beam (normalized brightness = 8×10^{10} A/m^{2}rad^2, divergence at full beam radius of 1 cm = 20 mrad) are made on the basis of analysis of the emittance data at z = 10.6 cm from the extraction slit.[11] The output beam from the ESQ LEBT is found converging ($\sim$ -25 mrad), and it shows an emittance growth by a factor of about 1.8 assuming a K-V type distribution of the beam. The emittance growth is identified as due mainly to chromatic aberrations.

The above analysis has been carried out further. Figure 1(a) shows the evolution of rms normalized emittance through the ESQ transport channel. The enhancement of emittance occurs essentially in the second and fifth lenses, when the amplitude of the beam envelope grows to more than 80% of the quadrupole aperture. The beam particles residing in the outer part of the envelope are responsible for the emittance growth, and these particles can be rejected by suitable use of the ground plates between the adjacent ESQ lenses (Fig. 10 in ref. 11) as beam scrapers. Two beam scrapers are inserted, one in front of the second lens and the other in front of the fifth lens. Figure 1(b) shows the evolution of emittance through the ESQ LEBT when 10% of beam particles are scraped out. The emittance growth is a factor of 1.4 here. This is an efficient way to deliver

an almost emittance-preserved beam to an RFQ. The above analysis has been carried out using typical parameters of H^- beams from a volume ionization source, here a BNL-type. Usually the beam from such sources has lower current density compared to, say, the Penning-Dudnikov case. Hence, a larger extraction slit (radius of extraction slit = 5.6 mm here as opposed to a radius of 1 mm in the Penning-Dudnikov case) is used to draw the same amount of current in the case of volume sources. Also the beam divergence at the extraction slit can be very small; almost a parallel beam can be extracted from the source. The estimated normalized brightness of this beam is about $3 \times 10^{10} A/m^2 rad^2$; all other parameters have been given earlier.[11]

Figure 2 shows the modified PARMILA results on distribution of the beam particles corresponding to an H^- beam from the volume source. Here the parameters corresponding to a 4 times rms ellipse, constructed by including 90% of the beam particles at the output of the ESQ LEBT, are: $X_{max} = 3.3$ mm, $Y_{max} = 2.7$ mm, $(X_{max})' = -13.5$ mrad, $(Y_{max})' = -14.9$ mrad. The maximum voltage on the ESQ lenses was 4.7 kV. The emittance growth of the beam is negligibly small, $\sim$ 4%. This result suggests that the characteristics of the input beam are very crucial to the issue of emittance growth in a transport system - - a parallel input beam is desirable.

The sensitivity of output beam parameters with variation of beam voltage, beam current, misalignment of the beam axis with respect to the LEBT system has been studied. The K-V code analysis suggests that the beam parameters do not change noticeably for a $\pm 1\%$ change of quad voltage (from the ideal setpoint) on all the lenses simultaneously. Similar insensitivity is noted for variation of beam current (ideal = 30 mA) within a few milliamperes. Preliminary analysis on the aforementioned misalignments is done using the modified PARMILA code (no image charge is included in the present code). With the variation of the amount of off-centering of the input beam, the phase-space distribution of the output beam remains almost invariant, while the beam centroid shifts coherently. A translational off-centering by 1 mil at the input is amplified by about a factor of 2 off-centering at the output of the LEBT; this also introduces an angular error of the beam centroid by about 2 mrad. An on-centered input beam with an error of 1 mrad in the injection angle shows an off-centering of the output beam by about 1.8 mil; the error in the angle stays almost the same through the LEBT channel.

III. Matching to an RFQ

The beam from the LEBT section needs to be matched with the RFQ in order to achieve a good transmission and preserve emittance through this channel. The typical Twiss parameters for the acceptance ellipse of an RFQ (e.g., BEAR and SSC RFQ) demand a beam convergence of about -90 mrad at the full beam radius of about 1.3 mm. It is an arduous task to satisfy these requirements of an RFQ by an ESQ LEBT alone without sacrificing the emittance growth. An LEBT composed of two modules — the ESQ lenses as a beam transport section and an einzel lens at the end as a matching section — seems to be a good choice in this pursuit.

Figure 3 shows a schematic of the ESQ LEBT with a short modular attachment containing an einzel lens. Preliminary analysis is done using the K-V code. The beam envelopes for the two situations are shown in Fig.4: (a) Penning-Dudnikov case, (b) volume source case. The beam parameters at the end of the einzel lens match well with the requirements of the RFQ as mentioned earlier. A high value (about 7.0) of the ratio of the aperture of the einzel lens to the beam size is taken here; hence, the einzel lens is expected to have an insignificant contribution to the emittance growth. This problem is being currently investigated to get a quantitative answer.

IV. Experiments and Discussion

The ESQ LEBT system has been constructed in-house. The overall mechanical alignment of the apparatus has been measured, and found to be within ± 1.5 mil. The power supply system for the ESQ lenses has been attached. Detailed voltage hold-off tests have been done, and the performance is satisfactory. It is planned to test this ESQ LEBT with an H^- beam from a magnetron source at the SSC Laboratory. The code results are being reviewed in the light of the beam parameters from the magnetron source.

It has been shown that a combination of an ESQ LEBT system with an einzel lens can be used very effectively to transport a space-charge dominated, high-brightness H^- beam over a distance of about 30 cm and focus the beam into an RFQ without any significant emittance dilution. This method appears to be attractive particularly to handle a highly diverging beam from an ion source. Such a scheme has a number of advantages: (i) flexibility to handle a wide range of input beam parameters from different types of ion sources, (ii) allow sufficient buffer space (not field-free) between an ion source and an RFQ for differential pumping, (iii) experiments with low-voltage power supplies over the major part of the transport, and (iv) ease of fine tuning. It is now a very important issue to determine the optimum length of the LEBT section to insure a reliable operation of the injector system in an accelerator. Carefully controlled experiments with various transport schemes are warranted and a good database is required to unravel the reliability of the computer simulation results.

Acknowledgments

This work is supported by ONR/SDIO.

References

1. "Site-Specific Conceptual Design of the Superconducting Super Collider", edited by J. R. Stanford and D. M. Matthews, Superconducting Super Collider Laboratory Rept. SSCL-SR-1056, July 1990.
2. J. G. Alessi, et al., Rev. Sci. Instrum. **61**, 625 (1990).
3. P. G. O'Shea, et al., Nucl. Instrum. & Methods in Phys. Res. **B40/41**, 946 (1989).
4. C. R. Chang, Proc. LINAC Conf., Albuquerque, NM, Sept. 10-14, 1990, p.399.
5. M. Reiser, et al., SPIE Proc. Microwave and Particle Beam Sources and Propagation **873**, 172 (1988); S. K. Guharay, et al., High Brightness Beams for Advanced Accelerator Applications, College Park, MD., June 6-7, 1991, AIP Conf. Proc.No. 253, p. 67.
6. O. Anderson, et al., Lawrence Berkeley Laboratory Rept. LBL-27953 (1989).
7. D. Raparia, Proc. LINAC Conf., Albuquerque, NM., Sept.10-14, 1990, p.405.
8. D. A. Swenson, et al., Proc. LINAC Conf., Albuquerque, NM, Sept. 10-14, 1990, p.39.
9. J. G. Alessi, (private communication)
10. J. G. Alessi, High Brightness Beams for Advanced Accelerator Applications, College Park, MD., June 6-7, 1991, AIP Conf. Proc. No. 253, p. 193.
11. S. K. Guharay, et al., SPIE Proc. Intense Microwave and Particle Beams III **1629**, 121 (1992).
12. H. Matsuda and H. Wollnik, Nucl. Instrum. & Methods **103**, 117 (1972).
13. C. R. Chang, et al., SPIE Proc. Intense Microwave and Particle Beams **1226**, 483 (1990).

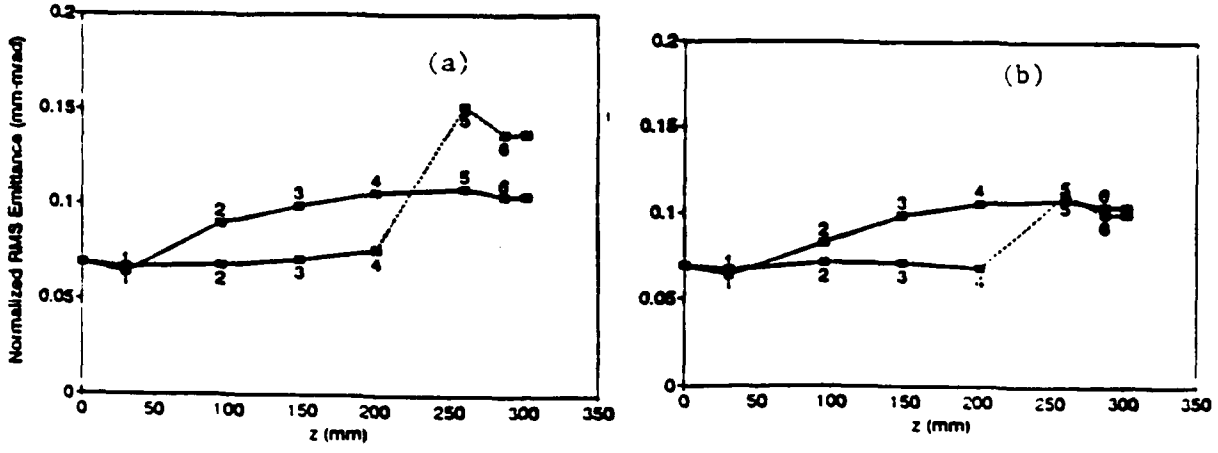

Fig. 1. Evolution of rms normalized emittance (solid line: X-component; dashed line: Y-component) through the ESQ lenses for an H^- beam from the Penning-Dudnikov source: (a) without any beam scraper; (b) with beam scrapers, one in front of the second lens and the other in front of the fifth lens. The numbers inside the figure identify the location of the downstream endpoint of the corresponding lens.

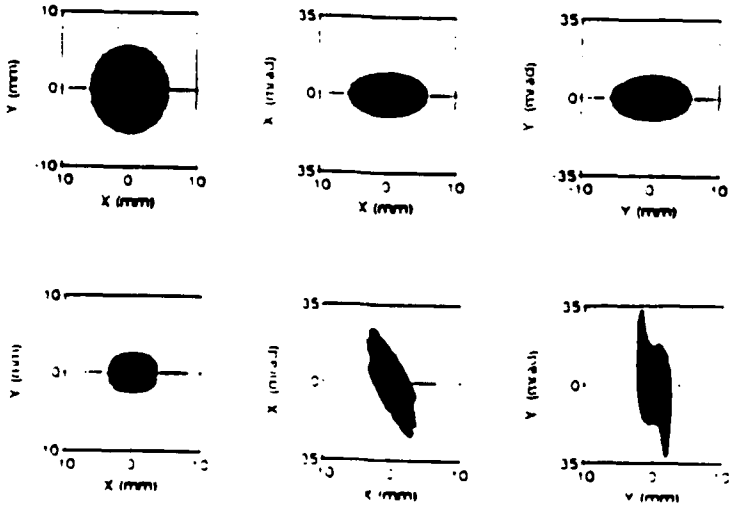

Fig. 2. Modified PARMILA results of distribution of beam particles for an H^- beam from the BNL volume source: Input beam (top figure); Output beam (bottom figure).

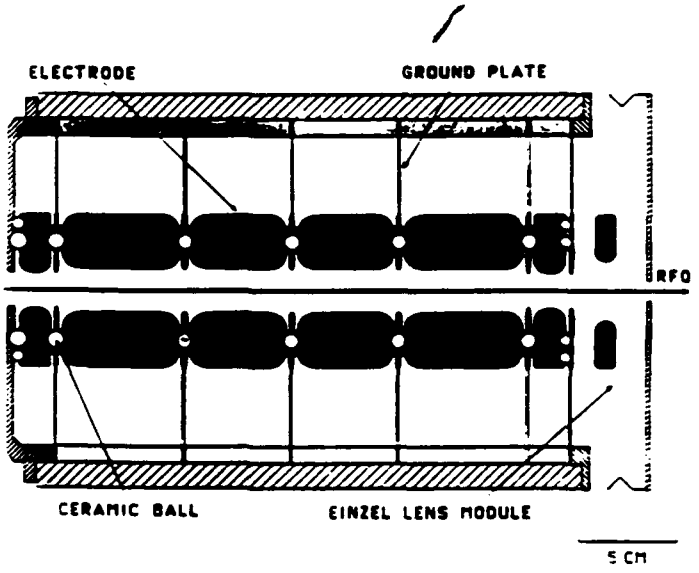

Fig. 3. Schematic of the LEBT system.

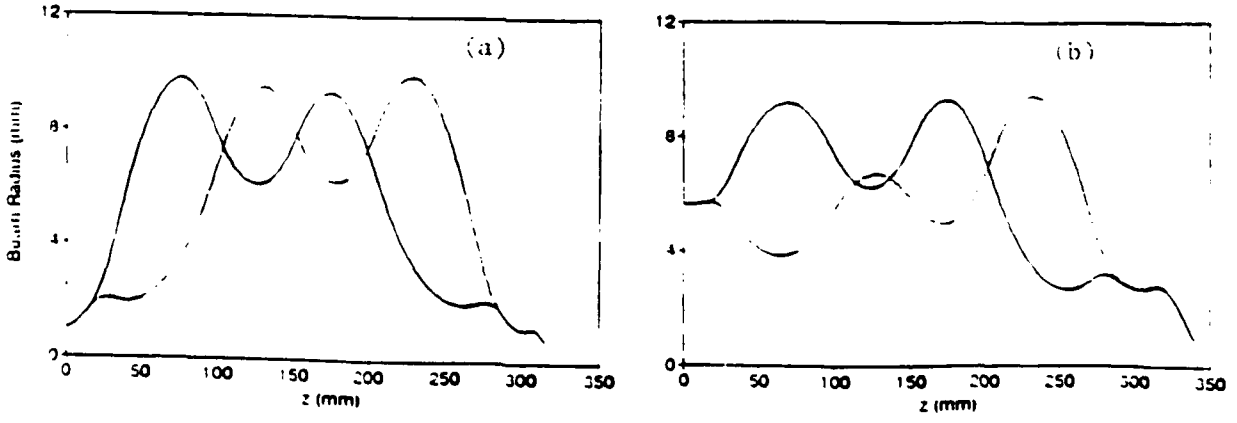

Fig. 4. K-V envelope solution (solid line: X-component; dashed line: Y-component) for the matched beam to an RFQ using H^- beam parameters corresponding to: (a) Penning-Dudnikov source; (b) BNL volume source.

AIP Conf. Proceedings on Computational Accelerator Physics

SOLUTION OF LAPLACE'S EQUATION BY THE METHOD OF MOMENTS WITH APPLICATIONS TO CHARGED PARTICLE TRANSPORT*

C. K. Allen, S. K. Guharay, and M. Reiser
Laboratory for Plasma Research
University of Maryland, College Park, MD 20742

ABSTRACT

A fast approximation method to the 3D electrostatic problem is developed. The method of moments procedure is outlined for the particular case of Laplace's equation. The resulting matrix-vector equation is solved by a conjugate gradient algorithm. These techniques are then implemented with a computer code running on a PC and used to solve example problems.

1. INTRODUCTION

We are interested in the transport of low energy ions beams, specifically, we have been engaged in the design and analysis of Low Energy Beam Transport (LEBT) section of an accelerator column[1,2]. To avoid gas focusing we use electrostatic lenses for the relatively slow moving ions. The action of such lenses is completely characterized by their spatial potential distribution ϕ. Thus, analysis of electrostatic lenses invariably requires the solution of Laplace's equation.

Although simple in form, this equation must be solved numerically for most geometries of practical interest. Many approximation techniques are very successful to this end (e.g. finite differences) and are covered extensively in the literature. However, for a fully 3D treatment computation and machine storage usually become extreme. Manipulation of the solution data also becomes quite cumbersome. Consequently, these situations require special hardware such as a supercomputer. We present an approximation technique which is fully 3D and remarkably computational efficient. Ideally, we wish to implement this technique as CADware for the IBM PC.

The technique relies on a combination of the method of moments and fast iterative techniques for solving linear systems. Specifically, we proceed by reformulating Laplace's equation into an integral equation over the boundary surface, reducing the dimensionality of the original system. The new problem is approximated by the method of moments[3] to yield the matrix-vector equation $Ax=y$. We then use conjugate gradient algorithms[4] to solve this equation.

---

*Supported by ONR/SDIO

2.0 PROBLEM FORMULATION

In this section we clarify the physical system which we wish to model. Figure 1 depicts an abstract geometric representation of the electrostatic problem. We have a closed surface Γ in Euclidean 3-space E^3 which represents the boundary of our problem. Γ separates E^3 into two regions Ω_i and Ω_e representing the (bounded) interior of Γ and the (unbounded) exterior of Γ, respectively. Typically we associate the union of Γ and Ω_i as a conductor in 3-space while we are interested in the potential ϕ in the region Ω_e external to the conductor. This is an example of the so called *exterior Dirichlet problem* and can be classified mathematically as follows:

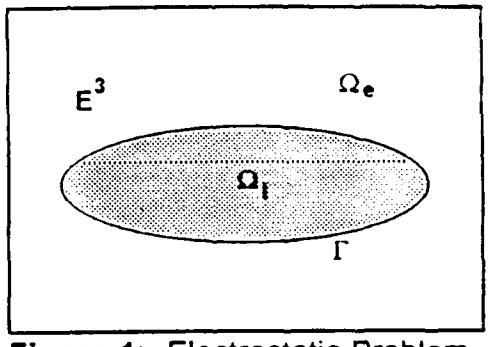

Figure 1: Electrostatic Problem

$$\begin{aligned} \nabla^2\phi(x) &= 0 \qquad \forall x\in\Omega_e, \\ \phi(x) &= f(x) \qquad \forall x\in\Gamma. \end{aligned} \tag{1}$$

The function f is the given set of boundary values and it constitutes the data of the problem. For a conductor f is a constant over the boundary Γ. In addition, we usually impose the physical restriction that ϕ vanishes at infinity.

Also of interest is the *interior Dirichlet problem* where we are concerned with the distribution ϕ in the region Ω_i. This situation is formulated mathematically below.

$$\begin{aligned} \nabla^2\phi(x) &= 0 \qquad \forall x\in\Omega_i, \\ \phi(x) &= f(x) \qquad \forall x\in\Gamma. \end{aligned} \tag{2}$$

Notice that both problems take the same boundary values, namely f. Typically for the interior problem we also require that ϕ remains bounded in Ω_e.

We may reformulate both of these problems into a single integral equation on Γ[5]. The alternate problem is achieved by the introduction of an intermediate function σ defined on Γ.

$$f(x) = \int_\Gamma G(x,x')\sigma(x')dx' \qquad \forall x\in\Gamma \tag{3}$$

where

$$G(x,x') = \frac{1}{4\pi}\frac{1}{|x-x'|}. \tag{4}$$

The potential distribution ϕ is then related to the function σ by the equation

$$\phi(x) = \int_{\Gamma} G(x,x')\sigma(x')dx' \qquad \forall x \in \Omega \tag{5}$$

where Ω is the union of Ω_i and Ω_e. Thus equation (5) is valid in all space except the boundary Γ. We recognize G(x,x') as the free space Green's function for Poisson's equation and equation (5) as the potential due to a surface charge density σ in free space. It is interesting to note that even though problems (1) and (2) are not related in any obvious manner, solution of (3) yields the correct σ in both cases given the same boundary values f.

3.0 THE METHOD OF MOMENTS

We now approximate σ in equation (3) using the method of moments. It will be convenient to rewrite (3) by defining the operator K. We have

$$K\sigma \triangleq \int_{\Gamma} G(x,x')\sigma(x')dx' = f \qquad f \in L_p(\Gamma) \tag{6}$$

where we have chosen f in L_p in order to analyze convergence. We see that K is a compact linear self-adjoint integral operator with kernel G(x,x'). Since Γ is compact, we may choose a countable set of functions $\{u_n\}$ which are dense in $L_p(\Gamma)$, that is they form a basis for the vector space $L_p(\Gamma)$. These functions are usually referred to as the set of expansion functions. Accordingly, any element of L_p may be approximated arbitrarily well by a linear combination of these functions. Thus,

$$\sigma(x) = \sum_{n=1}^{\infty} a_n u_n(x) \tag{7}$$

for some set $\{a_n\}$ of coefficients. By substituting (7) into (6) and using the linearity of K we have

$$\sum_{n=1}^{\infty} a_n K u_n = f. \tag{8}$$

Now we choose another set of functions $\{v_m\}$ in L_q (where $1/p + 1/q = 1$) to be used as a set of weighting functions. By taking the inner product of (8) with each of the v_m's we get a set of equations of the form

$$\sum_{n=1}^{\infty} a_n \langle Ku_n, v_m \rangle = \langle f, v_m \rangle \qquad m=1,2,3,\ldots \tag{9}$$

where $\langle\ -,\ - \rangle$ denotes the usual inner product

$$\langle u, v \rangle = \int_{\Gamma} u(x)\bar{v}(x)dx. \tag{10}$$

Note that since f is given and $\{u_n\}$ and $\{v_m\}$ are selected arbitrarily, the only unknowns are the coefficients $\{a_n\}$. To obtain an approximation for σ we must truncate the indices n and m at a finite value. If we choose the same value for both indices, say N, we are then left with the following matrix-vector equation.

$$\begin{pmatrix} \langle Ku_1, v_1 \rangle & \cdots & \langle Ku_N, v_1 \rangle \\ \vdots & & \vdots \\ \langle Ku_1, v_N \rangle & \cdots & \langle Ku_N, v_N \rangle \end{pmatrix} \begin{pmatrix} a_1 \\ \vdots \\ a_N \end{pmatrix} = \begin{pmatrix} \langle f, v_1 \rangle \\ \vdots \\ \langle f, v_N \rangle \end{pmatrix} \tag{11}$$

which can be written more compactly as

$$Ax = y. \tag{12}$$

The matrix A is known in the literature as the moment matrix for (6), since we take the moments of $K\sigma$ with respect to the weights $\{v_m\}$. Equation (12) may be solved by standard matrix techniques to yield a solution for x, the vector of coefficients $(a_1, \ldots, a_N)^T$. We then have our approximation to σ according to equation (7).

COMMENTS

(1) The method of moments generates solutions that converge in the mean, i.e. in the L_p norm. The exact L_p space where convergence occurs depends on the choice of expansion and weighting functions.

(2) When we chose $\{v_m\} = \{u_m\}$, we have Galerkin's method which is known to be equivalent to the Rayleigh-Ritz variational method[3]. Thus, we see that the method of moments is a generalization of the Rayleigh-Ritz procedure. For Galerkin's method we have convergence in the L_2 norm (mean-squared convergence), where the approximate σ lies in span $\{u_n\}$.

(3) By choosing $\{v_m\} = \{\delta(x-x_m)\}$ where δ is the Dirac delta function and the x_m's are some set of points on Γ, we have a point-matched solution. Such solutions are known to converge in the L_1 norm (pointwise convergence).

(4) For valid solutions we must make sure the set $\{Ku_n\}$ spans the range of K. Otherwise, we converge to solutions to the problem $K\sigma = Pf$ where P is the projection operator onto the space span$\{Ku_n\}$.

(5) K^{-1} is unbounded and there exists f in L_p such that (8) has no solution σ in L_p (such solution may however be interpreted distributionally). However, K is a positive operator, indeed $\langle K\sigma,\sigma \rangle$ is recognized as the electrostatic energy in the system. Consequently, in the discrete approximation, 0 is not an eigenvalue of A (it is in the limit $N \to \infty$, though).

4.0 CONJUGATE GRADIENT ALGORITHM

We now turn our attention to the task of solving the matrix-vector equation (12). The traditional approach is to use some direct method such as

LU decomposition or Gaussian elimination. With these techniques the amount of computation necessary to solve an N^{th} order system is known *a priori*. For example, it is known that inversion of (12) requires $O(N^3)$ operations. Instead, we have chosen an iterative technique where the amount of computation is not known in advance.

The conjugate gradient algorithms are a specialization of the more general technique of conjugate directions methods. These techniques are expressly developed to solve the problem[6]

$$\min_{x \in \mathbb{R}^N} \; g(x) = \frac{1}{2} x^T A x - y^T x. \qquad (13)$$

It is assumed that the matrix A is positive definite so that a solution does exist. Note that the solution to this problem, obtained by setting the gradient of g to zero, is given by $x = A^{-1}y$. Conjugate direction methods are based on the idea of generating a complete set of linearly independent vectors $\{d_n\}$ which have the property $d_n^T A d_m = 0$ whenever $m \neq n$. This is known as A-orthogonality, or A-conjugacy.

Instead of solving (12) directly, in conjugate gradients we choose to iteratively minimize some functional, for example g in the above equation. The value of x furnishing this minimum is the solution to (12). The method starts with an initial guess for x_0, then it generates a sequence x_i that minimizes the functional. The sequence $\{x_i\}$ will converge to the exact solution x in a finite number of iterations. Even if the matrix A is not invertible in the classical sense (0 is an eigenvalue of A), the conjugate gradient algorithm will converge to a solution in the least squares sense. The algorithm we have chosen was taken from Sarkar *el. al.*[4] The functional which it minimizes is the (l_2) norm squared of the residual $r_i = y - Ax_i$ (i.e. minimize $\|y - Ax_i\|^2$).

5.0 IMPLEMENTATION

To apply the method of moments it is necessary that we select an appropriate set of expansion functions $\{u_n\}$ and weighting functions $\{v_m\}$. Since our aim is to minimize computation, we have selected a point-matching procedure. Thus, our weighting functions $\{v_n\}$ are given by the set $\{\delta(x-x_n)\}$ where the x_n's are the match points in Γ to be determined. This technique yields the least computing time, and the procedure is straightforward. It also yields good results as long as one is careful in the selection of the match point locations[7,8].

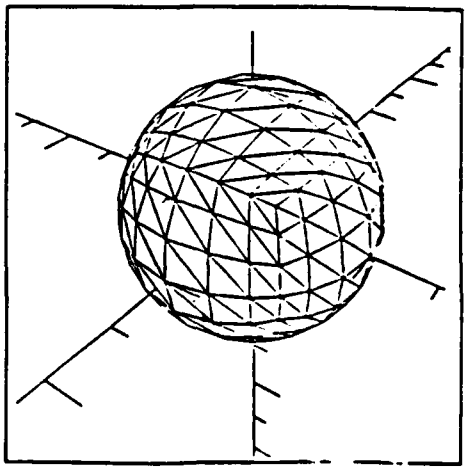

Figure 2: Triangulated Sphere

We choose a set of piecewise constant functions for $\{u_n\}$. First, Γ is

divided into triangular subdomains, denoted by the set $\{T_n\}$ where n runs from 1 to N. If Γ has curvature then we have an approximation to Γ as well (for example figure 2 depicts the triangulated approximation to a sphere). Now let the u_n's be a set of piecewise constant functions on each T_n.

$$u_n(x) = \begin{cases} 1 & \text{if } x \in T_n \\ 0 & \text{if } x \notin T_n \end{cases} \tag{14}$$

It can be shown that such a set is dense in L_p so σ may be approximated arbitrarily well[9]. Thus, according to comment (4) we must be certain that Pf = $\{f(x_n)\}$ is in the span of $\{Ku_n\}$. We shall see later that this criterion places restrictions on our triangulation of Γ. We have chosen the matching point set $\{x_n\}$ to be the centroids of each triangle T_n. Since this is the center of mass for our constant expansion functions, it seems to be a reasonable approximation to f across the triangle face.

In order to form equation (11) we must determine the inner products $\langle Ku_n, \delta(x-x_n)\rangle$. For our choice of expansion functions, this amounts to the evaluation of the following integral.

$$\begin{aligned} a_{n,m} &= \int_{T_m} G(x_n, x')\,dx' \\ &= \frac{1}{4\pi}\int_{T_m}\int \frac{1}{\sqrt{(x_n-x')^2+(y_n-y')^2+(z_n-z')^2}}\,dx'dy'dz' \end{aligned} \tag{15}$$

This can be done completely numerically, hybrid analytic and numeric, or completely analytically[10].

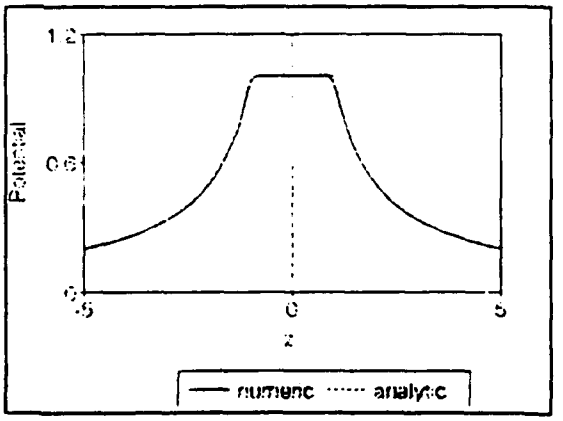

Figure 3: Conducting Sphere Axial Potential

6.0 EXAMPLES

We have implemented the above techniques in a computer program written in Borland C++. The platform is an i486 PC operating at 33 MHz and running Windows 3.1 operating system. All examples were run in single precision arithmetic except where noted. We have taken arbitrary units.

CONDUCTING SPHERE

The analytic potential distribution for a conduction sphere of radius 1 and held

at a potential 1 is known to be

$$\phi(x) = \begin{cases} 1 & \text{if } |x| < 1, \\ \dfrac{1}{|x|} & \text{if } |x| \le 1. \end{cases} \qquad (16)$$

Figure 3 shows a comparison of this analytic formula with the numerical results achieved for a triangulated sphere of 432 triangles (shown in figure 2). The solution converges to a norm squared residual error < 10^{-9} in 75 iterations taking about 7 minutes real time (double precision required 42 iterations within 5 minutes).

A single number which is indicative of solution quality is the capacitance. This value may be calculated by recognizing σ as surface charge density. We numerically calculated the capacitance to be 110.2 pF for the above situation in MKS units, the true value is 111.3 pF.

EINZEL LENS

An einzel lens was modeled as two cylindrical pipes of radius 5 and length 10, separated axially by a distance of 3. Both pipes were capped with plates having an inner radius of 1/2. A conducting plate with outer radius 5 and inner radius 1/2 was centered between the two pipes at position z=0. The center plate was driven to a potential of 1 while the two outer pipes were grounded. El-Kareh provides an approximate analytic axial potential distribution given by[11]

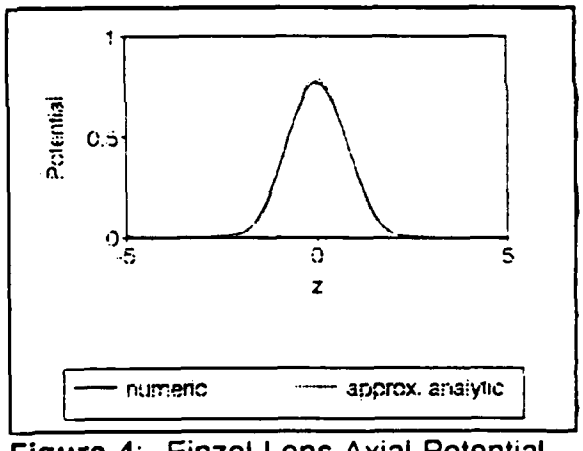

Figure 4: Einzel Lens Axial Potential

$$\phi(z) \approx \frac{2}{3\pi}\left[\frac{2z+3}{2}\tan^{-1}(2z+3) + \frac{2z-3}{2}\tan^{-1}(2z-3) - 2z\tan^{-1}(2z)\right]. \qquad (17)$$

This approximation assumes three infinite plates of inner radius 1/2 with uniform fields at $z = \pm\infty$. The discretization was made with 464 triangles. This system took 261 iterations to converge to the usual error criterion (about 18 minutes of real time). What is happening here is that our boundary function f of equation (8) is almost outside the range of $\{Ku_n\}$. Fortunately, our iterative technique is indicating this situation by slower convergence! In order to avoid such situations it is necessary to reevaluate the triangulation of the system to insure that $\{Ku_n\}$ spans the space of boundary functions. Even though our patch model was borderline ill-conditioned, the stability of the conjugate

gradient method still yielded reasonable results (see figure 4).

7.0 CONCLUSION

The method outlined in this paper exhibits enough computational efficiency to allow practical implementation on a PC. It yields accurate results in a reasonable amount of real computing time. Moreover, the conjugate gradient algorithm furnishes suitable error criterion to judge the quality of the solution. However, the method does require more work to implement than, say, the rather straightforward technique of finite differencing.

REFERENCES

1. S. K. Guharay, C. K. Allen, and M. Reiser, Conf. High-Bright. Beams, College Park, AIP Conf. Proc. 253 (1992), pp. 67-76.

2. S. K. Guharay, C. K. Allen, M. Reiser, K. Saadatmand, and C. R. Chang, AIP Conf. Proc. on Product. and Neut. Negative Ions (1993) (to appear).

3. R. F. Harrington, Field Computation by Moment Methods (Krieger, Malabar, FL, 1968).

4. T. K. Sarkar and E. Arvas, IEEE Trans. Antennas Propagat., vol. AP-33, no. 10, pp. 1058-1066, Oct. 1985.

5. I. Stakgold, Green's Functions and Boundary Value Problems (Wiley, NY), pp. 508-517.

6. D. G. Luenberger, Linear and Nonlinear Programming 2nd Ed. (Addison-Wesley, Reading, MA, 1984), pp. 238-257.

7. T. K. Sarkar, A. R. Djordjevic, and E. Arvas, IEEE Trans. Antennas Propagat., vol. AP-33, no. 9, pp. 988-996, Sept. 1985.

8. A. R. Djordjevic and T. K. Sarkar, IEEE Trans. Antennas and Propagat., vol. AP-35, no. 3, pp. 353-355, March 1987.

9. H. L. Royden, Real Analysis 3rd Ed. (Macmillan, NY, 1988), p.282.

10. S. M. Rao, A. W. Glisson, and D. R. Wilton, IEEE Trans. Antennas and Propagat. vol. AP-27, no. 5, Sept. 1979, pp. 604-607.

11. A. B. El-Kareh and J. C. J. El-Kareh, Electron Beams, Lenses, and Optics Vol. 1 (Academic Press, NY, 1970), p. 187.

Proceedings of the 1993 Particle Accelerator Conf., May 1993, Washington, DC

An ESQ Lens System for Low Energy Beam Transport Experiments on the SSC Test Stand

S. K. Guharay, C. K. Allen, M. Reiser
Laboratory for Plasma Research, University of Maryland, College Park, MD 20742, USA
and K. Saadatmand
SSC Laboratory, Dallas, TX 75712, USA

Abstract

A low-energy beam transport system is designed with the aim of transporting a 30 mA, 35 kV H^- beam from a volume source and focusing it into an RFQ. The characteristics of the beam from the source are determined analyzing the emittance data. The behavior of the beam through the LEBT is studied using simulation codes. The system parameters are optimized so that the LEBT has a very modest contribution to the emittance growth (here a factor of about 1.5) and the emittance budget of the linac section is maintained.

I. INTRODUCTION

One of the vital considerations in modern high-energy accelerators is related to the design of an efficient low-energy beam transport (LEBT) section so that an intense, high-brightness beam (here we consider an H^- beam) can be transported over certain distance and finally focused into the commonly used RFQ accelerator in the linac section. The emittance growth in the LEBT is the key issue in developing a good scheme at the low-energy end of the accelerator chain. Thus, in order to achieve a good beam quality and match it to the acceptance of an RFQ a systematic study of beam dynamics in the preceeding sections including the extraction optics of the ion source is warranted. We have experienced that emittance measurements of the beam from an ion source and an analysis of the data to characterize the beam at the extraction electrode are two important problems in the context of designing an efficient LEBT. Earlier we reported [1,2] on the beam characterization and beam dynamics through a LEBT for H^- beams from a Penning-Dudnikov type [3] and magnetron type sources. In recent years significant progress has been made in the performance of volume sources [4,5]; normalized beam brightness approaches about 10^{11} A/(m-rad)^2 for H^- beams. This article highlights on the study of H^- beams from the SSC volume source with the aim of designing a LEBT system to deliver a 30 mA, 35 kV beam matched with the RFQ input.

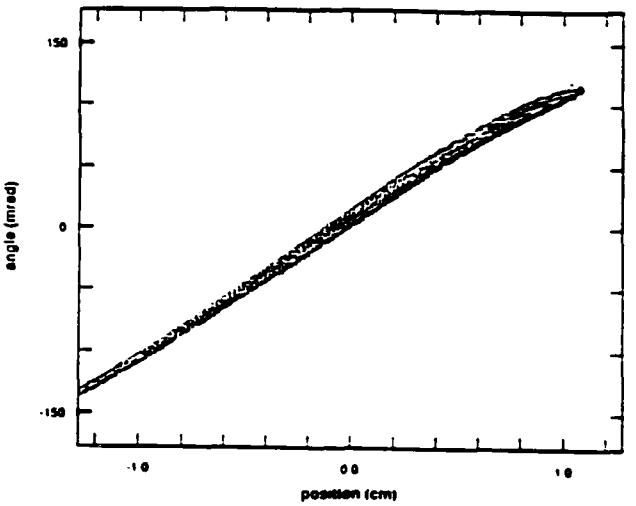

Figure 1: Contour emittance plot.

II. BEAM CHARACTERISTICS

A. H^- Beam from the Ion Source

The H^- beam from the SSCL volume source is measured at 10.13 cm downstream after the electrons (ratio of initial electron to ion current $\sim$ 40) are deflected away from the extracted beam current by a 10 cm long magnetic trap. Figure 1 shows the contour plots in the $x - x'$ space from emittance diagnostics; the flattening of the distribution in the upper half is possibly caused by the space-charge force due to the electrons deflected upward. The beam parameters at z = 10.13 cm are: beam size D = 2.38 cm, full divergence $\Delta\theta$ = 260 mrad, $\pi\tilde{\epsilon}_n = 0.1537\pi$ mm-mrad. These data are used in an envelope simulation code to estimate the beam characteristics at the extraction electrode; space-charge effects due to the electrons in the extraction region are included. Figure 2(a) shows the assumed space-charge correction factor, f, due to the electrons. Note that f is

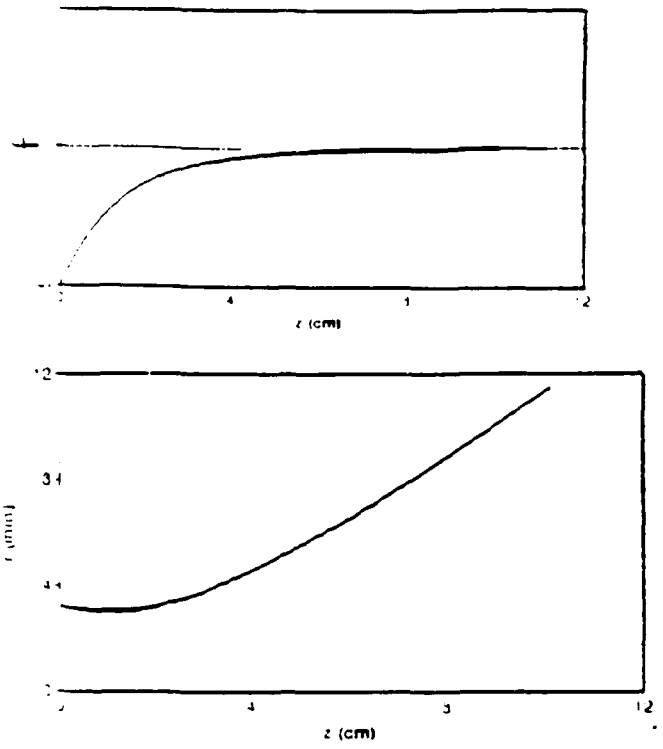

Figure 2: (a) Space-charge correction factor f; (b) beam envelope. z = 10.13 cm corresponds to the location of emittance measurements.

negative here and the beam perveance is to be multiplied by the factor $(1 - f)$. The beam envelope in Fig. 2(b) is evaluated by integrating the K-V envelope equations using a fourth-order Runge-Kutta method. This analysis suggests that the beam at the extraction electrode emerges nearly parallel, and the beam size is close to the aperture radius (= 4 mm).

B. Desired Output Beam Parameters from the ESQ LEBT

The purpose of the LEBT section is to isolate the RFQ from the ion source for a clean operation and also to deliver a matched beam to the RFQ. The SSC RFQ acceptance for a 30 mA, 35 kV H^- beam is given by the Twiss parameters: α = 1.26, β = 1.86 cm/rad, $\pi\tilde{\epsilon}_n = 0.2\,\pi$ mm-mrad. As the normalized rms emittance of the H^- beam from the source is about $0.1537\,\pi$ mm-mrad (Fig. 1), the LEBT is to be designed under a very tight emittance budget. The matching condition dictates that the beam parameters at the tip of the RFQ vane should be: beam radius = 1.3 mm and the corresponding slope of the beam envelope = −89 mrad; this is located at about 3 cm downstream from the front wall of the RFQ. It has been shown earlier that a short (about 5 cm long) single einzel lens module between an ESQ LEBT and the RFQ will be a good choice in satisfying the aforementioned stringent conditions of the RFQ [2]. The ESQ LEBT transforms the highly diverging beam from the ion source into a moderately converging one without any significant emittance dilution, and the einzel lens provides the final strong focusing. This analysis showed that the parameters of the output beam from the ESQ LEBT should follow: beam radius ~ 3 to 5 mm, the corresponding slope of the beam envelope ~ −30 to −50 mrad.

III. BEAM TRANSPORT THROUGH THE ESQ LEBT

The design principles of the ESQ LEBT follow the scheme as discussed earlier [1,2]. The present configuration of the magnetic trap in the extraction region of the SSCL volume source restricts the ESQ LEBT's distance to the extraction aperture to about 10 cm. This causes the beam to blow up significantly (Fig.1). After a detailed analysis with such a beam it is recognized that the goal to deliver a matched beam to the RFQ for the full beam current (30 mA) is a very difficult task. Our analysis suggests that a shorter magnetic trap (about 5 cm long) will be a better choice. Figure 3 shows the beam envelope through the ESQ LEBT when a hard-edge focusing function for the external field is assumed. An initial drift space of 5 cm long is considered, and a profile of the space-charge correction factor due to the electrons (Fig. 3, bottom) is assumed. The beam parameters at the extraction aperture are taken from the analysis of Fig. 2. The maximum aperture radius of the quadrupoles is 22 mm; it was taken as 12 mm when the LEBT was closer (1.5 cm) to the extractor [1].

The distribution of the beam particles through the ESQ LEBT is estimated using a modified PARMILA code [6]. Figure 4 shows the particle distribution in phase space for I = 30 mA. The estimated output beam parameters are: X = 3.5 mm, Y = 3.5 mm, X' = −51.7 mrad, Y' = −50.8 mrad, $\tilde{\epsilon}_n^x/\tilde{\epsilon}_n^y$ = 1.5. The emittance growth is primarily due to chromatic aberrations.

IV. CONCLUSIONS

Emittance measurements of a 30 mA, 35 kV H^- beam from the SSCL volume source have been studied. The simulation results suggest that the H^-

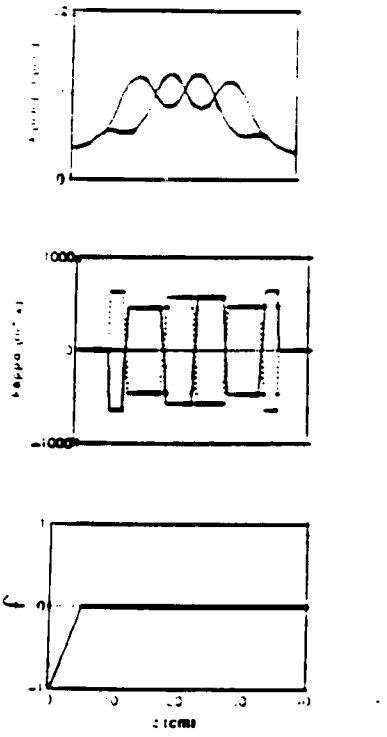

Figure 3: K-V envelope solution.

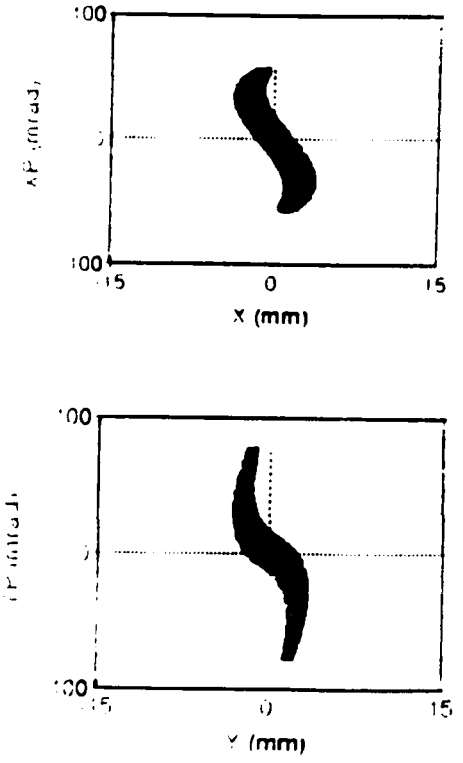

Figure 4: Particle distribution at the output of the ESQ LEBT.

beam envelope has a waist at the extraction aperture. With this definition of the input beam and a given set of characteristic parameters of the RFQ acceptance, we have designed a LEBT system. The particular design of the LEBT consisting of six ESQ lenses and a short einzel lens can transport the full beam current and match it to the RFQ.

Beam transport experiments with a prototype ESQ LEBT will be conducted to validate the simulation predictions. Further, the 3-D LAPLACE simulation scheme is being improved using a method of moments where any arbitrary boundary can be represented numerically and the practical problems will be simulated more realistically [7].

This work was supported by ONR/SDIO and DOE.

IV. REFERENCES

[1] S. K. Guharay, et. al., *Proc.1991 Particle Accelerator Conf.*, p. 1961.

[2] S. K. Guharay, et al., *BNL Conf. on Production and Neutralization of Negative Ions and Beams*, Nov. 1992 (to be published in AIP Proc.).

[3] P. G. O'Shea, et al., *Nucl. Instrum. & Meth. in Phys. Res.* **B40/41**, 946 (1989).

[4] K. N. Leung, *BNL Conf. on Production and Neutralization of Negative Ions and Beams*, Nov. 1992 (to be published in AIP Proc.).

[5] K. Saadatmand, these proceedings.

[6] C. R. Chang, Ph. D. Thesis, Univ. Maryland, 1989.

[7] C. K. Allen, et al., these proceedings.

1992 LINAC Conference Proceedings, Vol. 1, page 338

A COMPACT ESQ SYSTEM FOR TRANSPORT AND FOCUSING OF H⁻ BEAM FROM ION SOURCE TO RFQ*

S.K. Guharay, C.K. Allen, M. Reiser
University of Maryland, College Park, MD 20742 USA
and
K. Saadatmand and C.R. Chang
Superconducting Super Collider Laboratory, Dallas, TX 75237 USA

Abstract

A compact, 6-lens electrostatic quadrupole (ESQ) LEBT system has been constructed at the University of Maryland to transport a 30 mA, 35 kV H^- beam over a distance of about 30 cm. A short einzel lens section is included at the end of the ESQ LEBT to establish a good matching of the beam to the radio-frequency quadrupole (RFQ) accelerator, and to meet the emittance requirements of the linac in the Superconducting Super Collider. Computer code predictions on the beam dynamics through the LEBT with experimentally measured input beam data are discussed.

Introduction

An efficient ion source-cum-low energy beam transport (LEBT) section is highly desired to deliver a good-quality beam to the low-energy booster (LEB) in the collider ring chain of SSCL. The intrinsic emittance of the H^- beam from an ion source, volume-ionization or magnetron type, is typically about 0.12 π mm-mrad (rms normalized value); the LEB requires that the transverse beam emittance at the output of the linac section be $< 0.3\pi$ mm-mrad [1]. The components of the linac between the ion source and the LEB are: LEBT, radio-frequency quadrupole (RFQ) accelerator, drift-tube linac (DTL) and coupled-cavity linac (CCL). Computer code analyses of the beam dynamics through the DTL and the CCL suggest that the emittance growth in these two sections is not significant, being in the range of 10-15% [2]. The performance of the RFQ, e.g., beam transmission and emittance growth, depends primarily on the Twiss parameters of the beam at its input; the transverse rms normalized emittance of the input beam is desired to be $< 0.2\pi$ mm-mrad. Hence the LEBT's contribution to the emittance budget must be maintained within a factor of 1.6 of the input beam emittance. This suggests that the ion source-cum-LEBT section plays a critical role in the performance of the linac.

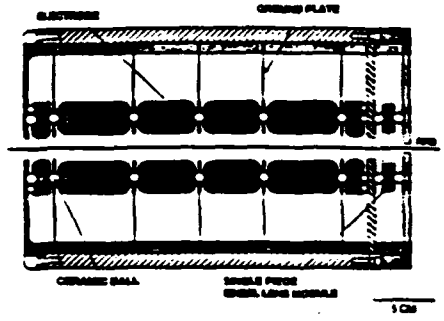

Figure 1: The LEBT system.

This article addresses some important problems in designing an efficient LEBT system. Here, an ESQ lens system is primarily considered: two other variants of the LEBT system, einzel lenses and a helical quadrupole lens, are also being investigated in the present context at SSCL [3]. The analyses are based on computer code simulations, where the input beam parameters are mostly taken from experimental measurements.

Beam Dynamics, Design of LEBT and Discussions

In our previous paper [4], we described a 6-lens ESQ LEBT system developed at the University of Maryland. The predicted performance of the ESQ LEBT are now examined in the light of beam parameters relevant to the SSCL program. Two types of H^- sources are considered in the SSCL injector development – a volume source and a magnetron source.

In the context of the volume source, we have used the beam parameters corresponding to a Brookhaven National Laboratory (BNL)-type source [5]. A 30 mA, 35 kV H^- beam is extracted through a 1 cm^2 circular aperture. A parallel beam is assumed to emerge from the extraction aperture. The beam envelope through a compact 6-lens ESQ LEBT section (Fig.1), which has been constructed in-house at

*Supported by ONR/SDIO and DoE Contract #DE-AC35-89ER40486.

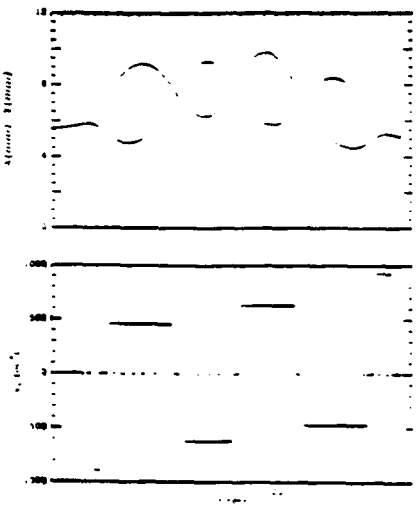

Figure 2: Linear beam optics result for a parallel input beam. Top: Amplitude (X, Y) of the beam envelope through the ESQ LEBT along x (solid line) and y (dotted line); bottom: focusing function, κ. z is the direction of propagation of the beam.

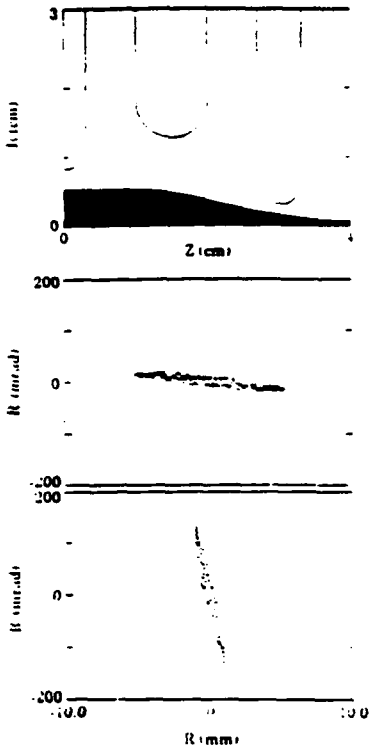

Figure 3: SNOW-2D results for the einzel lens module. Top: Beam trajectory through the einzel lens module. The center electrode is at −36 kV and the two end electrodes are grounded. Middle: Phase-space distribution of the input beam. Bottom: Phase-space distribution of the output beam.

Maryland, is computed by integrating the K-V envelope equations using a fourth-order Runge-Kutta method. Figure 2 shows the beam envelopes, when a linear external focusing force represented by a hard-edge focusing function, $\kappa(z)$, is assumed. As mentioned in the previous article [4], the SSCL RFQ requires a circular beam of about 1.3 mm in radius and a beam convergence of about −90 mrad at r_{max}. To match these conditions without sacrificing the emittance growth, an additional unit, a single-piece einzel lens module, is included at the end of the ESQ LEBT section (Fig.1). The particle distribution at the output of the ESQ LEBT is computed using a modified PARMILA code [6], and it does not show any significant emittance growth, $\lesssim$ 5%. Results in a similar situation have been shown earlier [4]: this point is not elaborated further. The einzel lens turns the moderately convergent (∼ −20 mrad) beam from the ESQ LEBT into a strongly convergent (∼ −110 mrad) beam with a negligible emittance dilution, $\lesssim$ 5%. The behavior of the beam through the einzel lens section, predicted by the SNOW-2D code, is shown in Fig.3.

The aforementioned analyses have been carried out using the parameters of a 30 mA, 35 kV H^- beam extracted from the SSCL magnetron source. The characteristics of the beam are measured at a distance of 11.75 cm downstream from the tip of the extraction cone. Using these results as initial beam conditions, the beam parameters at the tip of the extraction cone are predicted. A plausible estimate of the beam parameters at the tip of the extraction cone is: beam radius = 1.1 mm, and divergence at r_{max} = 72 mrad.

The lens aperture in the ESQ LEBT in Fig.1 is not large enough to accommodate the highly diverging H^- beam from the magnetron source. A preliminary design study reveals that the aperture of the ESQ lenses, second through fifth in Fig.1, is to be increased by a factor of 2; this demands a higher voltage on the quadrupoles. The beam dynamics through the ESQ LEBT is followed using the modified PARMILA code. Figure 4 shows the output beam distribution (bottom figure), when a K-V type input beam (top figure) is assumed. The ground plate in front of the second lens in Fig.1 has been used as a beam scraper to reject about 15% of the beam particles, which contribute significantly to the emittance growth. The output beam in Fig.4 still suffers from some distortions, giving rise to an emittance growth by a factor of about 1.5. Further optimization of the ESQ LEBT is warranted to improve the present situation. Nevertheless,

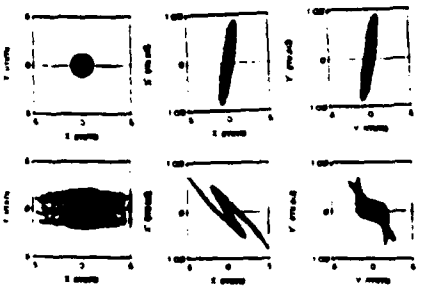

Figure 4: Modified PARMILA results on particle distribution for H^- beam from the SSCL magnetron source. Top: input to the ESQ LEBT. Bottom: output from the ESQ LEBT.

an output beam current of $\gtrsim$ 25 mA, as required for the SSC RFQ, is achievable from the ESQ LEBT. In regard to matching the beam to the RFQ, an einzel lens module is included at the end of the ESQ LEBT. Figure 5 shows preliminary results of beam transport through the einzel lens module. The smooth nature of the input beam is an artifact of modeling it from an estimate of the effective values of beam parameters in Fig. 4. The einzel lens does not contribute to the emittance growth: the beam parameters at the front end of the third electrode (at ground potential) match closely to the acceptance ellipse of the SSCL RFQ.

The above analyses for the LEBT have been done in two separate stages– first the ESQ lenses with modified PARMILA and then, the einzel lens with SNOW-2D. The simulation predictions will hold well, if the matching between the two codes is complimentary. An effort is being made to include the option of an einzel lens in the modified PARMILA, when a more reliable design tool will be available.

Conclusions

The problem of low-energy beam transport and its matching to an RFQ has been studied in reference to two special cases of the input H^- beam: (i) a parallel beam, and (ii) a highly divergent beam. The computational results suggest that the key point in designing an efficient H^- injector (ion source-cum-LEBT) relates to achieving a well-conditioned beam, e.g., unaberrated and near-parallel, from the ion source. An emphasis is laid here to develope an LEBT apparatus with compactness, mechanical stability and flexibility for easy modifications. A combination of a 6-lens ESQ module and one short einzel lens module, as adapted in the present LEBT design, appears to be a good choice in this respect. An experiment is being planned on the SSCL test stand to study the beam characteristics through the ESQ LEBT system developed at Maryland, and test the reliability of simulation predictions.

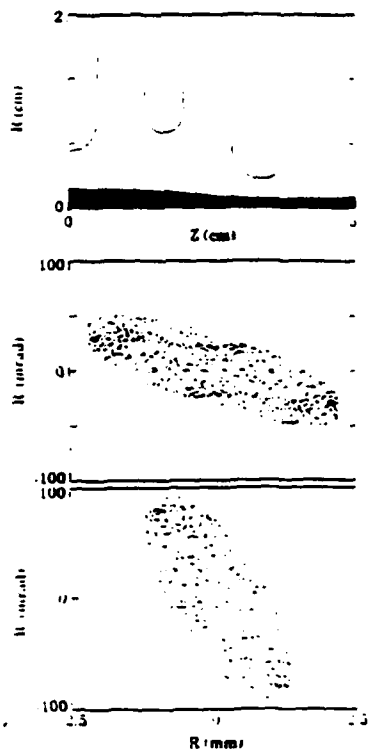

Figure 5: SNOW-2D results for the einzel lens module. Top: Beam trajectory. The center electrode is at −36 kV. Middle: Phase-space distribution of the input beam (Effective values from Fig. 4 are used to model it.) Bottom: Phase-space distribution of the output beam.

References

[1] L.W. Funk, these Proceedings, paper #MO1-2.

[2] D. Raparia, et al., these Proceedings, paper #MO4-65; ibid, paper #MO4-66.

[3] K. Saadatmand, et al., these Proceedings, paper #MO4-20.

[4] S.K. Guharay, et al., Proc. 9th International Conf. on High-Power Particle Beams, Washington, D.C., May 25-29, 1992, paper #PB36 (to be published).

[5] J.G. Alessi, private communication.

[6] C.R. Chang, et al., SPIE Proc. on Intense Microwave and Particle Beams, vol.1226, p.483 (1990).

Paper submitted to Nuclear Instruments & Methods in Physics Research.

Study of Beam Dynamics for an Intense, High-Brightness H^- Beam to Design an Efficient Low-Energy Beam Transport Using ESQ Lenses

S. K. Guharay, C. K. Allen, M. Reiser

Laboratory for Plasma Research, University of Maryland, College Park, MD 20742, USA

Abstract

With an aim of transporting an initially diverging high-perveance (generalized beam perveance $2I_b/I_0\beta^3\gamma^3 = 0.003$), high-brightness (normalized brightness $\sim 10^{11}$ A/(m-rad)^2) H^- beam and finally focusing it without any significant emittance dilution, a detailed simulation scheme has been set up incorporating the various nonlinear forces due to the beam and the external focusing elements, e.g., due to space charges, geometrical and chromatic aberrations. The analysis is done following a particular hierarchy to identify the mechanism of emittance growth; this procedure is used to optimize the lens parameters. A combination of six electrostatic quadrupole lenses is configured to deliver a satisfactory solution. The estimated emittance growth is a factor of about 1.6, and this is mainly due to chromatic aberrations. A relatively small group of particles is found to be responsible for the emittance growth. The analysis highlights a number of important issues, e.g., sensitivity to the beam distribution, beam current, lens misalignments, etc. An ESQ LEBT system with some novel features in terms of compactness and mechanical rigidity is developed, and its essential characteristics are described.

1. Introduction

The study of high-brightness charged particle beam transport has great relevance in many modern applications. In today's and next generation's high energy colliders, e.g., Tevatron, SSC, NLC, etc., one of the vital requirements is to achieve luminosity of colliding charged particle beams of order 10^{31} cm^{-2} s^{-1} or higher; this demands that beam brightness also be very high [1]. H^- beams, with normalized brightness of $\gtrsim 10^{12}$ A/(m-rad)^2, are required in space defense for generation of intense particle beams to probe any foreign objects. The importance of high intensity, high-brightness beams is also evident in heavy-ion fusion (HIF), free electron lasers, etc., and of late, in an attractive scheme for radio-active waste transmutation [2]. The recent trends of ion-beam related research in accelerators and fusion reveal that major activities have been initiated with H^- beams due to their merits over proton beams:

(a) Given a phase-space area, the intensity of an H^- beam can be enhanced significantly by adapting the principle of non-Liouvillian stacking. This is particularly useful in modern accelerators.

(b) The charge-exchange cross section at energy $\gtrsim$ 100 keV is much higher for H^- beams; hence, H^- beams are used for the development of high-energy neutral beams in magnetic fusion research and also in space defense.

During its long travel through the various components in an accelerator, the characteristics of an ion beam are significantly determined by its behavior in the early stages, e.g., extraction optics in the ion source and subsequently, the low-energy beam transport (LEBT) section. The crux of the problem is to obtain a high quality beam (usually defined by the beam emittance) from an appropriate ion source with minimum distortions due to aberrations and nonlinear forces, and to preserve its quality, as much as possible, in the transport and acceleration chain. This article focuses on the LEBT section as a systematic study on this part is still missing, particularly in relevance to transport and focusing of space-charge dominated, high-brightness H^- beams.

The LEBT section isolates the first stage of acceleration, e.g., a radio-frequency quadrupole accelerator (RFQ), from an ion source providing a buffer space for differential pumping; also, it presents a clean, matched beam to an RFQ. The gas focusing scheme, usually supplemented by magnetic quadrupoles or solenoidal magnets, has been mostly used as a LEBT system [3-5]. The advantage of the scheme is that the experimental hardware is simple, and it is capable of handling large beam current, $\gtrsim$ 100 mA. However, this scheme is not well suited to beam pulses shorter than the gas neutralization time, typically > 50 μs. Also, due to the complex nature of atomic and molecular processes involved, it is difficult to set up accurate computer simulation models and obtain reliable predictions apriori. Thus our understanding of this approach remains at a qualitative level, and there is some ambiguity in the definition of the control parameters in experiments. One of the most impressive applications of the gas focusing scheme has been in the context of the BEAR (Beam Experiment Aboard a Rocket) accelerator program at Los Alamos [4]. Results on the sensitivity of beam parameters to variations of the gas pressure suggest that a reproducible operation of such a scheme is very difficult. The other LEBT schemes include radio-frequency quadrupole (RFQ) lenses [6] and electrostatic lenses [7-12], e.g., einzel lens, electrostatic quadrupole (ESQ) lens, and helical electrostatic quadrupole (HESQ) lens. Until now, the utility of RFQ lenses has been least explored. In the category of electrostatic lenses, einzel lenses are commonly used. The conventional einzel lenses have a drawback in that plasmas may build up in the field-free region, rendering the system susceptable to beam-plasma instabilities. Anderson's "ring" lens version appears to be free from this problem [8]. The einzel lenses require power supplies close to the beam voltage, typically $\sim$ 30 kV for a 35 kV beam; the ESQ lenses have an edge over the einzel lenses in this respect. Several practical factors, e.g., tuning with low-voltage power supplies (typically $<$ 10 kV), elimination of any field-free region, and ease of computer modeling, make the ESQ system a very attractive choice as a LEBT. Reiser [13] reported briefly a comparative study of the aforementioned LEBT schemes. It is understood that in spite of a good deal of research involving LEBT systems, a systematic study of beam dynamics and optimization of LEBT parameters has not been made in the context of transporting intense,

high-brightness H^- beams. In order to obtain insight into the problem and advance the present state-of-the art of LEBT systems, detailed simulation studies should be first made, and the simulation predictions compared with experimental results. In a recent article Bru enumerated a beam transport program in which all the forces are considered linear [14]. The present article addresses in detail for the first time the beam dynamics issues relevant to designing an ESQ LEBT for intense, high-brightness H^- beams incorporating the various nonlinear effects due to aberrations, fringe-fields, etc.; a special emphasis is given here to understanding emittance growth and methods to control it. Typical beam parameters of a Penning-Dudnikov type ion source are considered in which the generalized beam perveance $K = 0.003$ and normalized beam brightness $B_n \sim 10^{11}$ A/(m-rad)^2). Here, K is defined as the ratio of $2I_b/I_0\beta^3\gamma^3$, where I_b is the beam current, I_0 is the characteristic current (3.1×10^7 A for H^- beam), $\beta = v/c$, $\gamma = (1-\beta^2)^{-1/2}$.

Some key physics issues on emittance growth in an ESQ LEBT and its control are investigated in detail. The simulation scheme is developed in steps. A linear beam optics code is written to integrate the well-known K-V envelope equations. The lens parameters are approximated from this analysis. A 3D Laplace solver maps the equipotentials of the lens system, and the fringe fields are evaluated. Several articles have dealt with fringe fields [15-20]. Following the method of Matsuda and Wollnik [19], the effect of the fringe fields is included here in a particle simulation code, which essentially is a modified version of the well-known PARMILA code [21]. The evolution of emittance through the ESQ LEBT channel is determined from the modified PARMILA code. This simulation scheme is iterated until a satisfactory solution is obtained. The analysis is made here in the context of transporting an initially round (radius = 1 mm), diverging (slope = 20 mrad at the full beam radius) 30 mA, 35 kV H^- beam over a length of about 30 cm and transforming it into a round (radius $\sim$ 1 mm), converging (slope ~ -40 mrad) beam. The control parameters of an ESQ lens can be simulated reasonably well, and this permits to delineate an in-depth investigation of the various sources of emittance dilution. This study thus establishes a strong foundation for designing an efficient LEBT system. Some comments are made on the development of

the LEBT system and its experimental tests; details are beyond the scope of this paper and these issues will be reported elsewhere.

Section 2 pertains to the beam dynamics. Some characteristic features of the LEBT system are given in Section 3. Section 4 includes conclusions.

2. Beam Dynamics through the ESQ LEBT

A. Linear beam optics calculations

The study of beam dynamics in an ESQ LEBT system is developed from a rather simple, idealistic model in order to set up the lens parameters grossly. Afterwards, the simulation is done including various practical features , e.g., real geometry of the electrodes, fringe fields, aberrations, etc. First, a beam optics code, which includes a linear external focusing force, here a hard-edge type, in the K-V envelope equations is used; this integrates the following coupled equations by fourth-order Runge-Kutta method and gives the behavior of the beam envelope.

$$X'' + \kappa_x(z)X - \frac{2K}{X+Y} - \frac{\epsilon_x^2}{X^3} = 0,$$

$$Y'' + \kappa_y(z)Y - \frac{2K}{X+Y} - \frac{\epsilon_y^2}{Y^3} = 0.$$

ϵ_x and ϵ_y are the x and y components of the unnormalized beam emittance, respectively. The focusing function due to the externally applied force is $\kappa = V_q/(V_b R_q^2)$, where V_q is the applied voltage on the quadrupole, V_b is the beam extraction voltage, and R_q is the aperture radius of the aperture radius of the quadrupole. The derivatives are taken with respect to z, which follows the direction of propagation of the beam. The amplitude of the beam envelope, $X(z)$ and $Y(z)$, is determined using certain values of the input beam parameters and an assumed configuration of the lens geometry. In the case of any gas accumulation in the channel, which may occur at the interface between an ion source and a LEBT, the above equations are solved with the beam perveance term K multiplied by $(1 - \gamma^2 f)$; f is the charge neutralization factor and $\gamma = (1 - \beta^2)^{-1/2}$.

In order to validate the results predicted by the linear beam optics code, the various nonlinear contributions, namely due to aberrations, fringe fields and image effects, are to be

minimized. The following constraints control the nonlinear effects [22].

(i) If the maximum beam excursion is not allowed to exceed 10% of the length of a quadrupole l, spherical aberrations may be kept at low level.

(ii) To reduce chromatic aberrations, the change in the beam energy due to the quadrupole focusing field should be less than about 5% of the total beam energy qV_b.

(iii) The image field may be neglected if the maximum excursion of the beam envelope remains within 75% of the quadrupole aperture radius R_q.

The following empirical relationship is satisfied to avoid any voltage breakdown [27]

$$d\ (\text{cm}) > 1.4 \times 10^{-3} V^{3/2}\ (\text{kV}),$$

where d is the interelectrode spacing and V is the voltage difference.

Due to limited accessibility in the neighborhood of the beam extraction region, it is difficult to obtain a reliable knowledge of beam parameters at the extraction point; this introduces some ambiguity in the initial values of the beam parameters which are given as input to the code. Usually measurements are made at a distance of about 10 cm downstream from the extraction slit and the data are interpolated using some simulation model to predict beam parameters at the extraction point. Table 1 lists the estimated values of the H^- beam parameters corresponding to the Penning-Dudnikov source used in the BEAR experiment, when the nominal emittance data [24] measured at a distance of 10.6 cm downstream from the extraction aperture have been used.

The desired solution is obtained after several iterations, when the lens parameters (e.g., aperture and dimensions of the individual lenses, spacing between the lenses, and number of lens elements) are adjusted at each step. As mentioned earlier, the beam envelope is constrained at each stage through the LEBT system so that distortions due to aberrations and image effects are minimized. The LEBT system has been thus configured using a set of six ESQ lenses. The geometrical parameters of the lenses are given in Table 2. Here l is

the length of an electrode and L is the separation between adjacent lenses. Note that the geometrical parameters conform to a symmetric triplet configuration.

Figure 1 shows the K-V envelope solution (top figure), when the input beam parameters correspond to Table 1 and a hard-edge type focusing function (bottom figure), $\kappa(z)$, is assumed. The voltages on the three sets of similar lenses (1 and 6, 2 and 5, and 3 and 4) are, respectively, 7.825, 3.875, and 3.820 kV. The envelope parameters of the output beam (designated by subscripts f) at two locations are given in Table 3 to elucidate the nature of focusing. $z = 287$ mm corresponds to the end of the last lens in the LEBT. These results suggest that the ESQ LEBT system can deliver a converging, round beam to the next stage, typically an RFQ in the linear accelerator section, and the beam will be well matched if the RFQ entrance is very closely (< 1 cm) coupled to the last lens of the LEBT.

An intriguing feature in the present LEBT is that the combination of the four lenses (number 1, 2, 5, and 6) is used to transform the diverging input beam into a converging one, while the other two lenses (number 3 and 4) act as a FODO transport section providing an adequate length of the LEBT. The FODO section may be cascaded to obtain any desired length of the LEBT.

B. 3D field mapping and evaluation of fringe fields

The exact geometry of the lens system is used, and the equipotentials are mapped solving the 3D Laplace equation. Cylindrical electrodes with some shaping of the end faces following Laslett [25] and Dayton et al. [26] are used, when the field is expected to be quadrupolar within about 90% of the lens aperture. In order to minimize interference between two adjacent lenses [27], a grounded plate is inserted between the lenses. Figure 2 shows the equipotentials of the ESQ lens system. Following the notations of Matsuda and Wollnik [19], the potential distribution due to a quadrupole lens follows a symmetric behavior as

$$\begin{aligned} \phi(x,y,z) &= -\phi(-x,y,z), \\ \phi(x,y,z) &= -\phi(x,-y,z), \\ \phi(x,y,z) &= \phi(x,y,-z), \end{aligned}$$

if the four electrodes in a lens are biased at alternately positive and negative potentials. The

potential distribution ϕ can be expressed as

$$\phi(x,y,z) = \frac{k(z)}{2}(x^2 - y^2) - \frac{k''(z)}{24}(x^4 - y^4) + \ldots,$$

up to the fourth order, while the electrostatic field components are governed by

$$\begin{aligned} E_x(x,y,z) &= -k(z)x + \tfrac{k''(z)}{6}x^3 + \ldots, \\ E_y(x,y,z) &= k(z)y - \tfrac{k''(z)}{6}y^3 - \ldots, \\ E_z(x,y,z) &= 0 - \tfrac{k'(z)}{2}(x^2 - y^2) + \ldots, \end{aligned}$$

up to the third order. The first term in the above expressions represent the field components of a pure quadrupolar field; the fringe field, which has a nonlinear behavior, contributes due to the second derivative term in k for E_x and E_y and is governed by k' for E_z. The function $k(z)$ is determined from the equipotentials. This result in conjunction with the values of the beam amplitude at various z-locations from Fig. 1 is used to evaluate a comparative estimate of the main field and the fringe field which the beam envelope is expected to encounter in our particular design. Figure 2(a), (b), and (c) show the field components, respectively, in x, y, and z-directions; Fig. 3 shows the effective magnitude of the field components. It is evident that the contribution of the correction terms due to the fringe field is very localized over a small region towards the edges of each lens in the ESQ LEBT, and the main field significantly dominates. This suggests that geometrical aberrations may not be serious in the present ESQ system.

C. Beam dynamics calculations and analysis of the sources of emittance growth

The results from the above two steps of analysis are used in a particle simulation code, PARMILA, to study the beam dynamics in further details. This code essentially pushes particles using a chain of transfer matrices, where the matrix elements are characterised by the factors governing the motion of the beam, e.g., space charge, drift space, lens elements, etc. This code adapts the following key points.

(a) The space-charge force is calculated assuming the beam as an ensemble of typically 5000 ring-like macroparticles. The macroparticles follow certain distributions in both configuration and phase spaces, e.g., K-V, waterbag, semi-Gaussian, Gaussian, etc.

(b) The electrostatic field due to the lens is decomposed into two parts: a main field of hard-edge type within the lens region, and fringe fields outside this ideal boundary. In order to get a realistic evaluation of the hard-edge boundary which can effectively represent the quadrupolar field component of a lens, an equivalent length is defined as

$$l_{eff} = \frac{1}{\kappa_0} \int_{z_2}^{z_1} \kappa(z) dz$$

where κ_0 is the peak value of κ in the flat-top region as shown in Fig. 2, z_1 and z_2 correspond to the zero-crossing locations of $\kappa(z)$ on the immediate two opposite ends of a lens. A set of integrals involving $k(z)$, as prescribed by Matsuda and Wollnik [19], is used to model the force due to the fringe field. This force is applied at the ideal hard-edge boundary, and the shifts and bends of the particle motion due to fringe fields are incorporated in the PARMILA code [22].

(c) The trajectory of the macroparticles is followed systematically with due considerations of field distributions over a cross-section of the beam. The energy conservation law is followed to tackle this problem

$$\frac{1}{2}mv_0^2 + eV_0 = \frac{1}{2}mv(r)^2 + eV(r).$$

where v_0 and $v(r)$ denote, respectively, the velocity of particles on the axis (this is equal to $(2eV_b/m)^{1/2}$) and at an arbitrary location r, and V_0 and $V(r)$ correspond to the electrostatic potential due to the lens at the respective locations.

Figure 4 shows the behavior of the particle distribution at the output of the ESQ LEBT when a K-V type distribution of the input beam particles is assumed. The distortions in the output beam are due to nonlinear effects, and this leads to some emittance growth. In this particular example, the emittance growth is a factor of about 1.6. The ellipses composed from the Twiss parameters for the output beam show a very similar nature in the two orthogonal planes; these ellipses are drawn using the effective emittance $\epsilon = 4\bar{\epsilon}$ due to Lapostolle [29]. The corresponding characteristic beam parameters are: $X_{\max} = 1.6$ mm, $Y_{\max} = 1.3$ mm, $(X_{\max})' = -41.7$ mrad, and $(Y_{\max})' = -39.2$ mrad; a better matching of the parameters

in the two orthogonal planes may be fortuitous. Various other types of distributions, e.g., waterbag, semi-Gaussian, Gaussian, have been also considered. The particle distribution of the output beam in its configuration space is shown in Fig. 5 for the various distributions. A small group of particles ($\lesssim 5\%$) is detached from the dense core group in the case of Gausian distributions; these particles are essentially lost from the system as their location corresponds to the boundary of the electrodes. The rapid blow-up of the beam for a non-KV distribution may be an artifact of excess energy in tail particles of the distribution function. For the sake of comparison of the beam behavior in the two extreme cases, the output beams are shown in Fig. 6 for K-V and Gaussian (with the tail cut off at 4σ) distributions of the input beam. The phase-space area occupied by the core group of particles seems to be similar in the two cases. The emittance of the output beam will practically follow the dynamics of a K-V type input beam if distribution is tailored to a low-temperature beam. As a K-V type distribution is commonly used in the literature for basic analysis of beam dynamics and also, it seems to represent well the beam distribution particularly in the case of a space-charge dominated, high-brightness beam [28], we have extended our analysis assuming a K-V type distribution of the input beam.

The evolution of emittance growth, as the beam propagates through the ESQ LEBT, is shown in Fig. 7. It is noted that the emittance is primarily enhanced at the second lens in the x-plane and at the fifth lens in the y-plane. This result conforms to the previous findings from the linear beam optics code when large beam excursions (Fig. 1) have been noted at the aforementioned two lens elements; nonlinear effects act strongly when the amplitude of the beam envelope is large. In our simulation studies it is possible to diagnose the principal contributors to emittance growth and reject some of the unwanted group of particles by using appropriately shaped ground plates between the lenses as beam scrapers, and thus the emittance growth may be controlled. Figure 8 shows an emittance growth by a factor of about 1.3 only when a beam scraper is introduced between the third and fourth lenses; about 15% of the beam particles is rejected here. This seems to be an easy way to control emittance of the output beam.

In an effort to further understand the effect of nonlinear forces, the architecture of the simulation code is made appropriately to evaluate the contribution of various factors piecewise, i.e., term by term. First, the transverse energy of all the beam particles is numerically maintained at a constant value through the entire LEBT. Figure 9 shows the output beam distribution. It is evident that the output beam is free from any major distortions. The emittance growth is estimated to be reduced by more than 90%. This suggests that the chromatic aberration is the principal contributor to emittance growth in the present case. Turning the fringe-field terms off in the simulation, it is noted that the emittance growth is reduced very insignificantly. This indicates that geometrical aberrations do not play a major role here.

The sensitivity of output beam parameters with variation of beam voltage, beam current, injection error has been studied. Using the linear beam optics code it is noted that the beam parameters do not change noticeably for a $\pm$ 1% change of quad voltage (from the ideal setpoint) on all the lenses simultaneously. Similar insensitivity is noted for variation of beam current (ideal = 30 mA) within a few milliamperes. The effect of an injection error is studied using PARMILA. With the variation of the amount of off-centering of the input beam, the qualitative nature of the phase-space distribution of the output beam remains almost invariant, while the beam centroid shifts coherently. A translational off-centering by 1 mil (= 0.0254 mm) at the input causes an off-centering of the beam by about 3 mil at the output of the LEBT; this also introduces an angular error of the beam centroid by about 1.5 mrad. An on-centered input beam with an error in the injection angle by 1 mrad shows an off-centering of the output beam by about 2 mil; the error in the angle does not change appreciably through the LEBT channel.

3. Development of the ESQ LEBT apparatus

The aforementioned guidelines are used to develop an ESQ LEBT system. Figure 10 shows a schematic of the LEBT system developed in-house at Maryland. The principal elements of the ESQ LEBT are: (i) six lenses, each consisting of four quadrupoles, (ii)

ground plates between the lenses, and (iii) precision ceramic insulating balls. The four quadrupoles of each lens are machined out of a single piece of finished cylindrical aluminium rod. The dimensional accuracy of each electrode is measured to be within $\pm$ 0.2 mil (average) of the designed value. The aluminium ground plates are 2 mm thick. Ceramic balls are used to develop an adjustment-free, self-aligned lens assembly. Two sets of precision balls with tolerance in sphericity within $\pm$ 0.025 mil are used. Larger balls of 3/8 inch diameter are used between two opposing quadrupoles of adjacent lenses; smaller balls of 1/8 inch diameter are placed between a quadrupole and its neighboring ground plate. The ceramic balls are hidden in the shadow of the electrodes in order that they remain mostly obscured to the field of the propagating beam. The entire lens assembly is mounted in a cylindrical housing, which is installed in a large vacuum vessel.

Voltage hold-off tests have been conducted on the lens assembly. With gradual conditioning of the surface of the electrodes by allowing some low-level corona discharges, the lens system could finally be driven at high voltage (up to about $\pm$ 14 kV) without any noticeable breakdown. This insures practicability of the present ESQ lens design.

4. Conclusions

This article addresses the problems of designing an efficient low-energy beam transport system, particularly in relevance to space-charge dominated, high-brightness H^- beams. Although several researchers used ESQ LEBT systems in the past and showed some interesting results, the input beam parameters were not as severe as considered in the present case in terms of space-charge forces, beam divergence, etc.; further systematic study of beam dynamics has thus been missing. An emphasis is given here on simulation studies to examine some beam physics issues critically. This approach lays a foundation to develop an efficient LEBT system; especially, the role of the various nonlinear forces on emittance dilution is studied in depth.

The lens assembly is designed following several iterations of the numerical scheme so that the lens geometry is optimized as much as possible. Typical beam characteristics of a

high-brightness H^- source, Penning-Dudnikov type (as used in the BEAR experiment [4]), are used in the analysis with an aim of transporting a space-charge dominated, diverging beam from the source over a length of about 30 cm, and yield a converging beam at the end without significantly deteriorating the intrinsic emittance of the beam. The beam dynamics is studied in detail using a particle simulation code, which enables us to study the influence of various factors in determining the emittance growth, e.g., nonlinear effects due to chromatic aberrations and fringe fields, various types of distributions of the beam, sensitivity of various control parameters, etc.

The main contributor to emittance growth in the ESQ LEBT is found to be chromatic aberrations. It is shown in the simulations that particles responsible for enhancing the emittance growth can be identified and subsequently, they are rejected by carefully using two intermediate ground plates as beam scrapers. Thus the emittance growth can be controlled without sacrificing the beam current appreciably. In the case of the H^- beam from the Penning-Dudnikov type source the nominal emittance growth through the ESQ LEBT system is estimated to be a factor of about 1.6, while this factor is reduced to about 1.3 by rejecting only 15% of the beam particles. Such a modest value of emittance growth attributes merit to the particular design of the ESQ LEBT.

The ESQ LEBT system developed in-house at Maryland own some uniqueness in its mechanical assembly. The entire system is self-aligned and it is very rugged mechanically. Each component is fabricated with a dimensional tolerance close to the designed value. Results on voltage hold-off tests of such a compact system are encouraging; no noticeable breakdown events occur up to a voltage level of about $\pm$ 14 kV.

Beam transport experiments are planned using the ESQ LEBT. Details of the experimental work and further studies on beam dynamics will be reported elsewhere.

Acknowledgments

This work is supported by ONR/SDIO. The authors acknowledge valuable discussions with Dr. P.G. O'Shea of Los Alamos National Laboratory.

References

1. D. A. Edwards and M. J. Syphers, AIP Conf. Proc. on High-Brightness Beams for Advanced Accelerator Applications, eds. W. W. Destler and S. K. Guharay, No. 253, p. 122 (1991).

2. R. A. Jameson, ibid, p.139.

3. J. G. Alessi, J. M. Brennan and A. Kponov, Rev. Sci. Instrum. **61** (1990) 625.

4. P. G. O'Shea, et al., Nucl. Instrum. & Meth. in Phys. Res. **B40/41** (1989) 946.

5. J. Klabunde, P. Spädtke and A. Schönlein, IEEE Trans. Nucl. Sci. **NS-32** (1985) 2462.

6. D. A. Swenson, et. al., Proc. Linear Accelerator Conf., Albuquerque, 1990, p. 39.

7. C. R. Chang, Proc. Linear Accelerator Conf., Albuquerque, 1990, p.399.

8. O. A. Anderson, et al., AIP Conf. Proc. on Production and Neutralization of Negative Ions and Beams, ed. A. Hershcovitch, No. 210, p. 676 (1990).

9. W. Chupp, et al., IEEE Trans. Nucl. Science, **NS-30** (1983) 2549.

10. S. Okayama, Nucl. Instrum. & Methods in Phys. Res. **A298** (1990) 488.

11. Y. Mori, et. al., Proc. Linear Accelerator Conf., Ottawa, 1992, p.642.

12. D. Raparia, AIP Conf. Proc. on Production and Neutralization of Negative Ions and Beams, ed. A. Hershcovitch, No. 210, p.699 (1990)

13. M. Reiser, Nucl. Instrum. & Meth. in Phys. Res. **B56/57** (1991) 1050.

14. B. Bru, Nucl. Instrum & Meth. in Phys. Res. **A298** (1990) 27.

15. H. Wollnik and H. Ewald, Nucl. Instrum. & Meth. in Phys. Res. **36** (1965) 93.

16. H. Matsuda and H. Wollnik, Nucl. Instrum. & Meth. in Phys. Res. **77** (1970) 40.

17. H. Matsuda and H. Wollnik, Nucl. Instrum. & Meth. in Phys. Res. **77** (1970) 283.

18. T. Sakurai, T. Matsuo and H. Matsuda, Int. J. Mass Spectrom. Ion Processes **91** (1989) 51.

19. H. Matsuda and H. Wollnik, Nucl. Instrum. & Meth. in Phys. Res. **103** (1972) 117.

20. L. Sagalovsky, Nucl. Instrum. & Meth. in Phys. Res. **A298** (1990) 205.

21. G. Boicourt and J. Merson, Los Alamos National Lab. Report LA-UR-90-127, 1990; and references therein.

22. C. R. Chang, Ph. D. Thesis, Univ. Maryland, 1989.

23. R. Keller, AIP Conf. Proc. on High Current, High Brightness and High Duty Factor Ion Injectors, No. 139 , p. 1 (1985).

24. P. G. O'Shea, private communication.

25. L. J. Laslett, Lawrence Berkeley Report No. HI-FAN-137.

26. I. E. Dayton, et al., Rev. Sci. Instrum. **25** (1954) 485.

27. H. Wollnik, *Optics of Charged Particles*, Academic Press, 1987.

28. I. Kapchinskij, private communication

29. P. M. Lapostolle, IEEE Trans. Nucl. Sci. **NS-18** (1971) 1101.

Table 1. Estimated H^- beam parameters

Beam current I_b	30 mA
Beam voltage V_b	35 kV
$v/c = \beta$	8.6×10^{-3}
Generalized beam perveance $K(= 2I_b/I_0\beta^3\gamma^3)$	3×10^{-3}
Initial rms normalized emittance $\tilde{\epsilon}_n\pi$	0.069 π mm-mrad
Initial beam radius a	1 mm
Initial divergence of beam envelope at $r = a$	20 mrad

Table 2. ESQ lens parameters.

	Lens Number		
	1 & 6	2 & 5	3 & 4
R_q (mm)	8.00	12.00	12.00
l (mm)	15.00	59.00	47.00
L (mm)	6.00	6.00	6.00

Table 3. Beam parameters at the output end of the LEBT.

z (mm)	X_f (mm)	Y_f (mm)	X'_f (mrad)	Y'_f (mrad)
293.0	1.39	1.37	−53.1	−53.7
302.0	1.03	1.00	−24.0	−24.3

Figure Captions:

Fig. 1. X and Y are the amplitudes of the beam envelope in x and y directions; z is the direction of propagation. $\kappa_y = -\kappa_x$. Note that X (and Y) = 12 mm corresponds to the maximum aperture of the electrodes.

Fig. 2. 3D LAPLACE results of the field components: (a) E_x , (b) E_y , and (c) E_z . Solid line: pure quadrupole field; dashed line: fringe field.

Fig. 3. Effective magnitude of the fields. Solid line: quadrupole field; dashed line: fringe field.

Fig. 4. Particle distribution in the output beam (right column) of the ESQ LEBT for a K-V type input beam (left column). Note that X (and Y) = 8 mm corresponds to the aperture of the first and last lenses.

Fig. 5. Configuration-space geometry of the output beam for various input distributions: (a) K-V, (b) waterbag, (c) semi-Gaussian, and (d) Gaussian.

Fig. 6. Comparison of phase-space distribution of the particles in the output beam for K-V (left column) and Gaussian (right column) input distributions.

Fig. 7. Spatial evolution of rms emittance through the ESQ LEBT. The emittance values are plotted at the end of each lens in the LEBT.

Fig. 8. Phase-space distribution of particles in the output beam when 15% of the beam is intercepted by two beam scrapers.

Fig. 9. Particle distribution in the output beam when all the particles are assumed to be transported with the same energy (35 kV).

Fig. 10. Schematic layout of the ESQ LEBT.

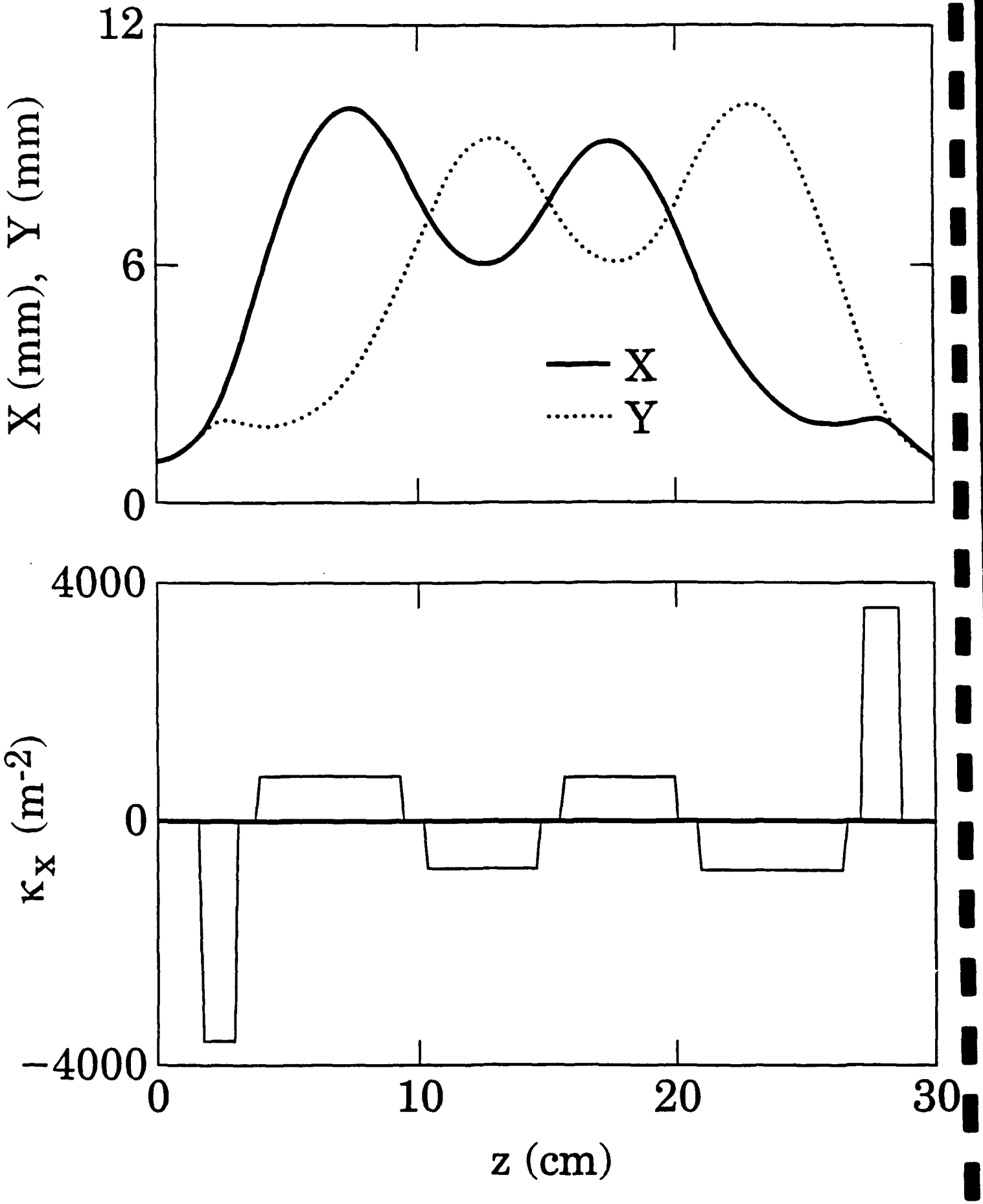
12
6
0
X (mm), Y (mm)
X
Y
4000
0
−4000
κ_x (m^{-2})
0
10
20
30
z (cm)

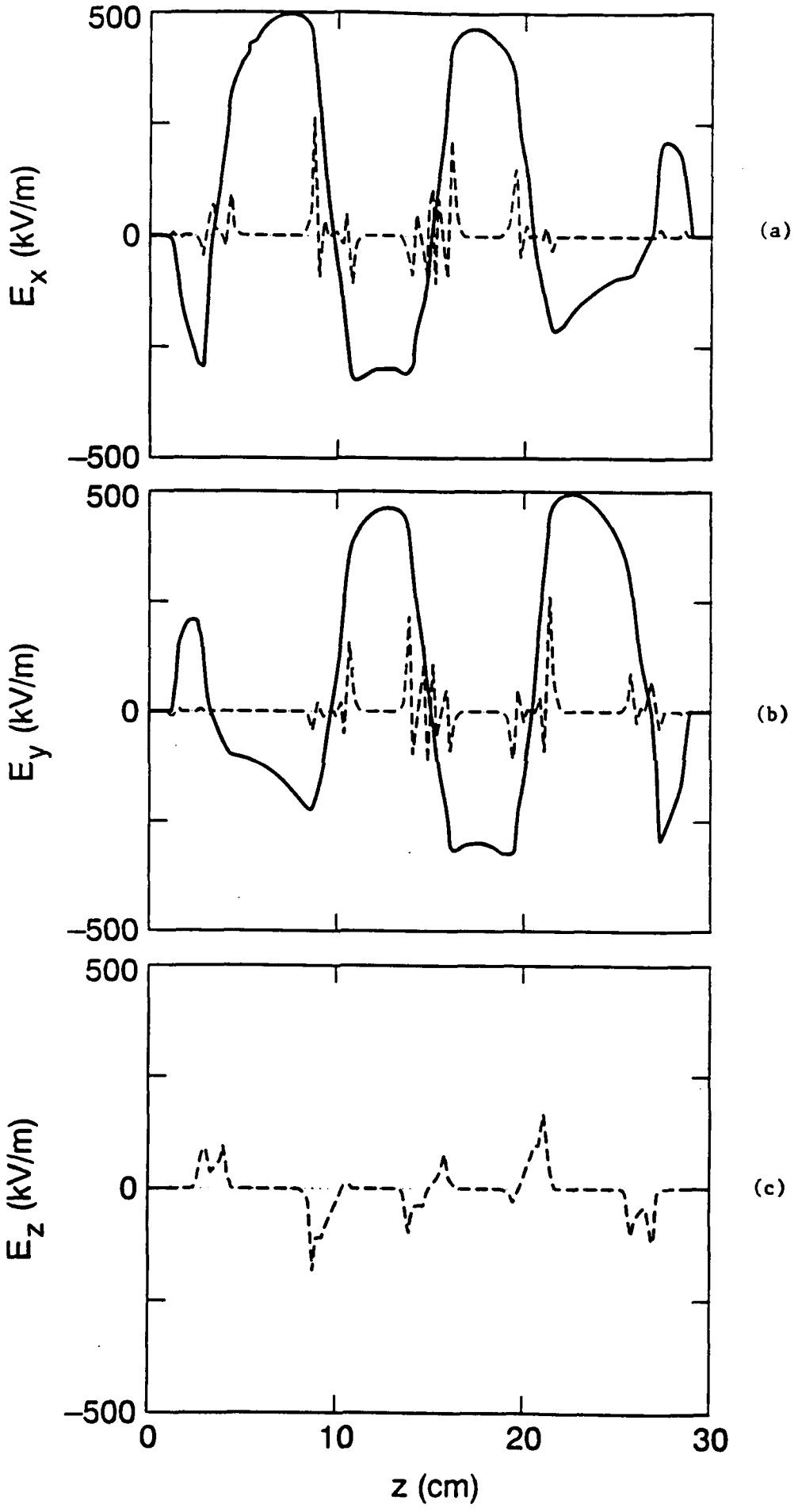
500
0
−500
E_x (kV/m)
(a)
500
0
−500
E_y (kV/m)
(b)
500
0
−500
E_z (kV/m)
(c)
0
10
20
30
z (cm)

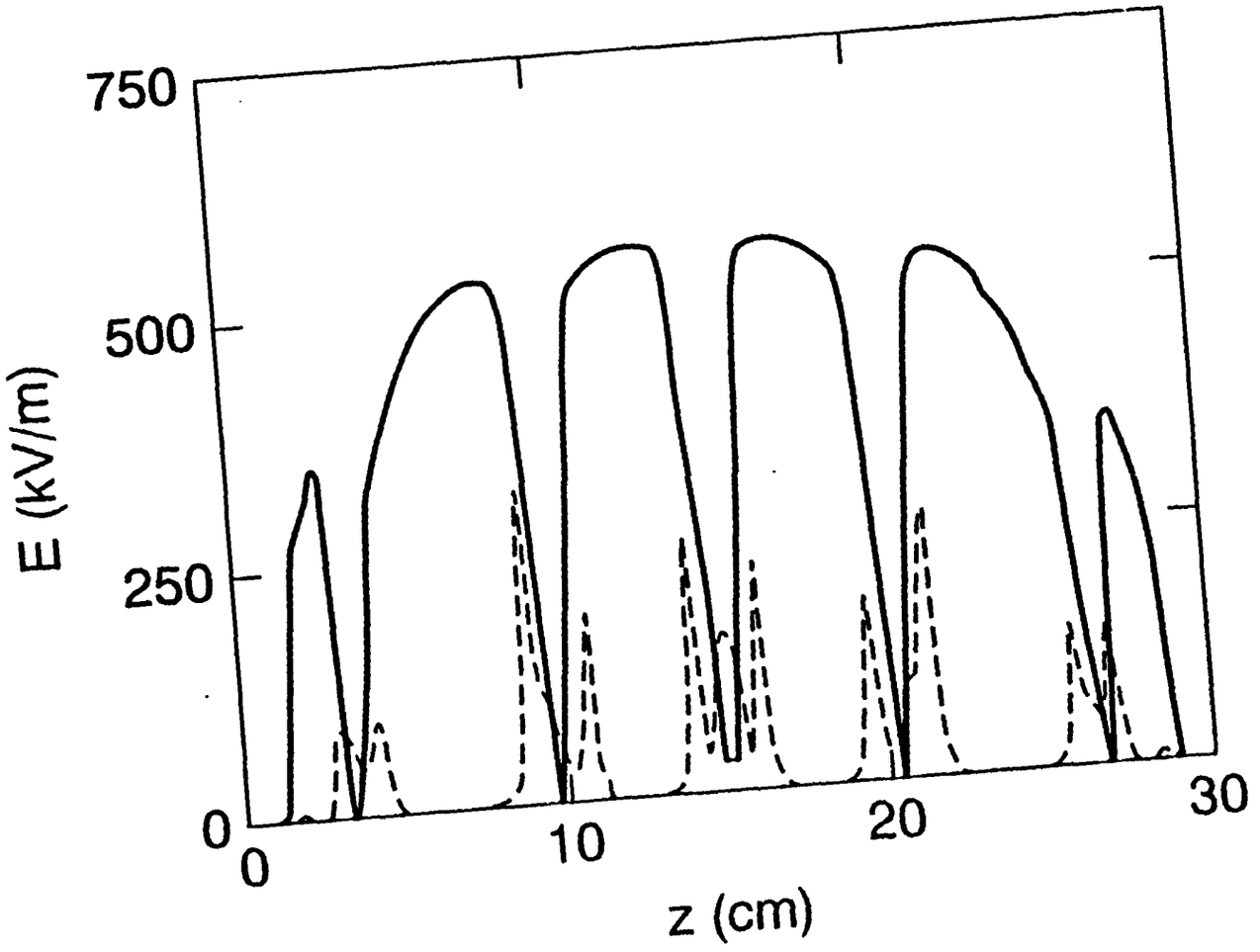
750
500
250
0
E (kV/m)
0
10
20
30
z (cm)

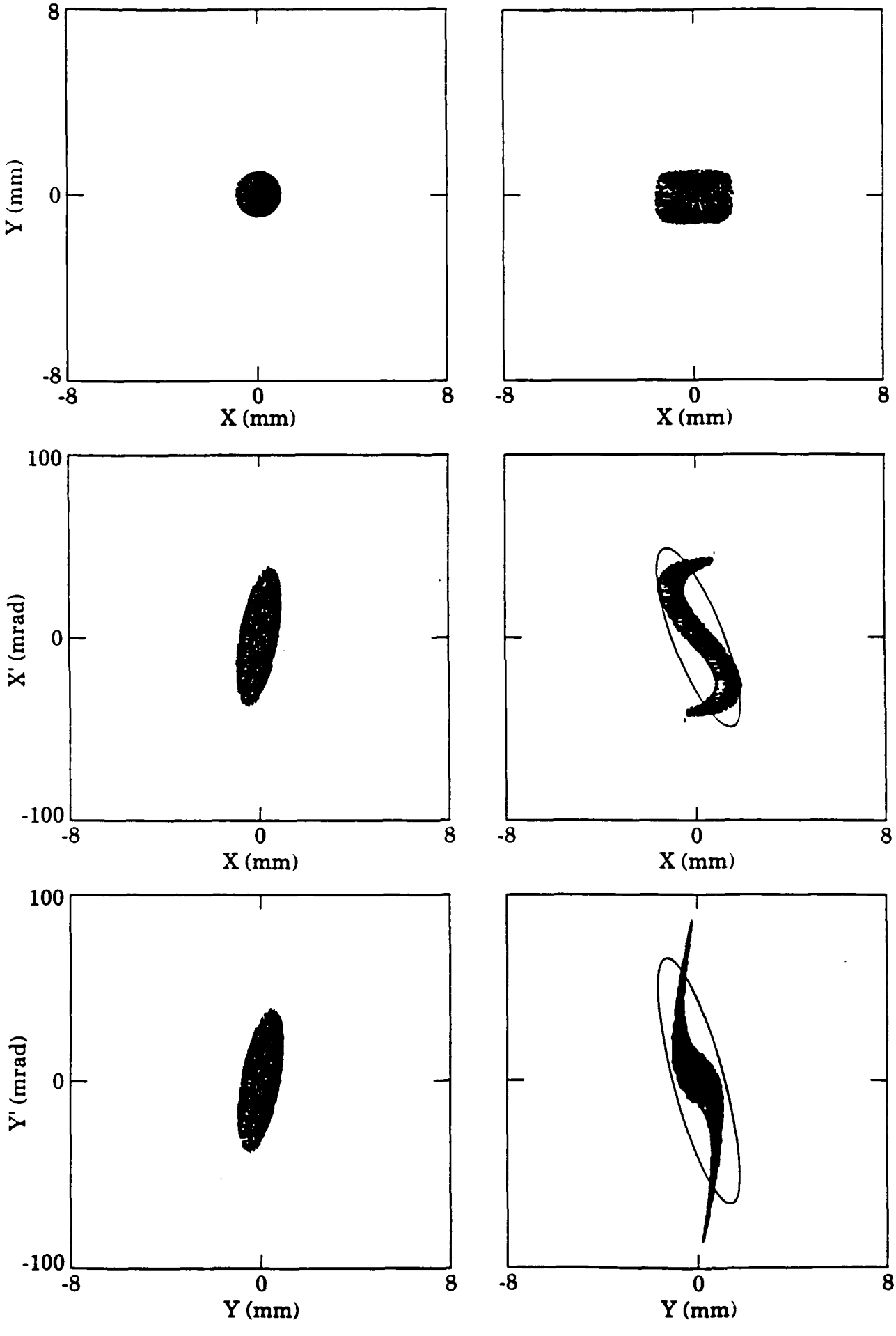
8
0
-8
Y (mm)
-8
0
8
X (mm)
8
0
-8
X (mm)
100
0
-100
X' (mrad)
-8
0
8
X (mm)
100
0
-100
Y' (mrad)
-8
0
8
Y (mm)
-8
0
8
X (mm)
-8
0
8
Y (mm)

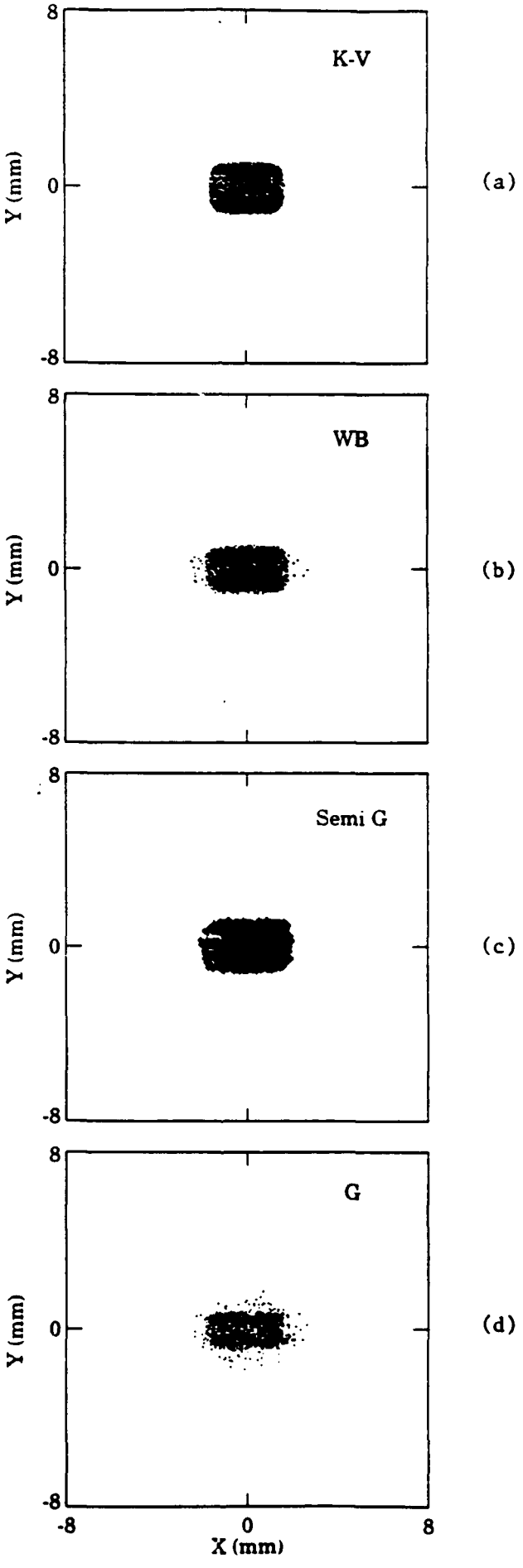
K-V
WB
Semi G
G
Y (mm)
X (mm)
8
0
-8
(a)
(b)
(c)
(d)

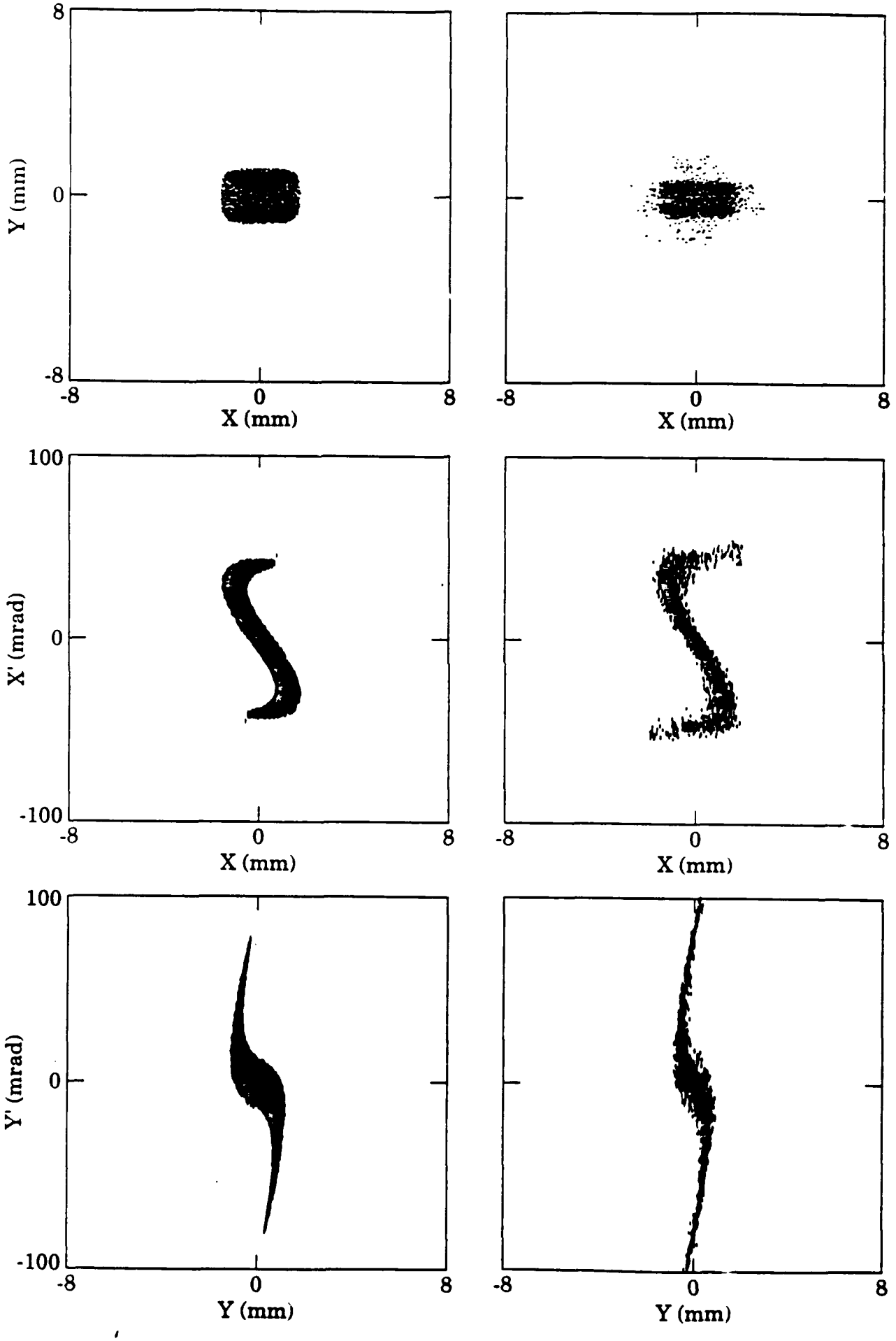
8
0
-8
Y (mm)
-8
0
8
X (mm)
100
0
-100
X' (mrad)
Y' (mrad)

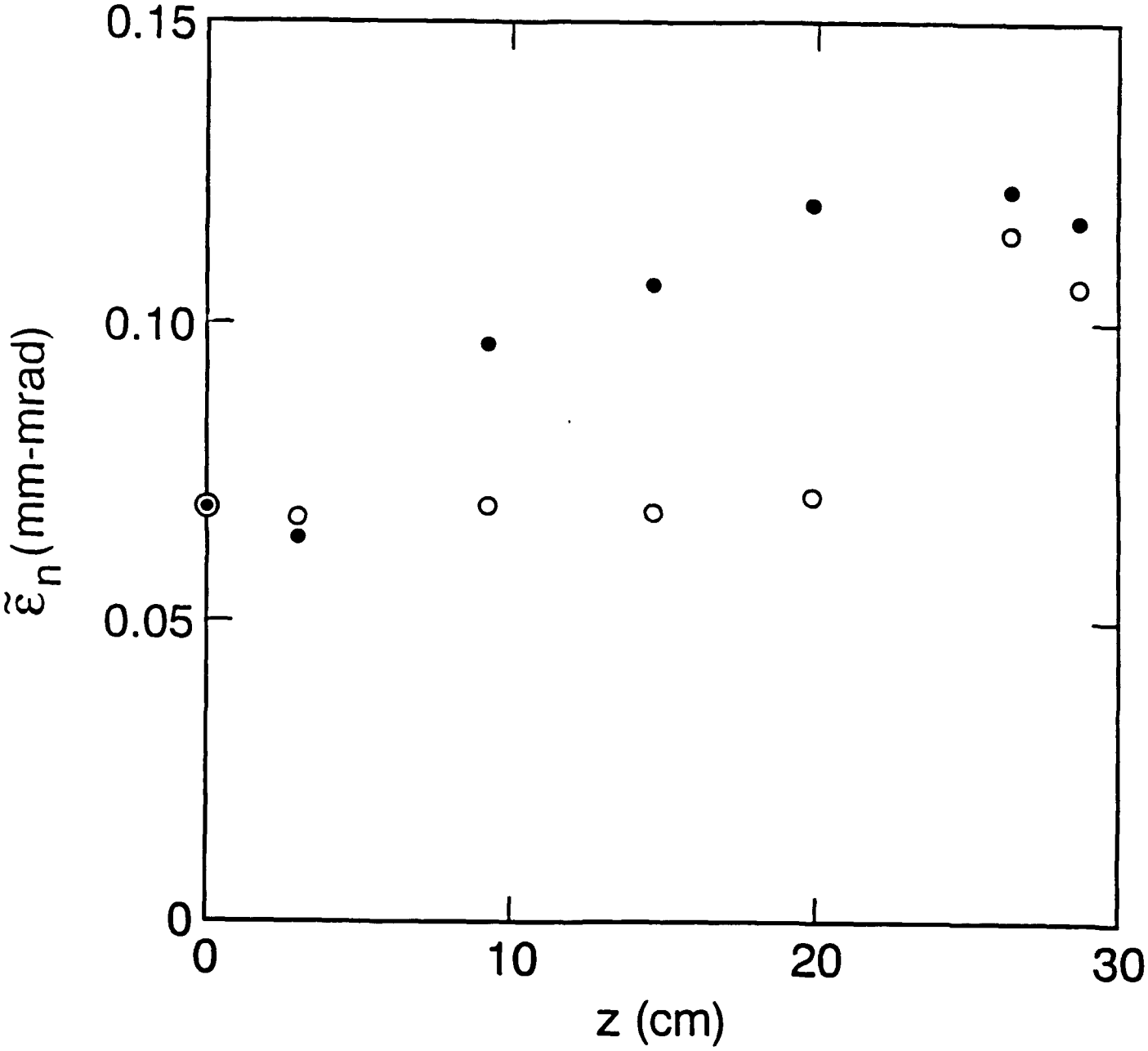
0.15
0.10
0.05
0
0
10
20
30
z (cm)
$\tilde{\varepsilon}_n$ (mm-mrad)

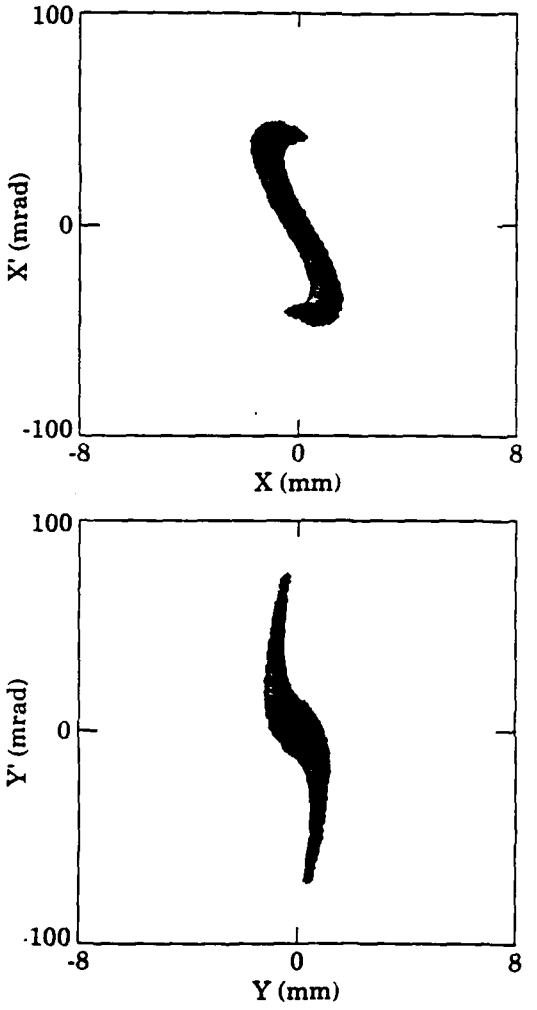
100
0
-100
X' (mrad)
-8
0
8
X (mm)
100
0
-100
Y' (mrad)
-8
0
8
Y (mm)

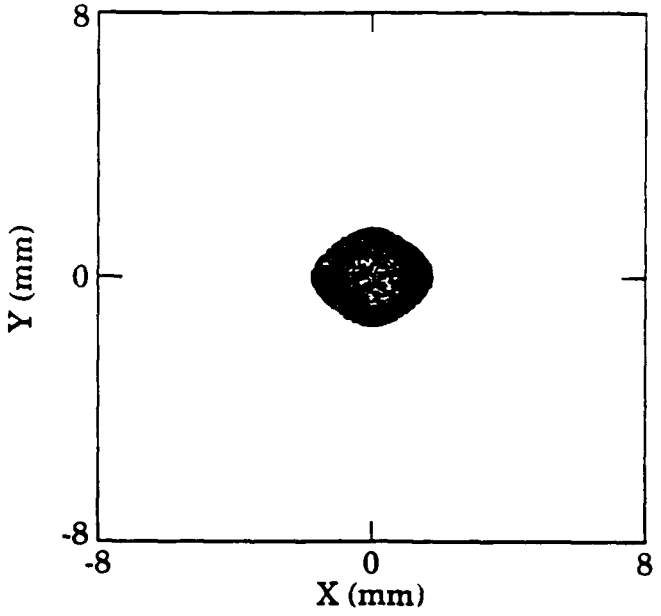
8
0
-8
Y (mm)
-8
0
8
X (mm)

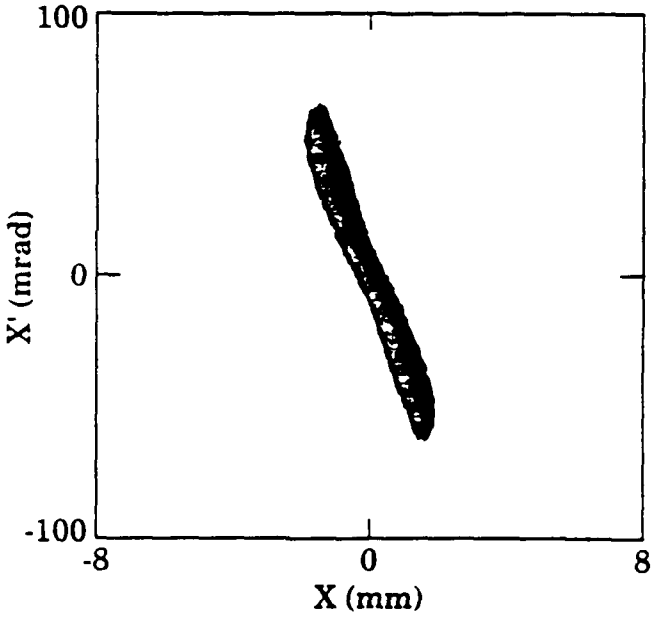
100
0
-100
X' (mrad)
-8
0
8
X (mm)

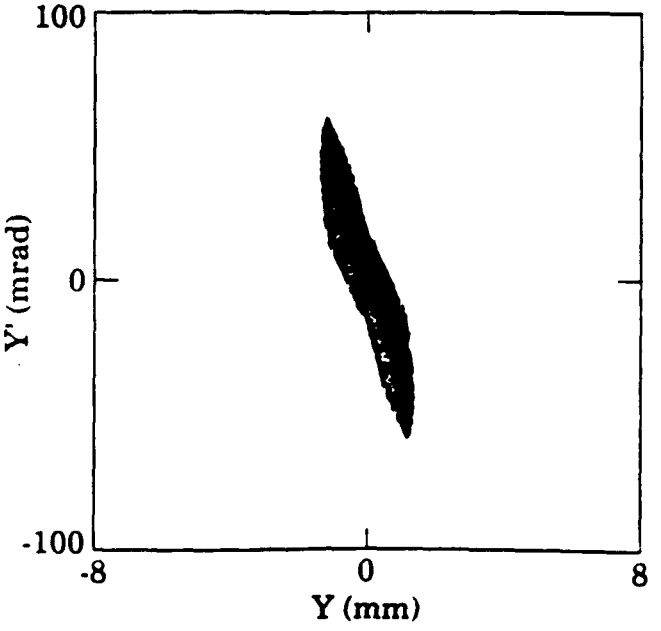
100
0
-100
Y' (mrad)
-8
0
8
Y (mm)

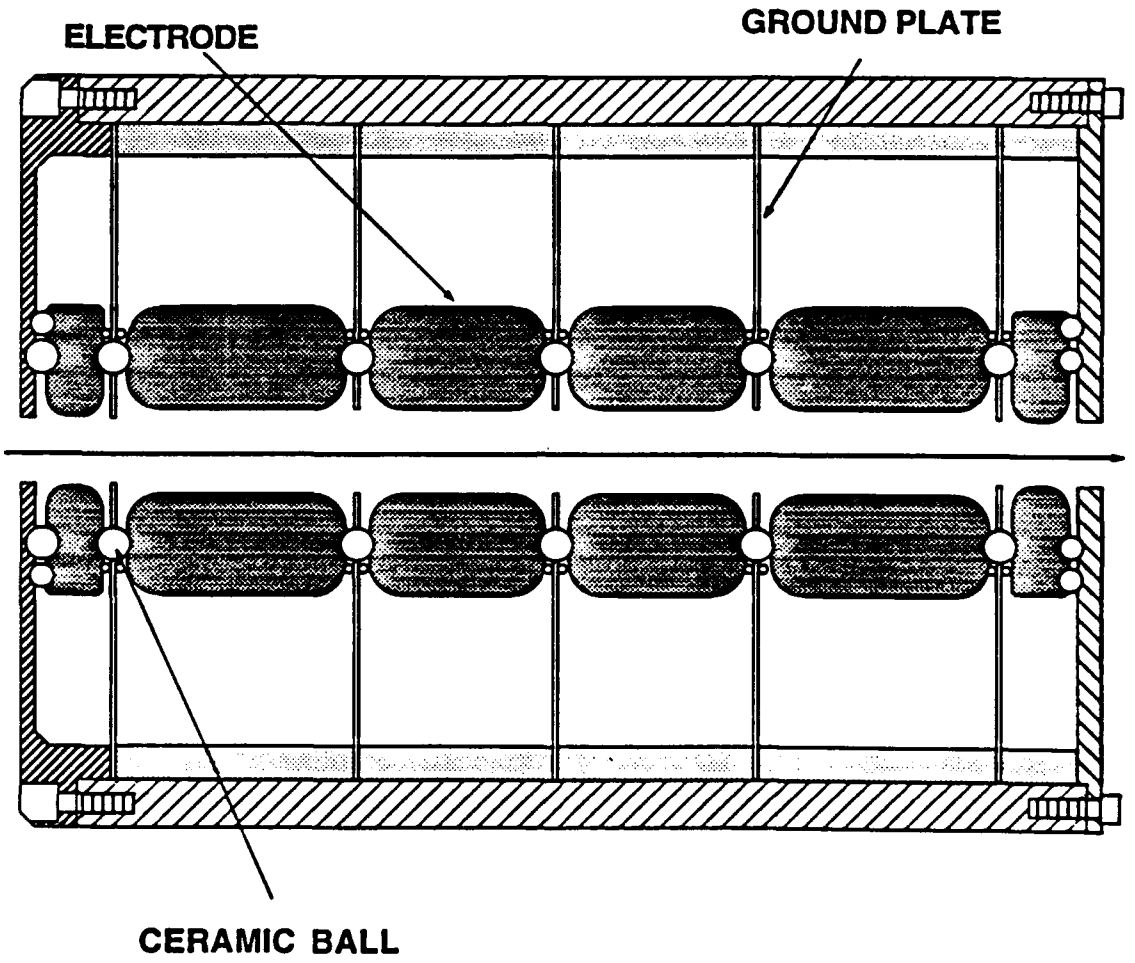
ELECTRODE
GROUND PLATE
CERAMIC BALL

Proceedings of the Particle Accelerator Conf., May 1993, Washington, DC

A Moment Method Laplace Solver for Low Energy Beam Transport Codes*

Christopher K. Allen, Samar K. Guharay, and Martin Reiser
Laboratory for Plasma Research
University of Maryland, College Park, MD 20742

Abstract

A moment method technique for solving Laplace's equation is presented. The technique is then extended to Poisson's equation to include space charge. The procedure is implemented on a PC and applied to the cases of an electrostatic quadrupole (ESQ) lens and an ellipsoidal bunch in a grounded pipe.

I. INTRODUCTION

Currently we are engaged in the design and development of a Low Energy Beam Transport (LEBT) section for H^- ion beams [1]. We have chosen to employ electrostatic lenses in this design, since for low ion velocities magnetic lenses fail to provide enough focusing for intense beams while gas focusing is intrinsically stochastic. The current prototype consists of 6 ESQ lenses. In order to model the action of such a lens it is necessary to solve Laplace's equation for the particular lens geometry. Once the lens is characterized electrically, the information may be used in other simulation tools to aid in design.

In general, numerical methods must be utilized to solve Laplace's equation. We present a technique which is fully three dimensional yet is efficient enough for implementation on a PC. The efficiency of the technique arises from the fact that it is based on an integral formulation rather than the more common differential form. Instead of solving for electrostatic potential directly, we solve for the surface charge density on conducting bodies. This results in a reduced dimensionality of the problem domain. The integral formulation also readily extends itself to Poisson's equation. Thus, we can model lenses in the presence of charge distributions. Also, since we know the surface charges, we may evaluate capacitances between various lens elements.

II. NUMERICAL TECHNIQUE

A. Laplace's Equation

Letting ϕ denote electrostatic potential, the problem is usually seen in the mathematical form

$$\begin{aligned} \nabla^2\phi(x) &= 0 \qquad \forall x\in\Omega, \\ \phi(x) &= f(x) \quad \forall x\in\Gamma. \end{aligned} \tag{1}$$

Here Ω is the 3D region of interest and Γ is its boundary (i.e. $\Gamma=\partial\Omega$). The function f represents the given boundary values and constitutes the data of the problem. Usually Ω represents the beam line and Γ is the surface of a focusing lens, thus f would be the lens voltage. A finite differencing method would typically attack this problem directly. However, we prefer to work with an integral representation of the problem rather than the differential form [2].

$$f(x) = \int_\Gamma G(x,\xi)\,\sigma(\xi)\,d^2\xi, \tag{2}$$

where

$$G(x,\xi) = \frac{1}{4\pi\,|x-\xi|} \tag{3}$$

is the free space Green's function for Poisson's equation. The function σ is introduced as the new unknown for the problem. It is recognized as the surface charge density on the boundary Γ. Once σ is known, ϕ may be recovered via

$$\phi(x) = \int_\Gamma G(x,\xi)\,\sigma(\xi)\,d^2\xi \qquad \forall x\in\Omega. \tag{4}$$

Note that the dimensionality of the problem has been reduced. In (1), ϕ must be solved on Ω, a 3D subset of E^3, while (2) is defined only on the 2D manifold Γ.

We employ the method of moments to solve (2), the details of which are presented in [3]. Qualitatively, the technique is vary similar to the representation of a quantum mechanical operator in matrix form. We choose a set of expansion functions $\{u_n\}$ on Γ which is used to approximate σ, that is $\sigma(x)=\sum a_n u_n(x)$, for some set of $a_n\in\mathbb{R}$. Another set of functions called weighting (or testing) functions $\{v_m\}$ is also selected. After expanding (2) in $\{u_n\}$ we take the inner product with each of the v_m's. We end up with a series of linear equations where the a_n's are the unknowns. This system may be solved by standard matrix methods. We apply a conjugate gradient algorithm to this end [4]: this is an iterative method which seems to provide fastest convergence.

For our moment method we chose for $\{u_n\}$ a set of piecewise constant functions, constant over the face of a triangle. Specifically, Γ is triangulated (approximated by triangles, for example see figure 1) and σ is assumed constant

*Supported by ONR/SDIO

over each triangle. This selection results in a finite element representation to (2). For the weighting functions we selected Dirac delta functions located at the centroid of each triangle (this is known as point-matching). This allows fastest evaluation of the inner products and yields good results as long as the triangles are sufficiently regular.

B. Extension to Poisson's Equation

If we wish to model a charge distribution ρ in the presence of our boundary Γ, it is convenient to exploit the linearity of the integral operator in (2). That is the potential at the boundary must be the sum of that due to both σ and ρ.

$$f(x) = \int_{\Gamma} G(x,\xi)\,\sigma(\xi)\,d^2\xi + \int_{\Omega} G(x,\xi)\,\frac{\rho(\xi)}{\epsilon_0}\,d^3\xi \qquad (5)$$

or

$$f(x) - \phi_\rho(x) = \int_{\Gamma} G(x,\xi)\,\sigma(\xi)\,d^2\xi \qquad (6)$$

where ϕ_ρ is the free space potential due to the charge distribution ρ, given by the second integral in (5). Equation (6) is similar in form to (2) and may be solved by applying the method of moments as before to the boundary data $f-\phi_\rho$. Therefore, it is only necessary to determine ϕ_ρ, the free space potential due to ρ, in order to apply the method to Poisson's equation. This may be done numerically or analytically (if available).

III. APPLICATIONS

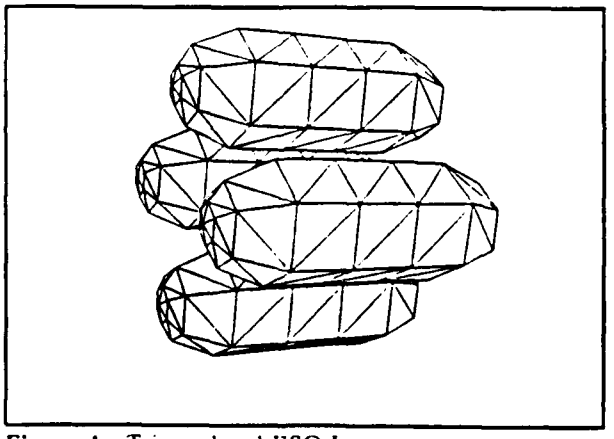

Figure 1: Triangulated ESQ Lens

The preceding technique was implemented using Borland C++ 3.1. The platform was an i486 PC operating at 33 MHz and running Windows 3.1 operating system. All examples where run in double precision arithmetic.

A. ESQ Lens

A 3D potential problem is the modeling of an electrostatic quadrupole lens. Figure 1 shows the computer model of an ESQ lens similar to the type used in [1]. It is formed from 4 cigar-shaped electrodes, the beam would enter from the left. Each electrode is 59 mm long and has a radius of 12 mm. The aperture of the entire lens is 10.5 mm. Two grounding shunts are located at z=±31 mm (they are not shown in figure 1 to avoid clutter) which provide isolation from adjacent lenses.

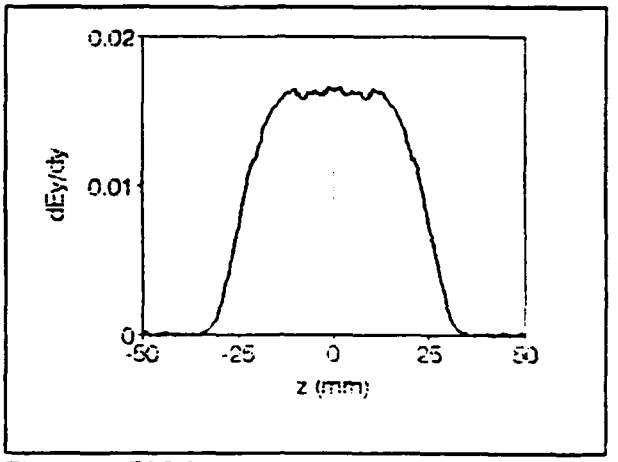

Figure 2: ESQ Lens Focusing Function

The single particle focusing effect (the kappa function $\kappa(z)$) from such a lenses can be determined from the derivatives dE_x/dx and dE_y/dy on axis. Figure 2 shows the computed data for the y-plane for the case in which the x-plane electrodes are driven to 1V and the y-plane electrodes are held at -1V. The grounding shunt at either end of the lens cause the rapid decay in dE_y/dy.

B. Ellipsoidal Bunch in a Pipe

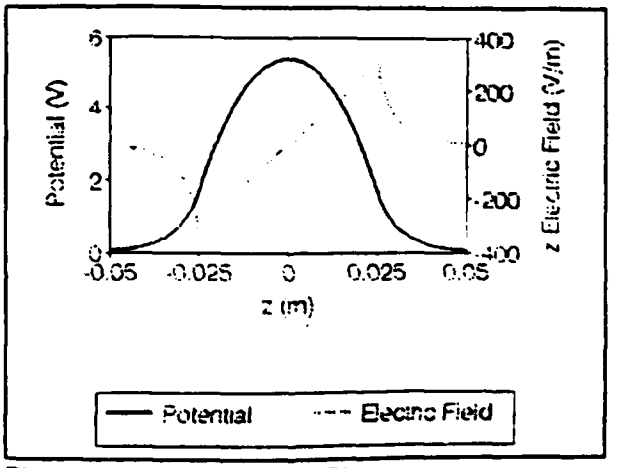

Figure 3: 2.5:1 Ellipsoid in Pipe

We can use the Poisson extension to simulate a uniform charge density ellipsoid in a conducting cylinder. This situation is useful in modeling cold bunched beams propagating through a beam pipe. There exists an analytic solution for the potential of such an ellipsoid in free space [5]. Thus, it is only necessary to model the pipe (surface charge) numerically.

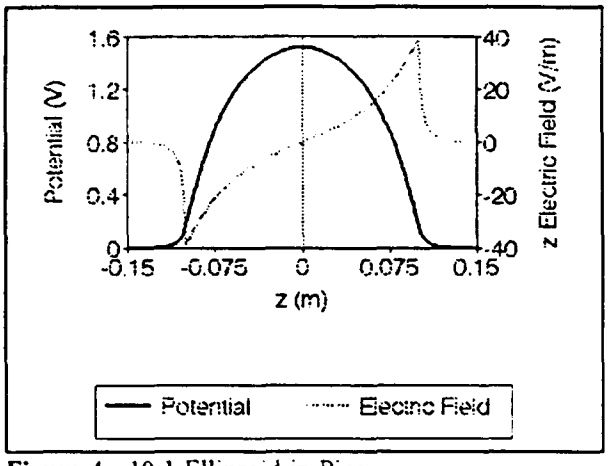

Figure 4: 10:1 Ellipsoid in Pipe

Figure 3 shows the axial potential and z component of electric field for the case of an axis-symmetric ellipsoid with major axis 2.5 cm and minor axis 1 cm inside a pipe of radius 2 cm. In this case the fields are still relatively linear, the image effects from the pipe are slight. However in figure 4 we see a very nonlinear field for the case of an ellipsoid with major axis 10 cm and minor axis 1 cm. We find that after the bunch length becomes comparable to the pipe radius the image effects play an increasing role. The total charge in both cases is 10^{-11} C.

The above simulations can be used to determine the so called "g-factor" for bunched beams in cylindrical pipes. A detailed discussion of these results can be found in [6].

IV. CONCLUSION

The method of moment technique has several advantages and disadvantages. The overall advantage of the technique stems from the fact that only surfaces are considered, rather than 3D regions. Hence, it is a good method to model complicated or otherwise arbitrary geometries. For the same system order, we get a higher boundary resolution as compared to finite differencing on a grid. Also, since the surface charges are solved for it is possible to calculate the fields anywhere in space, without interpolation. This fact allows us to apply the method to unbounded situations.

When dealing with the situation of conductors in a vacuum the moment technique is in general quite successful. However, if many dielectrics are present it is probably best to use finite differencing. Also, when it is necessary to know the fields over a large set of points, say when doing many particle simulations, it is probably best to use finite differencing. Computing the potential is a moderately expensive process, since we must evaluate (4) at each point, while finite differencing solves for the potential directly.

For the situations discussed the technique is well suited. We need full 3D solutions, yet only for the case of conductors in a vacuum. Also, we are only concerned with the solution data along the beamline axis. Therefore, the number of data points to compute is a minimum.

V. REFERENCES

[1] S. K. Guharay, C. K. Allen, M. Reiser, K. Saadatmand,and C. R. Chang, "An ESQ Lens System for Low Energy Beam Transport Experiments on the SSC Test Stand", (this conference).

[2] I. Stakgold, *Green's Functions and Boundary Value Problems* (Wiley, NY, 1979) pp. 508-517.

[3] C. K. Allen, S. K. Guharay, and M. Reiser, "Solution of Laplace's Equation by the Method of Moments with Applications to Charged Particle Transport", *AIP Conf. Proc. on Computat. Accelerator Physics*, Pleasanton, CA (1993) (to appear).

[4] T. K. Sarkar and E. Arvas, "On a class of Finite Step Iterative Methods (Conjugate Directions) for the Solution of an Operator Equation Arising in Electromagnetics", *IEEE Trans. Antennas Propagat.*, vol. AP-33, no. 10, pp. 1058-1066, Oct. 1985.

[5] R. L. Gluckstern, "Scalar Potential for Charge Distributions with Ellipsoidal Symmetry", Fermilab Report TM-1402 (1986).

[6] M. Reiser, *Theory and Design of Charged Particle Beams* (John Wiley & Sons, NY, to be published in fall 1993), Ch. 5.